

Tools from Above: Evaluating Drone-Borne Aerial Remote Sensing Systems for Archaeological Site and Feature Identification

Keywords:

Drones, Archaeology, Site Detection, Feature Identification, Digital Models, Remote Sensing, LiDAR, AI

Submitted to the Faculty of Graduate Studies in Partial Fulfillment of the Requirements for the
Degree of Master of Science in Archaeological Science
Department of Anthropology,
Lakehead University,
Thunder Bay, Ontario

© Nick A. Kuncewicz 2025

PERMISSION TO USE

Permission is hereby granted to the Lakehead University Library to reproduce single copies of this thesis and to lend or sell such copies for private, scholarly, or scientific research purposes only. If the thesis is converted to or otherwise made available in digital form, Lakehead University will inform potential users of these terms.

The author retains all rights associated with the copyright of the thesis, including but not limited to rights over the concepts, methodologies, and workflows developed or presented in the research. Except as explicitly permitted in this agreement, neither the thesis nor any substantial portion thereof, whether text, images, data, or processes, may be reproduced, published, or distributed in any material or digital form without the author's prior written consent. Any use of the research for purposes beyond personal or academic study, particularly commercial or derivative works, requires the express permission of the author.

ABSTRACT

Archaeological investigations are rapidly changing due to developing digital technologies. They affect data collection, processing, interpretation, and analysis, but have spawned new approaches to archaeological investigations. One aspect of this change includes remotely piloted aircraft systems (RPAS or Unmanned Aerial Vehicles or UAVs, also commonly known as drones) that have utility in improving cost-effectiveness of site characterization and feature identification but may not be appropriate for every archaeological situation. These RPAS are rapidly improving, and becoming more affordable, powerful, and accessible. When employed with digital data processing methods, they offer an important tool for investigating natural and cultural landscapes. Compared with imagery from modern satellite and manned aircraft, low altitude drone data offer advantages in resolution, accuracy, and flexibility. Important emerging considerations involve the development of diverse drone-deployed sensors coupled with geomatic analysis, machine learning, and computer-aided enhancement of detected spatial patterns.

This thesis explores the strengths and weaknesses of data collection and processing via aerial remote sensing, with particular attention to its utility for archaeological detection and characterization. It evaluates the efficacy and cost-effectiveness of unmanned aerial vehicles (UAVs) equipped with various sensors to aid archaeological investigation and site analysis. Further, a variety of data formats were integrated using geographic information systems (GIS). Information deriving from each of the remote sensing sensors used in this thesis demonstrated interpretive value. Efforts at validation of non-invasive archaeological interpretation involve direct visual confirmation of feature anomalies and positive spatial correlation of features of interest using optical remote sensing, legacy data, and georeferenced imagery.

This study represents the first systematic evaluation of UAVs and sensor technologies for archaeological use in the Canadian Prairies. The research addressed three key questions through examples using both consumer and professional-grade UAVs:

1. Can consumer and professional-grade UAVs provide more comprehensive tools for archaeological site characterization?
2. Can these UAVs help overcome the physical and financial challenges associated with archaeological fieldwork?
3. What technical and regulatory obstacles hinder the routine integration of consumer and professional-grade UAVs in archaeological investigations?

These questions are addressed with aerial data from three different archaeological site types from Manitoba, Canada: the pre-contact Lockport site (case study 1); the fur trade posts at Fort Ellice I and Fort Ellice II (case studies 2 and 3); and an undisclosed modern/historic cemetery (case study 4).

ACKNOWLEDGEMENTS

I would like to thank all the forces that brought me to this point in my life.

First and foremost, thank you to my loving partner in life, Megan Tymura for your steadfast support and for demonstrating to me what it means to strive for something you believe in and stand for. To Megan: Thank you for helping me find my way out of the basement. You are always looking out for me, and always there to help me figure things out. We have the unique ability to mirror our successes and we can do anything when we are together. You are the best teammate, and my best friend. I love you infinitely.

To my Dad, thank you for giving me a true understanding of space, peace, confidence, and patience. You taught me the meaning of balance and for this I will forever be grateful. Thank you.

To my Mom, You would never once hesitate to drop what you are doing for those who you care about and offered me a perspective on logic by always checking twice. For this I am thankful. You always lent an ear and helped me get through difficult times, if only by listening and being present.

To my Sisters Ashleigh and Chelsea, and to my Uncle Phil, thank you for taking interest in my endeavours and for offering your support, love, and help along the way. To the whole rest of my family, including my bros RJ and Cole, your humor, kindness, craziness, and reliability give me gratitude that is valued beyond words. Thank you greatly for listening to me drone on about drones.

To my other family the Tymuras, Don, Jer, and Claire, thank you for opening your doors to me and giving me a place to hang my hat. You've made it possible for me to call Thunder Bay my home away from home.

To John George: You built the biggest fire I've ever seen. It saved my life in more ways than one.

To Gord Hill and Perry Blomquist: Thank you for showing me that archaeology is about more than books. Your dedication to the field and approach to archaeology as a lifestyle is not lost on me. You equipped me with forever knowledge about true field archaeology and landscapes. From my first archaeological adventure at Nutimik Lake, Whiteshell to teachings at Bannock Point, thank you for instilling a long-lasting positive impact on me that persists to this day. You once told me I would make a good archaeologist and I believed this to be true; so much that I became one.

To Mike Sutherland and the PCSP team, including Mark Paxton-MacRae and Garth Sutton thank you for trusting me with this data, keeping open minds, and practicing archaeology the good way.

To Mireille (Mimi) Lamontagne, thank you for seeing the side of archaeology that is about relationships and culture, and always demonstrating respect and care for traditions. You are the real deal!

Thank you to my committee members Jill Taylor-Hollings and Dave Norris for supporting my ideas. Your professional and academic insights pass valuable knowledge regarding the field of archaeology. Jill, thank you for offering calm, positive vibes. Dave, thank you for helping me understand my value as an archaeologist.

Finally, thank you to Scott Hamilton for quietly understanding what this all means. Whatever forces brought me to your office in fall 2019 are now seemingly present in my everyday life. Thank you for always having an open door. Your guidance as a mentor of the archaeological discipline has proven invaluable to me on many occasions. Thank you for helping me keep my fire lit during this process. I look forward to what the future of archaeology holds for both of us.

This thesis is dedicated to those who make a conscious effort to follow their path even when it seems impossible to do so; one foot in front of the other.

TABLE OF CONTENTS

PERMISSION TO USE	i
ABSTRACT.....	ii
ACKNOWLEDGEMENTS	iii
TABLE OF CONTENTS	iv
LIST OF FIGURES.....	vi
LIST OF TABLES.....	vii
LIST OF ABBREVIATIONS	viii
 Chapter 1.0 Introduction	 1
1.1 <i>Background and context</i>	2
1.2 <i>Problem statement and research questions</i>	5
1.3 <i>Aims and objectives</i>	6
1.4 <i>Scope and limitations</i>	7
1.5 <i>Thesis layout</i>	9
 Chapter 2.0 Literature Review	 11
2.1 <i>History of aerial mapping and challenges for archaeological application</i>	11
2.2 <i>Key concepts and definitions of remote sensing</i>	18
2.2.1 <i>Photogrammetry</i>	22
2.2.2 <i>Multispectral</i>	23
2.2.3 <i>Thermography</i>	25
2.2.4 <i>LiDAR</i>	27
2.3 <i>Comparison of remote sensing techniques</i>	28
2.4 <i>Research in computer science</i>	37
2.5 <i>Archaeology of landscapes and GIS</i>	38
2.6 <i>Regulatory Issues</i>	39
2.7 <i>Theoretical frameworks and models</i>	41
2.8 <i>Digital Models</i>	44
2.9 <i>Overcoming challenges to systems and workflows</i>	47
2.9.1 <i>Data rights and ownership</i>	48
 Chapter 3.0 Case Studies	 50
3.1 <i>Introduction to case studies</i>	50
3.2 <i>Case study 1: Lockport (EaLf-1)</i>	50
3.3 <i>Case Study 2: Fort Ellice 1 (EcMh-3)</i>	54
3.4 <i>Case Study 3: Fort Ellice 2 (EcMh-10)</i>	57
3.5 <i>Undisclosed cemetery</i>	61
 Chapter 4.0 Methodology	 66
4.1 <i>Introduction to the methodology</i>	66
4.2 <i>Research design and approach</i>	66
4.3 <i>Data collection, processing, materials, and instruments</i>	68
4.4 <i>Hardware</i>	70
4.5 <i>Software</i>	74

4.6 <i>Sampling strategies</i>	77
4.7 <i>Data analysis methods and techniques</i>	81
4.7.1 <i>Ground Sampling Distance</i>	83
4.8 <i>Validity and reliability of the study</i>	85
Chapter 5.0 Results	89
5.1 <i>Introduction to the results</i>	89
5.2 <i>Examining workflow and making analytic inferences</i>	89
5.3 <i>Qualitative data analysis, themes, and visualization</i>	90
5.4 <i>Data interpretation</i>	93
5.5 <i>Summary of results and key findings</i>	115
5.6 <i>Comparison with existing literature</i>	120
Chapter 6.0 Discussion	122
6.1 <i>Introduction</i>	122
6.2 <i>Restatement of the research objectives</i>	122
6.3 <i>Comparison with existing literature and theoretical frameworks</i>	123
6.4 <i>Explanation and interpretation of the results</i>	125
6.5 <i>Implications for theory and practice</i>	127
6.6 <i>Limitations and future research directions</i>	128
6.7 <i>Workflow</i>	131
6.8 <i>Contribution of results from case studies</i>	138
Chapter 7.0 Conclusion	140
7.1 <i>Recap of the study</i>	140
7.2 <i>Conclusions and recommendations</i>	141
7.3 <i>Full Contribution of the study</i>	143
REFERENCES	146
APPENDIX	154
1) Results from Mavic Mini	154
2) Predictive model for grave predictions using NDRE	155
3) NDVI and NDRE grave statistics (marked and unmarked)	157
4) Cloud Compare Settings (CSF).....	160
5) VAT Algorithm Preset Values	161
6) DJI Mavic Mini Specs.....	162
7) MicaSense RedEdge-MX specs	166
8) DJI H20T Specs.....	167
9) DJI Zenmuse L1 Specs	168
10) D-RTK2 Base Station Specs	170
11) Juniper Systems GEODE-2 RTK Specs.....	172
12) Signed data permission letter from PCSP	176

LIST OF FIGURES

Figure 1. Map overview (Google satellite) of the Lockport Site location (EaLf-1).....	3
Figure 2. Map overview (Google satellite) showing FE1 and FE2	4
Figure 3. Electromagnetic spectrum taken from Khelifi et al., (2021: page3)	23
Figure 4. Illustration of the differences between digital elevation models (DSM, DFM, DTM) derived from aerial remote sensing data. Note. Source unknown. Used under presumed educational fair use.	29
Figure 5. RGB Orthophoto of EaLf-1 captured with a DJI Mavic Mini and processed with WebODM using 'Quick Orthophoto' option.	51
Figure 6. Digital Surface Model (DSM) of EaLf-1 capture with a DJI Mavic Mini.....	52
Figure 7. Comparison of the same features at EaLf-1 using RGB in Figure 5 (zoomed in) versus DSM in Figure 6.....	53
Figure 8. Drone capture of valley near beaver creek from overtop of FE-1 using a DJI Mavic Mini.	54
Figure 9. Google Earth screenshot showing the location of FE2 overlooking the Assiniboine River	58
Figure 10. RGB Orthophoto of FE2 captured using a Mavic 2 Pro	60
Figure 11. RGB orthophoto of FE2 captured using a DJI Mavic Mini	61
Figure 12. RGB orthophoto of undisclosed cemetery captured using a DJI Matrice 300 RTK drone equipped with a Zenmuse L1 LiDAR sensor	62
Figure 13. Undisclosed cemetery location showing multispectral orthophoto captured using a DJI M300 RTK drone and a MicaSense RedEdge-MX multispectral camera sensor	63
Figure 14. LiDAR VAT model of cemetery built using CloudCompare and GIS software	65
Figure 15. WebODM quality report. Note highlighted accuracies.....	73
Figure 16. Thermal heatmap of cemetery capture with a DJI M300 RTK drone equipped with a DJI H20T thermal camera sensor	92
Figure 17. Bar chart showing reconstructed features versus detected features for two different processing options in WebODM.....	96
Figure 18. GCP interface in WebODM allowing for PPK	98
Figure 19. NDVI model of isolated graves area showing high spectral reflectance	101
Figure 20. NDRE model of isolated graves area in the cemetery of case study 4 demonstrating high spectral reflectance signatures, likely indicating increased plant health, chlorophyll, and nitrogen.....	102
Figure 21. Raster histogram showing low frequencies of NDVI pixels using the mean of marked graves (black) and unmarked graves (red)	105
Figure 22. Raster histogram showing high frequencies of NDRE pixels using the mean of marked graves (black) and unmarked graves (red)	106
Figure 23. 10 graves selected for zonal statistics to analyze multiple pixels within a grave	107
Figure 24. Backgrounds for zonal statistics to understand surrounding environment in comparison to the spectral values of graves	108
Figure 25. Frequency histograms with implied value showing the range of means for NDVI compared to NDRE. Note the standard deviation for backgrounds and graves using NDVI are much wider, versus the narrow distributions of the NDRE data.	110
Figure 26. Thermal heatmap showing remnants of the FE2 palisade walls and other feature anomalies.	112
Figure 27. Thermal heat map of FE2 showing the remnants of an old baseball diamond. Measurements are consistent with the rules and regulations for noted baseball activity at this site during the same time. ...	114

LIST OF TABLES

Table 1. MicaSense RedEdge MX spectral bands.....	31
Table 2. Showing the RAM processing requirements for WebODM	95
Table 3. Showing 10 individual graves (marked) and 10 individual graves (unmarked) measured from a LiDAR VAT model. Note, there is a discrepancy where the Inside Cemetery and Outside Cemetery headings were incorrectly labelled, and they should instead read marked (for inside) and unmarked (for outside)	104
Table 4. Showing the temperature conversions at two different site locations after using data collected with a DJI H20T thermal camera sensor and in conjunction with an analysis tool called TermalMetrics	117
Table 5. UAV platform and sensor types used at each case study site location.....	119

LIST OF ABBREVIATIONS

AGC	Automatic Gain Control
AI	Artificial Intelligence
API	Application Programming Interface
CE90	Circular Error 90th Percentile
CMOS	Complementary Metal Oxide Semiconductor
CPU	Central Processing Unit
CRM	Cultural Resource Management
CRS	Coordinate Reference System
CSF	Cloth Simulation Filter
CSV	Comma Separated Value
DEM	Digital Elevation Model
DFM	Digital Feature Model
DGPS	Direct Global Positioning System
DSM	Digital Surface Model
DTM	Digital Terrain Model
FOSS	Free Open Source Software
GCP	Ground Control Point
GIS	Geographic Information System
GNSS	Global Navigation Satellite System
GPR	Ground Penetrating Radar
GPS	Global Positioning System
GPU	Graphics Processing Unit
ha	Hectares
GSD	Ground Sampling Distance
HBC	Hudson's Bay Company
HHRDD	Historic Human Remains Detection Dog
IMU	Inertial Measurement Unit
IRS	Indian Residential School

Km/hr	Kilometers per hour
LE90	Linear Error 90th Percentile
LiDAR	Light Detection and Ranging
LWIR	Long Wave Infra-red
MP	Megapixels
mRPAS	micro remotely piloted aircraft systems
MSRE	MicaSense RedEdge
NDRE	Non-Differential Red-edge
NDVI	Non-Differential Vegetation Index
NIR	Near-infrared
OSGPA	Ontario Standards and Guidelines for Practicing Archaeologists
PCSP	Peguis Consultation and Special Projects
PIC	Pilot In Command
PPK	Post Processing Kinematics
R-JPEG	Radiometric Joint Photographic Experts Group
RAM	Random Access Memory
RE	Red-edge
RGB	Red Green Blue
RPAS	remotely piloted aircraft systems
RTK	Real Time Kinematics
SDK	Software Development Kit
SfM	Structure-from-Motion
SIFT	Scale Invariant Feature Transform
TEK	Traditional Ecological Knowledge
TIR	Thermal Infra-red
UNDRIP	United Nations Declaration on the Rights of Indigenous People
VAT	Visualization for Archaeological Topography

Chapter 1.0 Introduction

The digital revolution of the 20th century introduced the world to personal computers and significantly transformed how archaeologists conduct professional site investigations. Computing capabilities have developed dramatically since the 1950s and over the last 20 years have become widely integrated into consumer electronics that complement daily life. In turn, these inventions have collectively impacted most academic disciplines, as increasingly more data is digitally collected, processed, stored, and shared. Modern archaeology follows this trend and continues to undergo profound change. It is reflected with the rapid development and ready availability of Unmanned Aerial Vehicles (UAV), also variously known as Drones, and Remotely Piloted Aircraft Systems (RPAS). RPAS and UAV are the most appropriate acronyms because they reference a suite of tools making up a system, but drone is more popularly used. All three of these terms are frequently used to generically reference the technology discussed in this thesis. This increasingly sophisticated technology offers utility for site prospection and will contribute to improvements in data collection, analysis, and interpretation.

This research summarizes a data collection and analytic workflow useful for archaeological investigations and geomatics while assessing the utility of RPAS to undertake archaeological mapping and site characterization. Important steps in this process are data acquisition, processing, analysis, interpretation, and dissemination. This evaluation of technology was conducted through four case studies in southern Manitoba where the machines were used to gather data and then build digital models for enhancing archaeological site detection and feature identification. This research considers both consumer and professional grade unmanned-aerial-vehicles (UAVs) and asks whether such approaches offer more comprehensive means of archaeological site characterization, whether they can help address the physical and financial hurdles confronting archaeologists, and

what technical and regulatory barriers impede their routine integration into the investigation process.

This research also assesses the utility of RPAS, described in the next section, to undertake archaeological mapping and site characterization. These range from a comparatively inexpensive consumer UAV that offers mapping capabilities via a red-green-blue (RGB) camera, through to the leading professional-grade machine capable of interchangeably mounting various sensors. The latter can also feature enhanced georeferencing capacity via communication with Real Time Kinematic (RTK) base stations. Evaluation of these methods are conducted through four case studies where machines were used to build digital models for enhancing archaeological feature identification, site discovery, and aerial reconnaissance.

1.1 Background and context

At its initial inception in 2021, this research sought to assess the utility and effectiveness of an entry level consumer drone (a DJI Mavic Mini) to undertake archaeological documentation and compare output to that collected by my academic supervisor Dr. Scott Hamilton, who was using a more advanced professional consumer or ‘prosumer’ drone (the DJI Mavic 2 Pro) (Hamilton, 2022). As the methodologies evolved, and as new technologies have emerged, the thesis scope and objectives have expanded to include evaluation of a professional-grade drone (the DJI Matrice 300) that deploys several different sensors, such as LiDAR, thermal, and multispectral tools that can collect new sorts of information. This latter equipment was used at four ‘case study’ localities: Lockport (EaLf-1), Fort Ellice 1 (EcMh-003), Fort Ellice 2 (EcMh-010) and an undisclosed cemetery location in Manitoba, Canada.

All four case studies derive from independent archaeological consulting projects and involve experimental application of RPAS-based mapping. The projects simultaneously consider

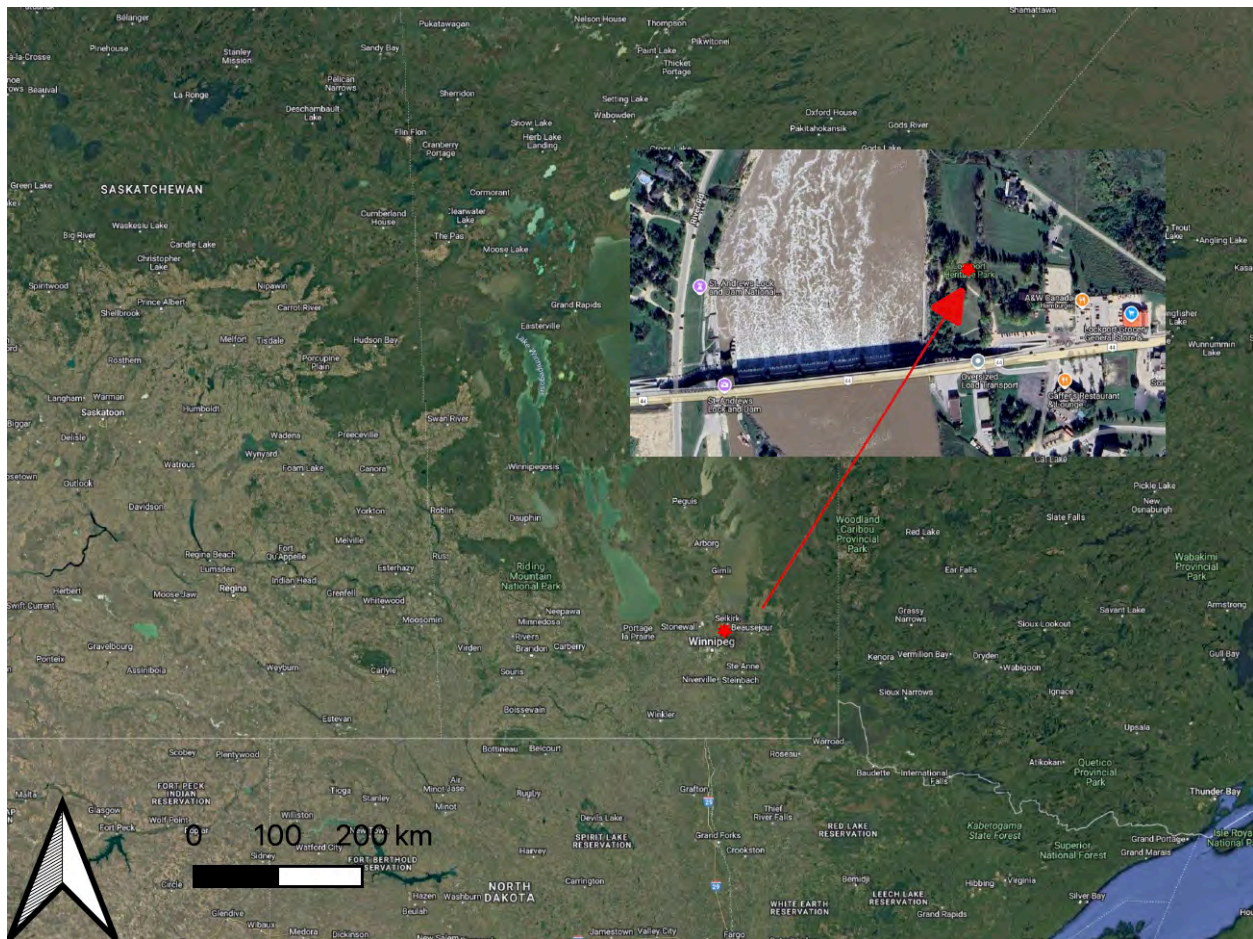


Figure 1. Map overview (Google satellite) of the Lockport Site location (EaLf-1)

the utility of such archeological approaches, and the efficacy of generated data for documenting subsurface archaeological features, including unmarked graves.

The first case study addresses the utility of an entry-level consumer drone (Mavic Mini) for rapid archaeological evaluative mapping as part of a conventional archaeological monitoring operation associated with urban infrastructure redevelopment along the east bank of the Red River at the Lockport Site near Selkirk, MB.

The Lockport Site was used for millennia as an aggregation place along the Lockport Rapids, with occupations representing some of the most northerly evidence of pre-contact Indigenous agriculture such as maize cultivation (Boyd et al., 2008). The site has been subjected to repeated archaeological investigation but lacks a well georeferenced large-scale map with which

to relocate former excavation zones and to monitor the rate of riverbank erosion. A micro-UAV, (DJI Mavic Mini) was used to rapidly generate an overview map of this locality to assess its utility for archaeological reconnaissance and site overview.

The second and third case studies address Fort Ellice 1 and 2, two 19th Century fur trade posts operated by the Hudson's Bay Company (HBC). These sites are situated near the junction of the Qu'Appelle and Assiniboine Rivers, close to the Manitoba/Saskatchewan border (*Figure 2*). These investigations sought to non-invasively relocate the fort compounds to further cultural and natural heritage interpretation of the property using walking trails and exhibits (Hamilton 2022a; 2022b). The work integrated aerial remote sensing with archival documents, using several RPAS and sensors including the DJI M300 RTK, Mavic 2 Pro, and Mavic Mini Version 1.

The final case study focuses on cemetery investigations conducted with permission from Peguis First Nation at an undisclosed location. For privacy reasons and in accordance with cultural

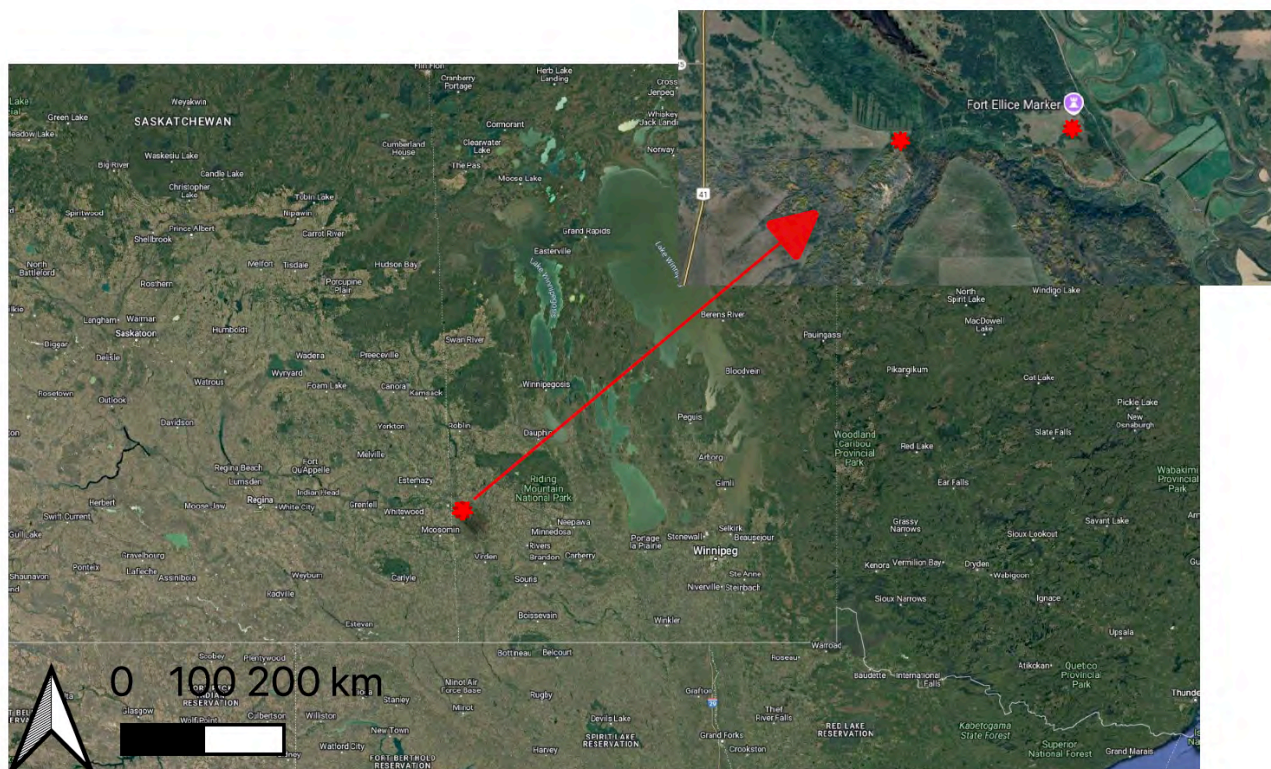


Figure 2. Map overview (Google satellite) showing FE1 and FE2

protocols, the geographic location and coordinate data for this site are not included. The flights were undertaken to assess the utility of RPAS methods for the detection of presently unmarked graves within this historic cemetery. The DJI Matrice 300 Enterprise drone was used to deploy four types of sensors to compare output from visible light, multispectral, thermal, and LiDAR methods.

1.2 Problem statement and research questions

This research evaluates several archaeological sites to assess efficacy of RPAS for general geographic characterization and under what site conditions can the various sensors document surface and subsurface features or localities of interest. This might involve use of photogrammetric and Light Detection and Ranging (LiDAR) methods to document topographic variability of archaeological interest. It may also involve documentation of subtle variability in the non-visible light spectra consistent with vegetation changes caused by human intervention. The latter might derive from plant light reflectance properties using multi-spectral sensors or patterned variation in solar heat absorption using thermal sensors. Such possible anthropogenic ground modification might be difficult to detect from the ground surface but can be more readily evident from an aerial perspective, particularly through use of sensors capable of detecting and enhancing such phenomena. Such site prospection and characterization requires identification, classification and interpretation to distinguish natural versus anthropogenic landscape features. As discussed in more detail below, this involves technical calibration of equipment, consideration of the optimal field conditions suited to each type of data collection, data processing workflows, and how to independently validate the output from remote sensing efforts.

In summary, this thesis outlines a geomatic data collection (using RPAS) and analytical workflow designed for archaeology. It considers data acquisition, processing, analysis, and

interpretation, and addresses under what conditions aerial remote sensing has utility in archaeological investigations. These questions are addressed with aerial data from three different archaeological site types; a pre-contact site (case study 1), a fur trade post (case studies 2 and 3), and a modern/historic cemetery (case study 4).

The research addressed three key questions through examples using both consumer and professional-grade UAVs:

1. Can consumer and professional-grade UAVs provide more comprehensive tools for archaeological site characterization?
2. Can these UAVs help overcome the physical and financial challenges associated with archaeological fieldwork?
3. What technical and regulatory obstacles hinder the routine integration of consumer and professional-grade UAVs in archaeological investigations?

1.3 Aims and objectives

To address the three research questions of this thesis, several objectives were developed. The central objective involved a comparatively straightforward evaluation of various RPAS and their efficacy for detecting and characterizing archaeological phenomena. This rather fundamental aim reflected the author's impression that many practicing archaeologists are slow to incorporate UAV mapping into site prospection methods. Pecci (2020) suggests some limiting factors include few published 'case study' exemplars, and that the rapid development of rather expensive technologies contribute to hesitation when and how to experiment with new archaeological approaches. Other more practical considerations involve the slowly resolving regulatory environment regarding RPAS.

While this research is heavily focused on data collection and analysis workflows in support of archaeological investigation, also of consideration is how such aerial remote sensing might contribute to non-invasive and non-destructive evaluation of archaeological and cultural heritage materials. This investigation tested three different RPAS to evaluate whether they generate analytically useful and replicable results. Specific attention was paid to investigative modalities being applied to various digital geospatial products, filters, algorithms, and workflows. This involved use of four optical remote sensing techniques capable of reading different classes of electromagnetic energy and plotting the output with precise 3-dimensional accuracy. The latter consideration was particularly important since it is essential for relocation of detected unconformities to further archaeological validation and testing.

1.4 Scope and limitations

Any evaluation of an emerging technology involves both a critical assessment at a time of rapid transformation of technical capacity and development of analytic/interpretative protocols. This impacted the thesis research and led to a priority shift to evaluation of diverse sensors mounted on UAVs. This includes consideration of appropriate deployment methods and the capacity of available equipment and software. It also begs questions how information deriving from diverse remote sensing methods can serve to validate or refute one other. While test cases for such advanced evaluation are beyond the scope of this thesis, aerial remote sensing may have considerable utility when used in concert with near-surface geophysical technologies such as ground-penetrating radar (GPR), or with satellite imagery that features rapidly improving absolute accuracy and higher image resolution, particularly in more populous southern regions, or where large-scale land transformation is anticipated. This is briefly addressed in the literature review section below.

Testing, validating, and effectively interpreting archaeological sites using non-invasive approaches can take several forms. It might include repeated data collection followed by data processing and analysis that is coupled with comparison of repeated ‘data runs’ to assess consistency of outcomes. If consistency of results is observed, it suggests good precision and perhaps relative accuracy but might not inform absolute accuracy; the concepts of which are expanded upon further in chapter 2. If replication of results is not revealed, then it speaks to the reliability of results interpretation. Issues of interpretative accuracy of spatially registered data occur at several levels. Accuracy might pertain to how closely the geospatial registration of the UAV-derived imagery conforms to real-world Cartesian space, typically assessed through Global Positioning Systems (GPS) or other coordinate-based reference systems. This form of accuracy is fundamental for ensuring that mapped archaeological features are correctly located relative to established spatial frameworks. Accuracy also refers to the sensor's ability to detect phenomenon that correctly and appropriately serve as ‘proxies’ of archaeologically interest, such as features and surface conditions. This latter form of accuracy is more interpretive and dependent on the sensors’ capacity and sensitivity, environmental conditions, and the specificity of its responses to different material contrasts. For instance, a thermal anomaly might suggest a buried archaeological feature, but without rigorous validation, it could just as easily be a product of biological or geological phenomena such as an ant mound, decomposing organic material, or vegetation with distinct heat retention properties. Therefore, while absolute accuracy is often crucial for spatially anchoring data, interpretative accuracy (repeated and validated detection of meaningful archaeological signatures) plays an equally critical role in establishing the reliability of remote sensing methodologies in archaeology.

While the equipment used in this thesis offers very significant improvements in map data resolution, density, and accuracy over conventional tools, it is associated with unexpected consequences. These methods generate enormous quantities of digital data that require storage, processing, analysis, and interpretation within a digital environment. Such data is vulnerable to loss, corruption, and data security issues if not handled correctly. This is particularly significant given the challenges associated with data management and the difficulty of recollecting lost or corrupted data, especially in workflows that involve extensive processing and large datasets. In addition, proper data management requires a significant investment in computer and software technology, and a major commitment to keeping up with changing general digital literacy.

1.5 Thesis layout

This thesis is organized in a series of chapters, divided into subsections to aid exploration of each case study with its discrete set of objectives. This emphasizes the workflows represented in data collection, processing, interpretation, and analysis to enable readers to critically evaluate strategies and outcomes and seek to replicate them with their own data. In effect this thesis offers a template on how to create and evaluate digital remote sensing products in ways that mimic standard approaches in archaeology.

Chapter 1 offers some background and context to the archaeological problems addressed in this thesis. The chapter provides some direction for the reader and an indication of things to follow.

Chapter 2 offers a literature review outlining the development of aerial remote sensing with particular attention paid to archaeological applications. This historical review addresses its origins with manned aerial vehicles, the development of high elevation satellite systems and the more recent emergence of computer assisted remotely piloted low elevation aircraft. The latter

are of quite recent derivation, particularly when considering the development of consumer and professional grade equipment equipped with increasingly sophisticated flight control and telemetry components and a rapidly expanding range of data collection sensors.

Chapter 3 offers details about the four case studies. This involves summarization of the research objectives associated with each test site, with detailed discussion how aerial remote sensing was integrated into those research operations.

Chapter 4 presents the methodologies employed at each test site and details the flight protocols, the level of georeferencing accuracy sought, the sensors used and how the data was collected, processed, analyzed, and interpreted. Particular attention is paid to case study 1 as an investigation of rapid mapping, case study 2 as an experiment for deriving optimal geospatial accuracy, case study 3 as an exploration of digital geospatial products for visual assessment by comparison while incorporating other remote sensing data, and case study 4 as a culmination of all techniques to achieve the highest grade possible of aerial investigation using enterprise tools for qualitative and quantitative analysis.

Chapter 5 presents the results generated from each case study complete with map imagery for visual representation. Some additional tables and figures about the technical information and equipment used during this study are found in the appendices.

Finally, Chapters 6 and 7 offering discussion and conclusions respectively where some future insights into the field of digital archaeology and remote sensing are provided and present an optimistic case for growth in these fields, gleaned from the examinations and results produced by this thesis.

Chapter 2.0 Literature Review

This section reviews the origins of photography and aerial remote sensing in general. It begins with the development and utilization of early technologies for mapping and reconnaissance and then introduces optical remote sensing in an applied setting. The final section offers a brief review of computer science research application, the development of Geographic Information Systems (GIS) and how this has impacted archaeology and landscape studies.

2.1 History of aerial mapping and challenges for archaeological application

While there is a growing number of publications contributing to aerial remote sensing, comparatively few directly address application to archaeology, and even fewer of these studies are conducted on North American sites. This is surprising given that archaeological field investigation and analysis often have a strong spatial and cartographic component. Perhaps this relates to the nature of North American climate and geography. It might also reflect the perspective that such methods are best suited for detection of monumental architecture, something less commonly associated with hunting and forager cultures that dominate North American culture history. This contrasts with Central America where pre-Columbia urban sites are being extensively studied with LiDAR, and European countries like Italy, Netherlands, and Switzerland that have strong computer-based digital archaeological programs. In any case, Canadian archaeological research and education programs are relative latecomers to aerial remote sensing, particularly using RPAS technology.

This section reviews the origins and development of aerial mapping methods and the evolution of equipment tools that make it possible. Development of these tools was driven by the need for better reconnaissance, often to support military intelligence collection. Such early aerial

surveillance dates to the turn of the 19th Century with Napoleonic military application using hot air balloons. More than a century after the first French use on November 21, 1783 (<https://www.nationalballoonmuseum.com/about/history-of-ballooning/>), the first successful powered flight was conducted by the Wright brothers on December 17, 1903, triggering rapid technological advances in powered flight (<https://www1.grc.nasa.gov/beginners-guide-to-aeronautics/wright-brothers-aircraft/>). Photographic technology was simultaneously rapidly developing, contributing to aerial surveillance and reconnaissance. Such applications relied heavily on oblique and nadir¹ image capture, with photographs requiring manual integration into cartesian maps. These methodologies rapidly improved through military application during World Wars 1 and 2, but cartographic integration remained a manual process. Modern UAV mapping is rooted in these earlier surveying practices that relied on cartesian grid systems such as Latitude/Longitude and later the Universal Transverse Mercator (UTM) System. Before development of the Ordnance Survey system, maps were created using techniques like stereopsis, which helped mapmakers understand spatial relationships between points. Early maps also used latitude and longitude for positioning, such as those based on the Mercator projection. The introduction of the Ordnance Survey system improved map accuracy by incorporating representative scales, allowing users to better visualize and interpret the relationship between locations and geographic features. Rapid technological development occurred throughout the 1960s and 1970s, stimulated by the development of computer technology, the Cold War and satellite surveillance systems. With the development of increasingly powerful computing technologies, digital data production and analysis became the primary mode of such mapping work. This era of sustained research and development of new digital technologies culminated in

¹ Nadir is a physical point of view where the camera angle is directly perpendicular to the landscape at -90° angle.

the 1980s with development of cruise missile systems that required the simultaneous development of satellite-based navigation systems. Even with the end of the Cold War, military applications of technology continued to drive development of emergent technologies, including remotely piloted aircraft (Maass, 2015). Since the early 2000s much of this technological innovation also drove civilian applications including drone development since the early 2010s.

Modern drone technology was initially driven by military application, but over the past decade, technology transfer and innovation has driven explosive product development for civilian recreational and professional users. The consumer market for such technology also triggered mass production to serve a global market and competition-driven innovation of new capacities.

While archaeological use of camera-equipped radio-controlled aircraft dates to the 1960s, over the past 15 years there has been rapid growth coinciding with digital photography, computer-assisted telemetry control, including IMUs (Inertial Measurement Units) and GPS, and high-capacity radio transmission of imagery (Keane & Carr, 2013). When this capacity is coupled with comparatively modest costs for consumer products, modern UAV applications are experiencing explosive growth. While several manufacturing companies exist, the Chinese drone manufacturer DJI is currently dominating the market, and all of the case studies feature use of various models produced by this company. This market dominance reflects equipment cost, ongoing development of new capacities, and integration of comparatively accessible software systems to support data processing and interpretation.

Central to the development of new aerial technologies is the parallel evolution and integration of several key systems. Computer systems and software engineering have enabled intelligent data processing, real-time image analysis, and semi-autonomous flight capabilities. Satellite-based navigation systems, such as GPS (USA), GLONASS (Russia), BeiDou (China) and

Galileo (EU), provide high-precision geolocation and route optimization, critical for both manual and automated drone operations. Advances in digital photography and sensor technology have improved image resolution and multi-spectral imaging, allowing drones to capture data across various wavelengths for detailed terrain analysis. The development of lithium-ion and polymer (LiPo) battery technology has extended flight durations, reduced weight, and increased power efficiency, making long-range aerial missions possible. Additionally, improvements in radio-communication systems have enhanced long-distance control, data transmission, and connectivity between drones and ground stations, ensuring reliable command and monitoring even in challenging environments. Continued technological innovation is driven by a global market for comparatively inexpensive consumer products featuring significant technical capacity. This thesis focuses on evaluating how such technologies can be harnessed to support archaeological investigation.

Since the earliest development of UAVs, they have been used for the observation and monitoring of landscapes. This capacity rapidly developed in concert with digital photographic technology. These innovations had widespread impact, including in the field of archaeology. Early efforts at gaining an aerial photographic perspective of archaeological sites, landscapes, and features involved cameras variously mounted on ladders, masts, poles, booms, and towers (Campana, 2017). Such approaches are cost-efficient but have operational height restrictions of approximately 20 m making it difficult to capture broad-scale terrain features associated with large archaeological sites. It is also difficult to capture nadir views and to georeference such imagery. Kites have been a popular choice for low-level aerial photography since the early 1970s (Campana, 2017). While kites can lift an acceptable payload to support aerial archaeology, specific wind requirements and erratic weather affect control and accuracy of deployment and is the main

drawback of this technology. Balloons and blimps require little or no wind to operate, but windy conditions make positional stability challenging. The expense of helium can also be a severe downfall. Helikites are a balloon and kite hybrid and offer the best of both worlds to reach higher altitudes, making them a viable technology for low-altitude photography (Campana, 2017). Unfortunately, the device's design makes it difficult to transport, set up, and launch (Verhoeven, 2009). Finally, manned aircraft enable broad spatial coverage while maintaining appropriate scale of resolution. For at least the last century, airplanes have been equipped to capture wide angle nadir and oblique photographs, and in recent years have deployed airborne laser scanning devices for terrain mapping. While conventional photography coupled with photogrammetry have demonstrated utility, this approach is constrained when the ground surface is obscured by vegetation. New innovations involving 'light detection and ranging' (LiDAR) devices overcome some of those issues since some of the laser light pulses can penetrate through vegetation canopies to generate a precise matrix of points representing surface topography. This is uniquely different from other forms of optical remote sensing that rely on digital photographic technology.

The widespread availability of consumer drone technology has been highly disruptive to the aerospace and surveying industries, fundamentally changing how aerial reconnaissance and remote sensing are conducted. Unlike traditional methods involving airplanes, helicopters or satellites, rotary wing drones are more efficient in low-altitude and small-area navigation. Their ability to operate in real-time allows for faster data acquisition, while their unmanned design significantly reduces operational costs and risks. These advancements in drone technology are closely tied to Global Navigation Satellite Systems (GNSS), which provide the geospatial precision necessary for accurate aerial mapping and remote sensing applications. This disruption ties into a broader democratization of aerial mapping. Consumer drones equipped with GNSS and

high-resolution RGB cameras enable individuals and smaller organizations to perform complex surveys and create detailed orthophotography. The rapid rise of online communities dedicated to refining drone-based survey techniques and remote sensing has accelerated this trend. These forums, along with advancements in free open-source software (FOSS) like WebODM and QGIS, have empowered users to produce professional-quality mapping and conduct spatial analysis without needing access to traditionally expensive and exclusive technological equipment. As a result, consumer drone technology has expanded access to aerial data, transforming industries such as archaeology by enabling rapid, cost-effective, and safer surveying solutions.

Drone technology has rapidly surpassed other aerial survey methods in archaeology, offering superior spatial data capacity, higher image resolution, and greater time efficiency for site detection and analysis. That said, it is still important to understand the trajectory of development of such technology to understand its specific advantages and limitations (Campana, 2017). A recurring theme that limits the utility of earlier technologies is the lack of absolute positional accuracy noted as either gyroscopic (roll, pitch, yaw, altitude) or geospatial (latitude, longitude, elevation, UTM). Campana (2017) emphasized that limited positional accuracy made production of 3D and photogrammetric digital models challenging because of the necessity to document and maintain positional control and to ensure suitable overlap between photographs. This problem has been solved with most modern remotely piloted aircraft systems (RPAS) that are equipped with onboard GNSS systems that simultaneously aid spatial positioning of the aircraft and provide georeferencing metadata attached to each photograph. The challenge is that these GNSS units are generally only capable of coordinate accuracy within 2-3 metres, and this accuracy varies in response to several uncontrolled factors. While this level of accuracy might be sufficient for many purposes, it is not appropriate for some archaeological applications. This is because global absolute

accuracy can indirectly affect relative accuracy through positional drift. When conducting multiple flights to capture repeated datasets, whether for change analysis over time or for deploying different sensors, it is crucial that absolute accuracy tolerances remain consistent. Even minor discrepancies in global positioning can lead to misalignment between datasets, making it difficult to spatially register information in the same locations across multiple surveys. Ensuring high positional accuracy is particularly vital for integrating data from different sensors, such as LiDAR, multispectral, and thermal imaging, where precise georeferencing is necessary to produce reliable and comparable results.

Modern, medium, and high-end drones have built-in GNSS capabilities, but also allow for differential GPS (DGPS) correction whereby the drone receives satellite corrections mid-flight, making it possible to use two different approaches during the data collection phase. Before expanding upon these approaches, it is important to distinguish between relative and absolute accuracy in this context. Relative accuracy refers to the precision of measurements within a dataset, ensuring internal consistency, while absolute accuracy pertains to how well those measurements align with true geographic coordinates in the real world. One technique using DGPS is called ‘real-time-kinematic’ correction (RTK) and involves in-flight refinement of GPS coordinates via simultaneous communication between navigation satellites, the RPAS and a stationary GPS base station. While RTK-enabled drones are currently quite expensive, they feature relative ‘ease of use’ compared to the more demanding workflow and expertise required when using ‘post-processing-kinematic’ techniques (PPK). PPK methods involve lab-based refinement of the georeferencing of aerial mapping products using ground reference points visible in the imagery that are associated with accurate geographic coordinates (absolute). Such refinement of spatial

accuracy significantly advances the utility of UAV technology particularly considering the general efficiency of image capture with reasonable time and cost (Marín-Buzón et al., 2021).

2.2 Key concepts and definitions of remote sensing

In order to understand the rapid development of remote sensing techniques, a general review of camera and sensor technology is essential. This is particularly important as the future developmental trajectory likely involves digital processing and analysis relying upon artificial intelligence (AI), and sophisticated filters and machine learning algorithms. This is closely connected to the increasing accessibility of sensors that detect wavelengths beyond the visible spectrum, supporting the viability of automated analysis techniques (Altaweel et al., 2022). These emerging approaches are only peripherally addressed in this thesis. Instead, it focuses on four key remote sensing techniques that are briefly introduced here: photogrammetry; multispectral; thermal; and LiDAR capabilities.

These four remote sensing techniques have utility in different situations. For example, *RGB photogrammetry* is useful for rapid reconnaissance mapping and the generation of surface relief models where minimal vegetation cover is evident, and modest georeferencing accuracy and relative relief is sufficient. This technique can also be effective for mapping archaeological excavations where repeated flights will document excavation progress, exposed features and artifact distributions. This is sufficient particularly if standard reference points remain visible in each flight, thereby enabling post-processing georeferencing refinement.

Multispectral sensors detect light reflectance beyond the visible light spectrum and have a primary agricultural application where plant age and species are uniform. They may have archaeological application since the sensor may detect differences in plant vigour and health that might be due to anthropogenic influences upon water and nutrient supply within the underlying

sediment. That said, core assumptions about plant uniformity of species and age need consideration.

Thermal sensors measure differences in thermal radiation emanating from the ground, structures or living objects. This has potential archaeological application in situations where archaeological features (mounds, filled depressions, buried foundations, refuse middens and earthworks) radiate heat in ways that contrast with the surrounding non-anthropogenic context.

LiDAR sensors operate by emitting laser light pulses at timed intervals and measure the time duration for those light pulses to be reflected back to the sensor. This might be light reflected from vegetation, structures, or the ground surface. When processed and classified, these data generate a dense ‘point cloud’ of X, Y, and Z data points that offer a detailed three-dimensional representation of the area of interest.

These four remote sensing techniques generate different characterizations of the locality that vary depending upon how the sensor responds to the local conditions. When used in concert they can offer powerful analytic capacity since each may identify discrete characteristics of interest, and each can aid in validating other classes of information. All involve collection, processing and analysis of digital information, the utility of which requires emergence of new archaeological methodologies inevitably tied to deployment of increasingly sophisticated computing technologies.

Effective digital remote sensing applications using RPAS have been contingent upon computer science and the rapid development of consumer electronics. Drone technology benefits greatly from automation and computational advancements, as it relies on GPS for navigation and remote control for data collection. Also important is the development of third-party applications that integrate with mobile devices and advanced remote controllers. These application

programming interface (API) kits broaden and enhance the flight capabilities designed by the original drone manufacturer. Computer science also contributes to efficacy of camera functions such as timing, electronics, and computational physics. Without some concepts of computer science acting as a media for reproducing virtual space, the process of digital modeling would simply fail. One such technological innovation is called bundle block adjustment that matches key tie-points and features in multiple overlapping, offset images (Stott et al., 202). During the bundle adjustment phase, drone sensors (camera, GPS, IMU) and photogrammetry algorithms work symbiotically. The hardware continually captures spatial data, such as external camera orientation and internal lens calibration, while the software interprets and adjusts this data to optimize the alignment of images. This interaction ensures that both the internal and external parameters are precisely refined for reliable spatial modeling (James et al., 2017). Offshoots of this innovation deriving from the IMU and external camera parameters also form the basis for collision avoidance sensors, aircraft positional awareness, and the coordination of speed and orientation to maximize performance and quality of data acquisition. In effect, the complex interaction of the sensors and information processing contributes to the deceptive ease of flight operations, particularly when conducting semi-autonomous mapping missions. Contributions from computer science are essential to archaeological science, especially in areas involving data processing and analysis. Diverse software programs, plug-ins, scripts, filters, and algorithms are associated with the development of digital models for landscape reproduction and georectification and are the basis of workflows that guide data analysis. There are even specific computer models designed for the detection and amplification of specific unconformities that may be of archaeological derivation.

Geographic Information Systems (GIS) are also strategic for the development of computational archaeology. While originally employed to store, manage and integrate thematic

data to support cartography, by the 1970s geomatics became widely used to address cultural landscapes and interpretation of the spatial component of social sciences data. Landscape studies framed from an archaeological perspective can address transformation of past environmental conditions and how anthropogenic processes shaped such landscapes. GIS offers functional capacity by enabling integration and comparison of spatial data and deriving new data using analytic tools and extensions. In the context of this thesis GIS is a core tool for comparison of accurately georeferenced thematic information deriving from each sensor type.

Much of the broader application of computing science to archaeology and other disciplines relates closely to the sharp reduction in size (and cost), coupled with expanding capacity of computer hardware components. With the 1958 development of the integrated circuit by Jack Kilby, research and development eventually led to microchips that enable equipment such as DJI drones to contain components responsible for diverse operational tasks and efficient management of information (Kilby, 2001).

These developments in electronic hardware act to rapidly further the fields of computation and software packages. For example, modern drone flight planning software requires integration of ‘software development kits’ (SDK), and ‘application programming interfaces’ (API). In brief, SDKs (also known as a dev kits), enhance interoperability to translate one computer language into another and allow programmers with a suite of tools to code new and unique software applications to be deployed on specific hardware. APIs used with UAV applications expand capacity for communication between a drone and a user. For example, in case study 1, 2, and 3 the DJI Mavic Mini drone used 3rd party software applications to enable "on-the-fly" capture of potential archaeological features. The DJI Mavic Mini was initially marketed as a simple hobbyist device and was not equipped with mapping software (i.e. capability to execute semi-autonomous flight

plans). This apparent market void offered an opportunity to companies such as Dronelink, Litchi and UGCS to develop APIs that enable flight planning software to communicate with DJI's proprietary hardware with minimal exposure of proprietary information and at a low security risk to DJI. Currently, there are many FOSS software applications available to the average drone user. The benefits of FOSS are clear but are countered by growing concerns over regulatory controls and who manages control of digital data such as sensitive cultural heritage information. Mapping approaches using FOSS also face some adverse risk that the data might inadvertently fall into public hands. Most FOSS currently allow users to access, interpret and even make changes to the structure of software tools and this contributes to further risk.

In the following sections the various approaches to remote sensing used in this thesis are briefly described, with some discussion of application to archaeology. Section 2.3 offers more comprehensive discussion when comparing the sorts of output generated from each sensor type.

2.2.1 Photogrammetry

Photogrammetry is a method by which multiple overlapping (nadir) aerial images, generally using RGB, are stitched together using computer algorithms to generate a mosaic. The algorithm uses the identification of unique points or features visible in multiple overlapping images, allowing them to be accurately linked together. Success of this tiling depends upon sufficient overlap within the adjacent images, as well as sufficient heterogeneity and uniqueness of features within the photographs. The stitching of the photographs within the software is done using a technique called Structure-from-Motion (SfM). This technique relies on two principles for defining similarities between images and their orientation in the image/within space: 1) the ability to create virtual depth perception through stereopsis and 2) the visual discrepancy of an object observed from a moving point (Abdollahnejad & Panagiotidis 2020). SfM is a photogrammetric

process using multi-view stereopsis. Similarly, to the way 3D glasses change the perspective of human vision, multi-view stereopsis derives 3D structure from duplicate points in overlapping images without the requirement of previously known 3D positions (Hirschmuller, 2008).

2.2.2 Multispectral

Multispectral sensors capture electromagnetic radiation across and beyond the visible spectrum (see *Figure 3*). While widely used in agricultural applications, their potential for archaeological prospection remains underdeveloped. Although effective, multispectral analysis can present challenges when compared to more comprehensive remote sensing methods. This is particularly relevant for studies focused on detecting subtle biochemical markers at the leaf level, which can indicate organic archaeological deposits.

The research discussed here used a MicaSense RedEdge-MX multi-spectral camera that captures 5 bands (red, green, blue, near-infrared (NIR), and red edge (RE)). NIR and RE bands are crucial for evaluating archaeological potential specifically for their roles in important vegetation indices known as Normalized Difference Vegetation Index (NDVI) and Normalized Difference Red Edge (NDRE) that will be discussed later. NIR and RE enhance the ability to detect subtle

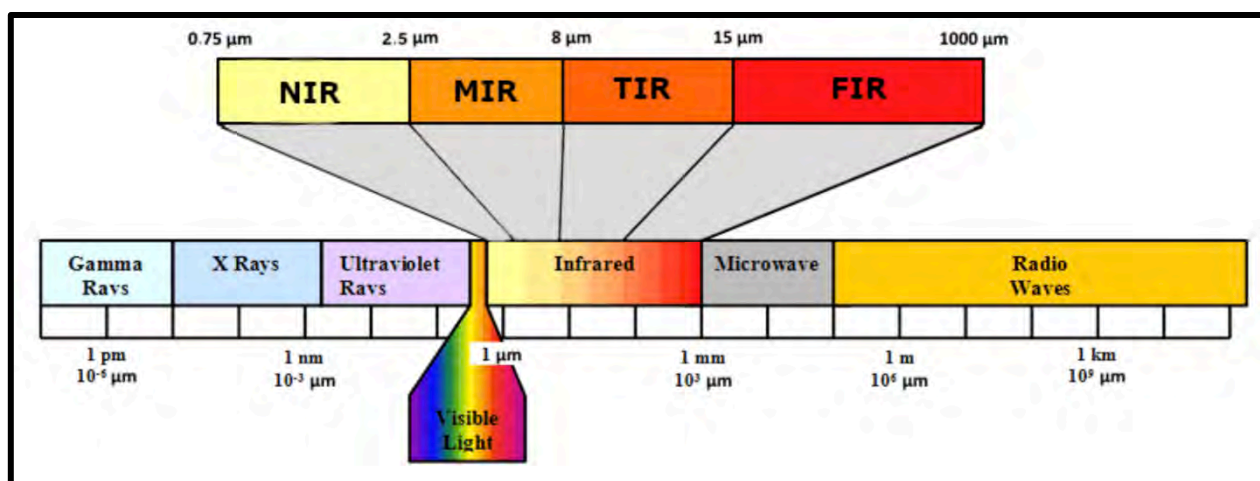


Figure 3. Electromagnetic spectrum taken from Khelifi et al., (2021: page3)

variations in vegetation and are useful for measuring changes in plant health and plant abundance. These characteristics are highly correlated with chlorophyll and nitrogen content that may indicate underlying soil nutrient load, moisture levels and buried features. Using fewer or different combinations of spectral bands can reduce the effectiveness of this analysis, limiting the ability to identify archaeological sites. Conversely, using hyperspectral cameras with over 100 bands could provide greater detail, but it remains unclear whether the additional data is interpretable and contributes meaningful insights. Proper segmentation of the wavelength spectrum is essential to balance the trade-off between detail and practicality in archaeological remote sensing.

In a study conducted by Abdollahnejad and Panagiotidis (2020), a version of the MicaSense multispectral camera was used, except their camera lacked a green band (MicaSense RedEdge-M). They demonstrated that a UAV (DJI S900) equipped with a multispectral camera can provide invaluable data for ecosystems management. This approach is transferable to archaeological applications if data collection protocols offer an appropriate scale and resolution. Such methods document vegetation health and have potential as an indicator of buried archaeological deposits (even human burials) since differential plant vigor might derive from anthropogenic nutrient enrichment or soil moisture differences. For example, in the context of documentation of unmarked graves, body decomposition releases high levels of Nitrogen into the surrounding soil to be taken up by plants (Rocke & Ruffell 2022). This localized nitrogen enrichment might be identifiable in plant leaves using the near-infrared spectrum detected with a multispectral camera (Brabazon et al., 2020, Rocke & Ruffell 2022, and Silván-Cárdenas et al., 2021).

2.2.3 Thermography

Thermal cameras measure light (heat) at a wavelength that coincides with the far edges of the infrared spectrum ($2.5\mu\text{m} - 25\mu\text{m}$) ([The EM spectrum \(utk.edu\)](#)). This may have archaeological application since earth heating and cooling rates can be affected by its sedimentary makeup, constituent materials, soil moisture, micro-relief, and vegetation cover- some of which might reflect anthropogenic origins. This requires production of a mosaic image using a thermal sensor with sufficient resolution to detect and delimit subtle temperature variation at the scale expected of archaeological features of interest.

The camera used in the case studies is the DJI H20T with a thermal FLIR sensor capable of reading wavelengths emitted between ($8\mu\text{m} - 14\mu\text{m}$) (<https://www.dji.com/ca/zenmuse-h20-series/specs>). The DJI H20T connects with the DJI M300 RTK using the DJI Skyport hardware, with data output being processed into a mosaic using DJI Terra with only a few parameter adjustments. One pitfall with this specific approach is that the mosaic generated using DJI Terra only generates a qualitative heatmap showing a gradient of differences between ‘hot’ and ‘cold’ spots. If quantitative data is required, temperature-specific values remain embedded in the metadata associated with each cell that makes up the raster mosaic output. Data extraction involves use of a portable version of Python and ExifTools to decode the embedded information. Once this information is retrieved, the values must be multiplied by 100 to get accurate temperature readings from pixel to pixel. While discussed in more detail below, this process was not attempted for this thesis but could be important in the future if archaeological features are identified within a specific emissivity range.

Agudo et al. (2018) explain that most archaeological applications of thermography rely on variation observed within crops characterized by uniform species and age. In such circumstances

variability in plant growth/vigor may reflect sediment conditions, including the existence and characteristics of subsurface archaeological features (Verhoeven & Vermeulen, 2016). Much like the conclusions drawn by Agudo et al. (2018), Case studies 3 and 4 demonstrate the applicability of thermography to archaeology. The quality of results will vary depending on many factors, the most important of which include the choice of sensors, soil type, time of day, ambient temperature, vegetative cover, and type of archaeological feature sought.

Successful thermography relies on four properties; thermal conductivity (the ability to transfer heat), volumetric heat capacity (the amount of thermal energy required to raise the temperature of an object by one degree from absorption), thermal inertia (the rate of heat transfer of different materials, and thermal emissivity (the effectiveness of emission or reflection of thermal radiation of a material) (Casana et al., 2017). Thermal conductivity differs between soil types, where wet sand results in a deeper transfer of energy below the surface, indicating high thermal conductivity. In contrast, dry clay-rich soil is considered to have low conductivity and will inhibit heat transfer (Casana et al., 2017). Thermal inertia also affects soils because the temperature of wet soils will also be more consistent than that of dry soils (Casana et al., 2017).

Casana et al. (2017) indicate that it is difficult to predict the optimal time for data collection from a seasonal and diurnal perspective. For documenting buried architecture or surface features such as pits, ditches, or earthworks, it is best to capture this imagery between sunset and sunrise. This is because vegetation will typically create the most thermal ‘noise’ shortly after sunset, making the differences between features less distinctive. As the ground cools through the night, differences in thermal inertia between soils and features will result in different appearances in the thermal imagery (Campana et al., 2017).

2.2.4 *LiDAR*

LiDAR is the abbreviation for Light Detection and Ranging techniques and holds considerable promise for non-invasive archaeological investigations. It involves emitting laser light pulses from a device with a known X, Y, and Z (3-Dimensional Space) position and measuring the timed interval until that light pulse is reflected back to the device. These coordinates represent movement in the east-west position (X), the north-south position (Y) and the vertical position (Z). The timed interval offers a precise estimate of range, while the spatial configuration of the reflective surface is represented by a dense cloud of X, Y, and Z points detected and stored within the LiDAR device. When aerial LiDAR is utilized correctly, it can create highly detailed surface models, often even when obscured by a tree canopy. This topographic relief model might represent natural undulations in the ground surface, or relief deriving from subtle archaeological surface features. The most widely published archaeological application of LiDAR mapping in heavily vegetated areas include mapping of tropical forests in Central and South America to document remnant structures obscured by the dense vegetation cover. Studies by Pingel et al. (2015), Chase et al. (2011; 2017), Inomata et al. (2018), and Iriarte et al. (2020) offer important examples of LiDAR application to archaeological prospection in Central and South America.

Of interest here is the limited application of LiDAR and other remote sensing technologies in Canada for documenting landforms and archaeological features that are often obscured by dense vegetation cover. Seasonal constraints, characterized by long winters and snow cover for a significant portion of the year, present logistical challenges for aerial surveys, particularly when compared to tropical regions where dense forest cover remains a persistent but surmountable obstacle year-round.

Beyond logistical and financial considerations, the global interest in archaeological discovery of monumental architecture also plays a role. Research in Central and South America, where remote sensing has revealed vast, interconnected temple complexes and cityscapes, often captures the imagination of both scholars and the public. In contrast, Canada's archaeological record, rich with Indigenous histories, cultural landscapes, and more ephemeral site types, has often been overlooked in mainstream narratives, contributing to the perception that its archaeology lacks the same level of exoticism or monumental appeal. This dynamic may further impact research priorities, funding allocations, and the visibility of digital archaeology efforts in the region.

2.3 Comparison of remote sensing techniques

The remote sensing literature examined in this section is organized by remote sensing type with particular emphasis on drone-based research. Aerial photogrammetry requires a sequence of stereoscopic images taken at approximately the same altitude (Fernández-Hernandez et al., 2015). This creates a virtual depth perception known as stereopsis that can be used to extract 3-dimensional geographic information. Photogrammetric output represents a 'merging' of overlapping photographs deriving from the identification of common points found in each image to enable accurate production of a mosaic image. The image becomes an accurate representation of geographic reality since the coordinates associated with each photograph allow the composite image to be reoriented and warped to conform to the cartesian space encompassed by the flight area. Photogrammetric processing also allows a 3-dimensional representation of the flight area using these 2-dimensional images. This involves arithmetic calculation of relief by observing the same point from two different perspectives represented in each overlapping photograph. Since the X, Y, and Z position of each photograph is approximately known via the on-board GPS and

barometric altimeter, this information enables an estimation of the cartesian coordinate of the observed points within the overlapping photographs. Ideally, the photogrammetric output is georeferenced within the accuracy possible of the on-board GPS and can be integrated with other similarly georeferenced data using GIS software. The surface relief model is usually represented as a raster image with each cell being assigned an 'elevation' value. They are often referred to as digital elevation models (DEM), digital terrain models (DTM) and digital surface models (DSM).

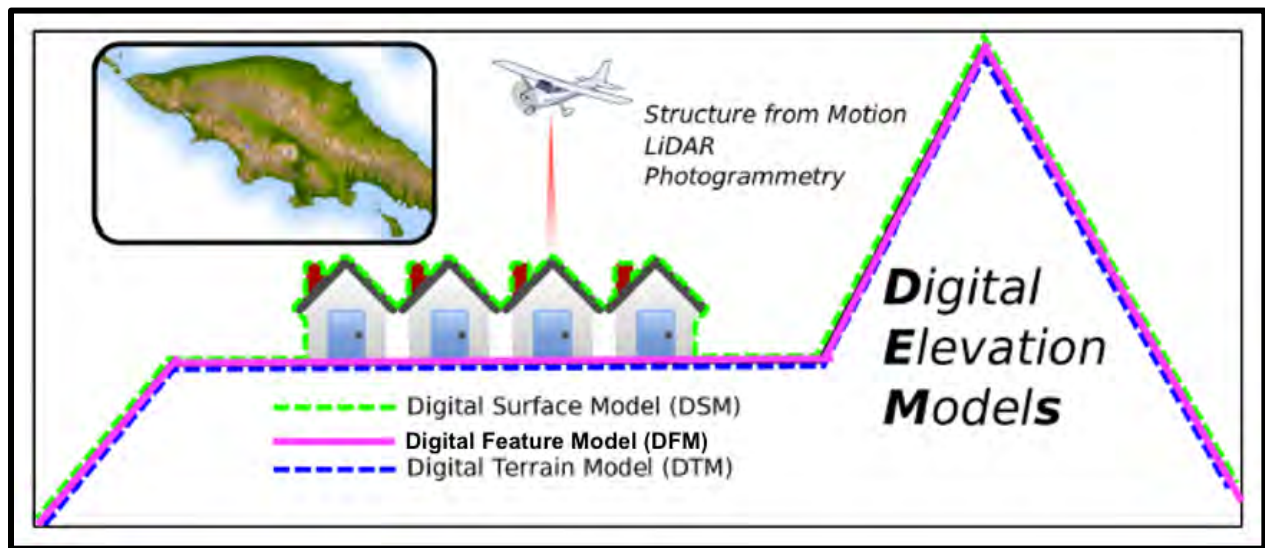


Figure 4. Illustration of the differences between digital elevation models (DSM, DFM, DTM) derived from aerial remote sensing data. Note. Source unknown. Used under presumed educational fair use.

These values can be utilized to visually represent relief using a 'false colour' gradient, can be subjected to contouring operations, or represented as 'hillshade' models. Photogrammetry most often relies on the red, green, blue (RGB) spectrum of visible light that is captured using digital cameras carried on most consumer-grade drones, though other types of imagery can be used in photogrammetric processes as well. This offers the most cost-effective remote sensing technique for archaeological investigation. Cost-effectiveness is crucial in archaeological investigation because research funding is often limited. Affordable remote sensing technologies, such as photogrammetry and consumer-grade drones, provide high-resolution data at a lower cost than

alternatives like LiDAR or extensive ground surveys. This allows archaeologists to survey larger areas, conduct repeated monitoring, and allocate resources more efficiently toward excavation, conservation, and analysis. Under certain conditions photogrammetric output can offer high-resolution documentation of the area of interest because of camera quality and the ability to undertake low elevation mapping missions. However, the utility of photogrammetric mapping can be constrained by the nature of vegetation cover mantling the area of interest. This is because the RGB camera records light reflected from the top surface. If the ground surface is visible, the elevation model might accurately represent that relief, but if vegetated, the output might reflect ‘false relief’ representing the top vegetation canopy.

As part of a forensics experiment, Silván-Cárdenas et al., (2021) demonstrated the utility of multispectral and thermal imagery to identify grave features based on body decomposition phases. They used pig remains as a proxy for human remains to study the decomposition process, and whether transformation of surface conditions might be detected using aerial remote sensing. Multi-spectral, hyperspectral, and thermographic techniques are all ways of quantifying electromagnetic radiation (energy) by measuring and interpreting the wave properties of light. Many spectra of light exceed the visual capabilities of the human eye and are rendered ‘invisible’. However, advances in remote sensing technology have made it possible to detect and interpret these otherwise invisible bands and can map this energy as a form of intensity, or brightness. Light in the spectral ranges associated with Red-edge, Near-infrared, and Thermal-infrared (TIR) also known as Long-Wave-infrared (LWIR) can be interpreted and utilized for archaeological purposes. The ways in which these spectra can be useful for archaeology are listed below in this section.

Multispectral sensors can detect subtle variations in vegetation health, making them useful for identifying buried features such as graves. Spectral indices, such as the Normalized Difference Vegetation Index (NDVI) and the Normalized Difference Red-edge Index (NDRE), highlight changes in plant vigor that often correlate with soil composition and nutrient levels. Since decomposition releases nitrogen into the surrounding soil, vegetation above graves may exhibit distinct spectral responses when compared to undisturbed areas. These indices are calculated using mathematical equations that process different wavelengths of reflected light to emphasize specific plant characteristics, particularly those related to water and nutrient availability (Silván-Cárdenas et al., 2021).

With Case Study 4 these techniques are applied using a MicaSense RedEdge-MX™ multispectral sensor to evaluate their effectiveness in detecting marked and unmarked graves. This dataset, collected from a cemetery and its surrounding area, provides a basis for identifying spectral signatures associated with human burials. A refined version of this workflow could have application in the search for missing children from Indian Residential Schools. The spectral attributes of the sensor used in this study are outlined in Table 1.

Table 1. MicaSense RedEdge MX spectral bands

MicaSense RedEdge-MX™				
Imager/Band Number	Band	Bandwidth	Center	Range
1	Blue	32 nm	475 nm	459–491 nm
2	Green	27 nm	560 nm	546.5–573.5 nm
3	Red	16 nm	668 nm	660–676 nm
4	Red-edge	12 nm	717 nm	711–723 nm
5	Near-infrared	57 nm	842 nm	813.5–870.6 nm

Whitehead et al. (2014) and Rocke and Ruffell (2022) are some of the few publications showcasing multispectral analysis using the Normalised Difference Vegetation Index (NDVI) for precision agriculture and archaeology respectively. NDVI is a metric for measuring biomass and is a good indicator of chlorophyll content and overall plant health generally. NDVI is used later in this thesis in case study 4. It is a result of the measured near-infrared light spectrum, minus the visible light spectrum, divided by the near infrared spectrum, plus the visible light spectrum or: $NDVI = \frac{NIR - VIS}{NIR + VIS}$. The sums and differences of NDVI are measured by the reflectance of wavelength in nanometers and are represented by this equation on a scale from -1 to +1 in the index.

Thermal analysis² is another form of remote sensing that relies on light derivation via electromagnetic energy. Much like the multispectral approach to acquire Red-edge and Near-infrared reflectance values from light intensity, using a thermal camera can produce temperature readings. The Thermal-infrared (TIR) electromagnetic radiation is diffused across a sensor array and the intensity data from each pixel is read, interpreted, and converted into pixel temperature values (<https://www.fluke.com/en-ca/learn/blog/thermal-imaging/how-infrared-cameras-work>). TIR ranges from 8-15 micrometers (µm) and is shown in *Figure 3* (Khelifi et al., 2021).

The characteristics of day and night are an important factor in the successful acquisition of thermographic data. Gompf and Anacelet (2019) describe these patterns in four (4) specific time cycles; diurnal (activity during light), nocturnal (activity during dark), crepuscular (activity during twilight), and cathemeral (activity during both day and night). Diurnal cycles are critically examined by Hill et al. (2020) to understand the thermographic effect these cycles have on archaeological feature identification. Using a DJI Phantom 4 drone, equipped with a gimbal

² The term thermal analysis is used interchangeably throughout this thesis with the terms thermography and thermogram.

mounted FLIR Vue Pro-R thermal camera sensor, Hill et al. (2020) repeatedly mapped the historic archaeological site of Enfield Shaker Village, New Hampshire. The FLIR Vue Pro-R is a radiometric sensor that can record proprietary radiometric JPG (R-JPEG) format directly to an SD card. The DJI H20T used in the case studies of this thesis has similar specifications aside from the ability of the H20T to record in 16-bit versus the 14-bit of the FLIR Vue Pro-R. Recording radiometric metadata is an important improvement over older thermal tech since this full spectrum method is enough to quantify data at the pixel level. Previous generations of thermal technologies were developed with automatic gain control (AGC) built-in such that the camera processed to an 8-bit image after evaluating the total range of thermal values apparent in each image (Hill et al., 2020). In this older technology, the relative variation in heat detected in each image is calculated across the available 8-bit range rather than recording the absolute heat associated with each pixel within the image. This is problematic for archaeological applications for several reasons. Primarily photogrammetric processes are difficult if images have different exposure values due to AGC fluctuations, but also high or low relative temperatures will cause AGC processing to mask subtle temperature variations of soil that might indicate subsurface archaeological features (Hill et al., 2020). Advances in thermal FLIR technologies are enabling solutions for quantifying thermal signatures of deeply buried deposits since these types of archaeological materials would display greater subtlety of temperature relative to thermal emissivity. Lastly, Hill et al. (2020) emphasize that data fusion is a more powerful approach to remote sensing than side by side comparisons of multiple datasets; a concept that is also explored more fully in this thesis. The Hill et al. (2020) study is noteworthy for identifying the role of dew point after dusk regarding feature detection. When the surface temperatures reach the dew point, features begin to disappear from the thermograms. The compilation of thermograms and other remote sensing techniques used by Hill

et al. (2020) demonstrate the effectiveness of data synthesis into a single interrogable space and conclude that diurnal heat flux is one of the most important factors affecting the visibility of archaeological features.

Further studies by Carmona et al. (2020) and Waagen et al. (2022) support depth as a determinant of thermographic resonance. Carmona et al. use a fixed wing UAV ebee system equipped with a third-party hardware application called thermomap. Once again, acquiring data at specific times throughout the diurnal cycle is regarded as ideal. Carmona et al. (2020) studied the Iron Age hillfort of Villasviejas del Tamuja (Cáceres, Spain) using aerial thermographic analysis. While there is some relevant information regarding general radiometric soil indices, this study lacked radiometric classification of the signal captured by the thermal sensor. Carmona et al. (2020) identified the site's sloped terrain and stratigraphic thickness as barriers contributing to weak thermographic signature attenuation. While this study successfully produced thermographic results relevant to archaeological investigations, further research is needed to better understand how stratigraphic thickness influences thermal response patterns. Carmona et al. (2020) also discuss differences in soil moisture due to seasonal variations and specific weather conditions as possible hindrances to efficient thermal data collection. The best images were taken at night during times of heightened thermal emissivity and active thermal inertia (Carmona et al., 2020). This is consistent with the observations of thermal data analysis in the case studies of this thesis. Carmona et al. (2020) emphasize the importance of establishing statistically significant criteria for differentiating, categorizing, and assessing the separability of archaeological features using thermal analysis. This is an idea elaborated on further in the discussion section 6.0 of this thesis regarding quantitative versus qualitative approaches to analysing data.

Waagen et al. (2022) recounts the archaeological investigation of two distinctly different sites using drone-based thermography. The sites of Acquarossa, Lazio, Italy, and Siegerswoude, Friesland, The Netherlands were specifically selected for their high probability of archaeological remains at shallow depths (20 cm - 50 cm DBS). In this study Waagen et al. (2022) used a DJI Zenmuse XT2 gimbal mount thermal camera with a FLIR TAU 2 radiometric sensor. While both sites are geographically different, they have similar soil types. The dense sandy soils are conducive to good thermal conductivity and diffusivity. The most optimal moment for thermographic capture in this study was yet again identified as directly after sunset. Waagen et al. (2022) is explicit about the effects of moisture content on thermal inertia. Between the two sites there is a difference of 8 °C in absolute diurnal heat flux. Since thermal anomalies were identified at both sites, the difference in diurnal heat flux is an indicator that the distance between minimum and maximum temperature values is less important than the sharp sequence of heating up and cooling down that occurs during crepuscularity (twilight). Waagen et al. (2022) makes an intriguing connection between soil moisture content and thermal radiation. Specifically, the moisture in the ground retains lower temperatures during the day while radiation increases the temperature of dryer soils to a relative high level making it traceable on thermograms due to contrast with the moist soil. Therefore, they (Waagen et al. 2022) infer that thermographic applications in archaeology don't pick up the spectral signatures of archaeological features, but instead thermal marks are created by the moisture conditions that appear affected by them.

Finally, a study conducted by Thomas (2017) demonstrates the utility of a relatively low-cost setup for conducting aerial thermographic archaeological investigations. At the time of Thomas' (2017) study DJI had not released a drone that had direct interchangeable operability with gimbal mount camera sensors. Thomas (2017) used the DJI Phantom 2 equipped with a FLIR Vue

Pro (non-radiometric) camera sensor. In this study a total cost of ~ USD \$4,400 was spent to acquire the setup. Overall, the study by Thomas (2017) was successful in attempts to visually assess archaeological features using thermography, however, this assessment is only qualitative and is not on par with output from equipment currently available in the market with comparable costing (~\$5,000 USD) for a technologically superior product (DJI Mavic Pro 3T) boasting greater resolution and battery life capabilities. While the medium-low-cost seems to negate the barrier for implementation of aerial thermography, this study is a telling example of how far aerial thermographic equipment has evolved since 2017 and this is also true for other remote sensing types, especially LiDAR equipment.

While the literature regarding aerial thermography presents as a viable option for archaeological site and feature determination, a deeper review suggests that digital archaeology is still plagued by contemporary issues regarding the appropriate use of quantitative and qualitative data.

Most research involving modern integrated LiDAR systems, particularly the DJI M300 paired with the Zenmuse L1 sensor (as used in this thesis), has focused on evaluating point cloud accuracy and density. Studies by Zhou et al. (2023) and Štroner et al. (2021) have assessed the performance of the DJI Zenmuse L1 by applying accuracy-correction algorithms such as multi-sensor triangulation and systematic shift correction, respectively. Rather than implementing these corrections themselves, both studies analyzed the effectiveness of these algorithms in improving LiDAR accuracy. Zhou et al. (2023) utilized a multi-sensor triangulation-based approach to align and calibrate multi-modal and multi-temporal datasets, ensuring a high degree of correlation between airborne and mobile mapping systems. Štroner et al. (2021) demonstrated that point

clouds processed using DJI Terra software, when corrected with ground control points (GCPs), achieved an RMSE of 20 mm to 50 mm at flight altitudes of 50 m AGL and 70 m AGL.

While these studies indicate improvements in geospatial accuracy, there is no clear consensus on what constitutes high accuracy, as tolerances vary depending on application and industry standards. Additionally, while extensive research focuses on quantitative accuracy improvements, there is comparatively little literature dedicated strictly to data filtering and interpretation algorithms. Štular and Lozić (2020) discuss filtering techniques to separate ground and non-ground points, aiding in the generation of detailed digital feature models (DFMs). Various ground-filtering algorithms exist, but this thesis specifically examines the Cloth Simulation Filter (CSF), which is applied in case studies 3 and 4 and further explored below.

2.4 Research in computer science

There are several key developments to the field of computer science that contribute directly to aerial remote sensing using drones. White (2016) identifies three trends that have created opportunities for archaeologists to generate, process, analyze, visualize, and contextualize data. These trends are commoditization, democratization, and miniaturization and all contribute to the increasingly routine application of supercomputing.

The contributions made by Kokalj et al. (2011) and Kokalj and Somrak (2019) involving computer algorithms and machine learning to model digital mock environments has implications for the subfields of digital and aerial archaeology.

Inevitably, advances in supercomputing, cloud processing, storage and new software options for DEM generation will provide a suite of tools for archaeologists for conducting non-invasive work. Aside from the current lack of independent validation via non-invasive methods,

evolution in computation appears to be a viable new tool for background information gathering, and for survey and reconnaissance missions associated with archaeology.

2.5 Archaeology of landscapes and GIS

LiDAR was initially developed and applied to support environmental monitoring and not specifically for archaeological purposes (Chase et al. 2017). The archaeological utility of LiDAR became evident when applied to studies of Stonehenge in the early 2000s whereby large landscape hill shade models revealed previously undiscovered features (Bewley et al. 2005). Since then, the archaeological application of LiDAR has been used to document sites featuring monumental architecture. More recently, high resolution data has been used to support landscape archaeology studies addressing more subtle features. At issue is how to capture relevant geospatial data of sufficient expanse and resolution to address archaeological problems while not becoming overwhelmed with massive quantities of data. This first problem involves the deployment of technology to efficiently capture geographic data of sufficient areal expanse, accuracy and resolution. The second problem is the development of data storage, processing and analysis capacity able to cope with large remotely sensed datasets. One Canadian example of such effort and landscape archaeology involves UAV deployed photogrammetry to document bison kill sites, specifically involving conventional photogrammetry.

Bison kill sites are widely associated with Great Plains communal hunting, the best known of which are jumps where bison were driven to their death over the edge of steep-edged plateaus or other steep slopes (Hamilton 2019). Other communal entrapment methods involved less dramatic landscape features, including incised stream valleys, or entrapment within sloughs, mires, sand dunes, snow drifts, coulees, or gullies (Speth 2017 in Hamilton 2019). In all of these cases, a key aspect of analysis involves modeling how humans utilized the landscape to guide bison herds

into the trap zone. Traditionally, this has been done through the interpretation of conventional analogue maps. However, with the availability of digital data and GIS capabilities, research has increasingly incorporated computer modeling, such as viewshed analysis, to better understand this behavior (Hamilton 2019). A significant challenge to such an approach lies in the availability of digital data of sufficient detail and resolution. UAV photogrammetry offers a strategy for collecting data of sufficient quality to undertake meaningful analysis, often using a multi-iterative approach.

2.6 Regulatory Issues

This chapter introduces new methods used for non-invasive surveys of archaeological sites, with particular attention on the value of UAVs to enable rapid and cost-effective data collection. Such discussion requires brief context of the Canadian regulatory environment governing mRPAS and their use. While most UAVs are governed by these regulations, because of their weight, mRPAS are not bound by the same regulations as standard-sized drones.

All flight operations in Canada are governed by the *Aeronautics Act* (R.S., 1985, c. A-2) (<https://laws-lois.justice.gc.ca/eng/acts/a-2/>) and overseen by *Transport Canada* via the *Canadian Aviation Regulations* (CARs) (SOR/96-433), see Part IX for Remotely Piloted Aircraft Systems (<https://lois-laws.justice.gc.ca/eng/regulations/SOR-96-433/FullText.html#s-900.01>).

Additionally, *NAV Canada* is responsible for issuing air navigation services, and the safety protocols they employ have been incorporated directly into the CARs.

Following this legislation, different regulations govern operation of drones over 250g take-off weight versus those under 250g take-off weight. Transport Canada specifies that any drone below 250g operating weight excluding the controller (i.e., mRPS) are exempt from the basic and advanced operating classes (<https://tc.canada.ca>). Transport Canada further states that flight of a

micro-drone does not require registration or licensing and thereby operators can fly mRPAS in non-restricted airspace without a Special Flight Operations Certificate (SFOC):

"Pilots of micro drone don't need to register their drone or get a drone pilot certificate to fly them. Pilots of micro drones are not bound by the same requirements as other drones... Micro-drones are considered aircraft under the Aeronautics Act and Canadian Aviation Regulations and are therefore prohibited to enter the following zones without the proper authorizations:

- *Class F Special Use Restricted Airspace*
- *Zones where a NOTAM for Forest Fire Aircraft Operating Restrictions has been emitted*
- *Zones where a 5.1 of the Aeronautics Act restrict the use of airspace to all aircraft has been emitted"*

Transport Canada (<https://tc.canada.ca/en/aviation/drone-safety/learn-rules-you-fly-your-drone/find-your-category-drone-operation>, Date Modified: 2021-02-19)

These regulations permit mRPS pilots to undertake flight operations in airspace not matching these restrictions. These minimal regulations, coupled with recent software development kits (SDKs) produced by companies like Dronelink and Litchi now enable operation using semi-autonomous flight plans capable of supporting mapping operations for photogrammetry. Notably, Ontario provincial heritage legislation does not directly address drone utility for archaeological site prospection, nor is the regulatory framework prepared to address UAV mapping. This leaves the application of drone technologies for non-invasive site survey within a grey area regarding heritage licensing, regulation and policies. The lack of regulatory clarity regarding UAV mapping

for archaeological site prospection likely contributes to the slow pace of policy implementation. Heritage legislation often lags behind technological advancements, as regulatory frameworks tend to be reactive rather than proactive. While drone technology has rapidly evolved to support semi-autonomous mapping and photogrammetry, heritage policies have not yet adapted to explicitly address its use. This creates a grey area, where drones are not explicitly restricted but also not formally recognized as a tool for archaeological research. Additionally, regulatory bodies may prioritize aviation safety and privacy concerns over heritage-specific applications, further delaying the development of clear guidelines for UAV-based site survey.

2.7 Theoretical frameworks and models

The study of human geography has significantly contributed to the development of landscape archaeology (Hill, 2014). The mid-late 20th century fostered the development of post-processual archaeological theory in reaction against the empiricism of the processual movement. This fostered an interest in the concept of subjectivity, and recognition that human representation of geographic space is essentially a cultural construct. Rather than providing an absolute representation of reality, maps and mapmaking are now understood as interpretive and stylistic processes that can contribute to the advancement of landscape studies and archaeology (Fleming, 2006). At issue is whether digital archaeology will follow this trajectory and how that might impact the application of phenomenology to the study of digital archaeology. The issue is whether digital archaeology will follow the same shift toward subjective interpretation as landscape archaeology did with post-processual theory. Traditional archaeology recognized that maps and spatial data are not purely objective but shaped by cultural and human perspectives. Digital archaeology, however, relies heavily on quantifiable, data-driven methods like remote sensing acquisition and GIS, which prioritize empiricism over human experience. The concern is whether this focus on technology

will downplay phenomenology, which emphasizes how people perceive and experience landscapes. This raises questions about whether digital tools will enhance interpretation or limit it to computational models, reducing the role of human perspective in archaeological analysis. While digital and aerial archaeology prioritize quantitative data collection, they do not necessarily eliminate subjective interpretation; rather, they offer new ways to integrate both empirical analysis and human experience. This thesis engages with phenomenology through use of visual assessment as a qualitative tool, recognizing that decision-making in archaeological interpretation is often shaped by experience. The influence of human geography and subjectivity has already expanded studies of human occupation, settlement patterns, and migration, while also incorporating non-conventional knowledge systems, such as oral histories. Digital tools, combined with evolving hardware, software, and diverse informational resources, enhance reconnaissance and investigation by making previously inaccessible features visible. Rather than replacing interpretive approaches, these technologies enable a hybrid methodology, where digital mapping and data analysis are informed by human perception, fostering a more nuanced understanding of archaeological landscapes.

Johnson (2012) argues that the concept of subjectivity of landscapes was born from human geography in the 1970s. Before adopting 'emotional' geography, most geographers viewed space and time from a Cartesian perspective. The progress of landscape studies in archaeology followed the same trajectory as technological advancements in other complex science fields. Specifically, where archaeological data is concerned, post-processual archaeologists of the 1990s became interested in the subjectivity of data itself. Last, Johnson (2012) argued that landscape archaeology followed a political agenda. These theoretical changes in landscape studies and new ways of thinking about geography are essential because they coincide with the development and evolution

of new technologies for digital archaeology. Moreover, the two concepts may be inextricably tied together and reliant upon one another.

The 'Gartner Hype Cycle for Emerging Technologies' (Oosterhoff & Doornberg, 2020) provides a framework for understanding how new innovations, including drones and digital archaeology, become integrated. This envisions a curve that progresses from a steeply inclined slope reflecting initial excitement over a new and promising innovation, followed by a trough reflecting initial disillusionment as unanticipated limits on utility become apparent. This is followed by a more modest upward inclining slope reflecting gradual acceptance as solutions to problems are resolved, followed by widespread adoption (plateau of productivity).

The first stage, the Innovation Trigger, represents the initial conceptualization and early development of a technology. In the case of drones and digital archaeology, this phase began when UAVs first became commercially viable, and researchers started experimenting with their applications for aerial photography, topographic mapping, and site documentation. During this period, the focus was on prototyping and testing, with limited real-world application.

The second stage, the Peak of Inflated Expectations, is characterized by hype, enthusiasm, and sometimes unrealistic expectations about what the technology can achieve. In archaeology, this was evident when UAVs were promoted as a revolutionary tool capable of replacing traditional survey methods entirely. Early adopters explored the potential of LiDAR scanning, multispectral imaging, and photogrammetry, but challenges such as regulatory constraints, high costs, and data processing limitations tempered initial optimism.

The third stage, the Trough of Disillusionment, follows as researchers and practitioners encountered practical limitations and setbacks. For UAV-based archaeological remote sensing, this phase involved recognizing the challenges of drone data integration, the requirement for

specialized expertise in GIS and photogrammetric processing, and limitations in penetrating vegetation or subsurface features. This also reflects skepticism regarding the consistency and accuracy of UAV data compared to traditional terrestrial surveys.

As the technology matures, it will move along the slope of enlightenment and towards the plateau of productivity whereby UAVs are increasingly recognized as a standard tool in digital archaeology rather than a novelty (Oosterhoff & Doornberg, 2020). This will involve widespread and routine use for long-term landscape monitoring, site preservation, change detection, and disaster response archaeology (Perry & Taylor, 2018).

2.8 Digital Models

Digital Elevation Models (DEMs) are raster-based representations of surface relief, capturing variations in elevation, slope, and aspect. These models apply metric values to topographic surfaces and can be manipulated and analyzed within a Geographic Information System (GIS). As virtual, mathematical abstractions of the physical landscape, DEMs offer flexible, iterative frameworks for modeling terrain across a range of spatial and temporal scales. While DEMs are typically raster-based, vector-based elevation models such as Triangulated Irregular Networks (TINs) are also used to represent terrain, particularly in applications requiring precise modeling of complex surface features. These models can be modified by incorporating new variables, can be reclassified to represent diverse data themes, and subjected to statistical analysis to assess the strength of perceived patterns. Such spatially ordered information can be subjected to repeated rounds of exploration in search of new patterns and can be modified to emphasize or exaggerate certain features consistent with the priorities of the creator. An example of this is how CloudCompare enables effective change detection by aligning and comparing multi-temporal point cloud datasets, highlighting structural and landscape changes through color-coding.

This approach is particularly useful for repeated archaeological surveys, allowing researchers to monitor erosion, site disturbances, and environmental impacts over time with high precision (Dawson et al., 2022). The integration of UAVs with various sensors has significantly expanded the ability to collect and analyze spatial data in a user-directed manner. These datasets can be processed, interpreted, and archived using specialized software, with GIS being one of the most common platforms for managing and visualizing such information. This thesis specifically examines how UAV-derived spatial data can enhance archaeological prospection and feature characterization, providing a more efficient and adaptable approach to site analysis and interpretation. This involves documentation of sometimes quite subtle topographic variation that has anthropological meaning, and detection of vegetative patterns that might serve as proxies for the nature and distribution of buried archaeological features.

Digital representations of elevation are categorized as digital surface models (DSM) and digital terrain models (DTM). The key distinction is that DSMs capture the elevation of all surface features, including buildings, trees, and towers, whereas DTMs represent the bare earth, with vegetation and man-made structures removed (Rogers et al., 2020). Both models serve valuable purposes: DSMs are particularly useful for analyzing urban environments, where surface features play a critical role in spatial analysis, while DTMs are more suitable for representing natural or rural landscapes with minimal obstruction.

Rogers et al. (2020) emphasize that advances in Light Detection and Ranging (LiDAR) technology have significantly improved the accuracy and resolution of digital elevation models (DEMs). Additionally, the increasing availability of government-funded LiDAR datasets through online public portals is expected to transform how users access and apply this data. However, while publicly available LiDAR appears to be a cost-effective alternative to UAV-derived DEMs, it

presents certain limitations, primarily due to its comparatively lower resolution, which can affect the accuracy of topographic representation. These trade-offs are further explored in a later chapter, where the feasibility of using publicly available LiDAR data is assessed as an alternative to UAV-based elevation models.

While legacy aerial photography is widely available from public repositories, such pre-digital era photographs may be associated with insufficient metadata for further interpretation (Verhoeven et al., 2012). Legacy aerial photographs are also often collected at high elevation using manned aircraft, exhibit inadequate resolution, may suffer from blurring and parallax distortion, and are seldom georeferenced. While often not offering data quality consistent with modern digital data, they do offer important historical and cultural context. According to Verhoeven (2012), the neglect of interpretative mapping through the ages was probably because of the time-consuming georeferencing process. This process supplies spatial information for users to interpret the context of aerial observations multi-temporally (Verhoeven, 2012).

Computer processing and machine learning can radically change the conduct of archaeological data acquisition, interpretation, and archiving. However, there is a blind spot regarding AI now, that is the lack of discretion in identifying real archaeological sites, versus only the parts that make up an archaeological site. It seems that in general, computer vision is very good at identification, but not so good at interpretation. Interestingly, a potential solution to rectifying this blind spot involves the use of predictive models such as Bayes theory of probabilities. Evolutions in computer processing and machine learning algorithms can identify things previously unrecognized in map products with higher resolution and more detail. In the future, it's likely that this detail could even provide context for intangible heritage assets through regular site mapping, monitoring, and reconstructing environments using virtual reality derived from drone data.

2.9 Overcoming challenges to systems and workflows

There are many obstacles regarding big data management in archaeology. First, to set up a system capable of processing and storing large quantities of data associated with modern digital archaeology, it is critical to have basic proficiency with computer hardware and software. Operational management and task orientation are two general principles needed for creating efficient systems for handling digital data. Selecting the appropriate hardware should be contingent primarily upon the size of database being processed, how this data is processed, data types, and storage capabilities. Modern computers have a central processing unit (CPU) with multiple cores capable of executing computation tasks independently (White, 2016). Computers also have random access memory (RAM) where data is temporarily stored for quick access while executing functions. The capabilities of WebODM used in this thesis are dependent upon large quantities of RAM. Additionally, there have been major advancements in graphics processing units (GPU) mostly due to the popularity of computer and video game industries. DJI Terra is another software that was used for data processing in this thesis that has specific operational requirements contingent upon use of high-capacity NVIDIA graphics cards. Building systems that can handle and store increasingly complex data is reliant upon access to such special hardware. Additionally, to operate a complex network of systems capable of working with this data, being able to transfer and use files for practical applications, a server system is required. Modern cloud capabilities allow for the spin up of virtual servers where large data files can be transferred and stored, but many of the available options currently offered are by large entities like Google and Microsoft. These options can be a challenge to use considering issues of data sovereignty and rights over ownership and control.

2.9.1 Data rights and ownership

Data ownership is a significant challenge facing the advancement of digital archaeology. One major concern is the potential misuse of digital data in site discovery and prospection, particularly for looting. This danger is amplified by the growing availability of archaeological information to the public. At the same time, digital tools have enabled broader access to and engagement with archaeological landscapes, often by individuals or groups outside the discipline. This has led to increased tension over who holds the authority to interpret and manage these landscapes. The growing availability of remotely sensed terrestrial data illuminates issues with data governance in contemporary archaeology and is a concern for both archaeologists and descendant communities (Gupta et al., 2020). OCAP (Ownership, Control, Access, Possession) are a set of guiding principles created to bolster Indigenous rights regarding digital data and digital data management. These principles are especially valuable, as they help alleviate concerns over the misuse, misappropriation, or exploitation of Indigenous data by external parties acting in bad faith. More specifically, there has been considerable debate in the past over the ownership and control of heritage data, and now the same tensions are being thrust upon digital archaeology, where questions of access, representation, and control over digital cultural materials remain unresolved. This debate becomes especially contentious in the context of Indigenous heritage, where ceremonial objects, burial items, and even human remains have historically been designated as the “property of the Crown” under colonial legal frameworks. Such classifications often disregard Indigenous laws, customs, and protocols for stewardship, leading to ongoing disputes over access, control, and the right to interpret or repatriate heritage materials. Typical problems result from the lack of dissemination of findings to descendant communities and the disregard for Indigenous involvement and consultation throughout the archaeological process. Though well

intentioned, OCAP and other similar concepts face problems with the ability to enforce such actions. To some degree, the principles of OCAP may be mandated by a court of law since they are supported by the United Nations Declaration on the Rights of Indigenous People (UNDRIP) and Section 35 of the Canadian Constitution Act. However, there are still many issues with copyright laws that would upend the enforcement of such principles (Gupta, 2016).

Issues in data management give rise to new ethical considerations related to the widespread use of the internet to access and redistribute information. An emerging issue affecting digital archaeology is differentiating between the rights and ownership of physical assets, including artifacts and archaeological sites, versus digital assets. In Canada, the United Nations Declaration on the Rights of Indigenous Peoples UNDRIP articles are not currently enforceable because most Canadian archaeology is governed by provincial heritage laws. In general, provincial rules and regulations pertaining to archaeology do not acknowledge intangible heritage assets such as digital archaeological products. However, the articles of UNDRIP do offer some acknowledgement of intangible heritage culture associated with archaeological sites along with a general progression towards protecting these assets. Bill C-15, which received Royal Assent on June 21, 2021, and requires by law, the federal government to work with Indigenous First Nations to align Canadian legislation with the rights outlined in UNDRIP including self-determination, control over cultural heritage, and free, prior, and informed consent (FPIC). While this movement can be considered a step in the right direction for cultural heritage protections, policy often obscures these actions at the provincial level, limiting descendants and consultants alike from accessing digital data by recognizing it as property of the Crown.

Chapter 3.0 Case Studies

3.1 *Introduction to case studies*

Four case studies are presented in this thesis. All employ RGB investigation methods but in different archaeological and environmental contexts. Two case studies examine thermal and LiDAR data, and one explores the use of multispectral data. In other cases, specific remote sensing methods were applied exclusively to a single study site based on the unique archaeological or environmental context. The rationales underlying selection of different methods of aerial remote sensing at these specific locations involve the following: understanding how remote sensing methods can be employed to non-invasively document fur trade era sites; how different sensors enable the detection of certain kinds of archaeological features; understanding the level of accuracy and precision required for consistently identifying archaeological features; investigating the utility of consumer drones for rapid mapping missions; and understanding the viability of aerial remote sensing as a tool for identifying and locating human burials.

3.2 *Case study 1: Lockport (EaLf-1)*

In late summer 2021, the historic human remains of two individuals were recovered from beneath the Lockport Bridge at St. Andrews Lock and Dam, Manitoba, Canada. Upon completion of the exhumation, the area and its surroundings were surveyed with a DJI Mavic Mini to georeference the burial locations and to better contextualize the finds relative to a nearby archaeological site found within a provincial park located 25-50 meters from the burial location. The Lockport site (EaLf-1) has been subjected to repeated investigations including excavation in 1951 by MacNeish (1958), with other work continuing from the mid 1980s to the early 2000s. It is a culturally rich locality, yielding evidence of pre-contact Indigenous agriculture, including the recovery of bison scapula hoes and other agricultural indicators. The drone flight was a rather



Figure 5. RGB Orthophoto of EaLf-1 captured with a DJI Mavic Mini and processed with WebODM using 'Quick Orthophoto' option.

hurried effort, occurring about one hour before heavy snow blanketed the area marking the beginning of winter and curtailing any further archaeological investigation.

Deployment of a UAV at the Lockport site sought to explore the utility of mRPAS as a tool for rapid archaeological investigation, particularly in environments with complex airspace regulations. It used the DJI Mavic Mini drone to rapidly deploy the aircraft to undertake *ad hoc* map documentation using the least expensive and least feature-laden mRPAS. Use of this small and light-weight drone does not require licensing, and its portability and comparatively low cost make it a viable option for routine early-phase archaeological evaluation. At issue is whether it has sufficient capacity to produce analytically useful output.

RGB photogrammetry relies on visible light reflections and is a fundamental technique for generating digital models using airborne remote sensing. Daakir et al. (2017) offer an early experiment with photogrammetric methods through a user-built UAV system equipped with a Sony RX1 camera and a single-frequency GPS module, integrated via a makeshift triggering device. While single-frequency (L1) GPS is less precise than dual- or triple-frequency systems, the study demonstrates that modifications can significantly enhance accuracy, achieving results of $2 \text{ cm} \pm 0.5 \text{ cm}$ without GCPs. Although the study was originally aimed at improving GPS synchronization for meteorological applications, its findings highlight an important balance between precision and practicality in photogrammetric workflows. While higher-frequency GPS improves accuracy, even basic GPS configurations can provide sufficient precision for rapid reconnaissance mapping, where efficiency and broad coverage take precedence over absolute positional accuracy. The rapid evolution of drone technology has further minimized these

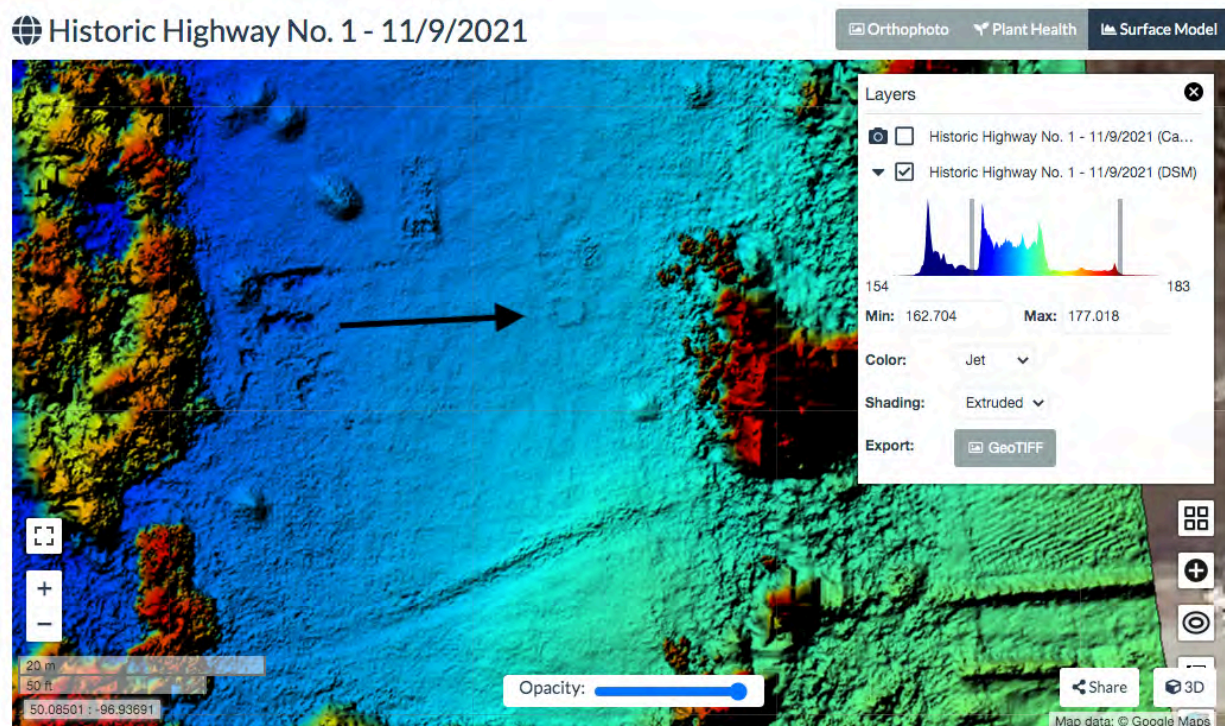


Figure 6. Digital Surface Model (DSM) of EaLf-1 capture with a DJI Mavic Mini.

limitations, as modern consumer drones now integrate high-precision GPS and camera systems into a single streamlined instrument.

At this location, the drone was flown at an altitude of 60 m AGL using a semi-autonomous flight plan (WebODM). Georeferencing relied on the on-board GPS, with no GCPs available to refine the georeferencing after data processing. During the first attempt the drone paused in mid-flight and began to return to the launch point, an automatic safety measure likely triggered by magnetic interference affecting the compass. This might have been caused by the nearby dam and bridge. The second attempt successfully collected the appropriate imagery within a flight of less than 30 minutes. The imagery was processed to generate a georeferenced RGB orthophoto and DEM (*Figures 5, 6, and 7*). The entire data processing workflow took less than four hours, and includes the organization of files, computer start-up and data processing, and preliminary review of the output in search of obvious flaws or errors.

This experiment demonstrates the effectiveness of the rapid deployment of mRPAS tools for aerial reconnaissance of archaeological sites and site features. It also emphasizes the operational value of such mapping flights to address a long-standing mapping deficiency at this important site, allowing future monitoring of site conditions through ‘change detection’ of the property by comparing georeferenced site maps collected in successive years, or considering

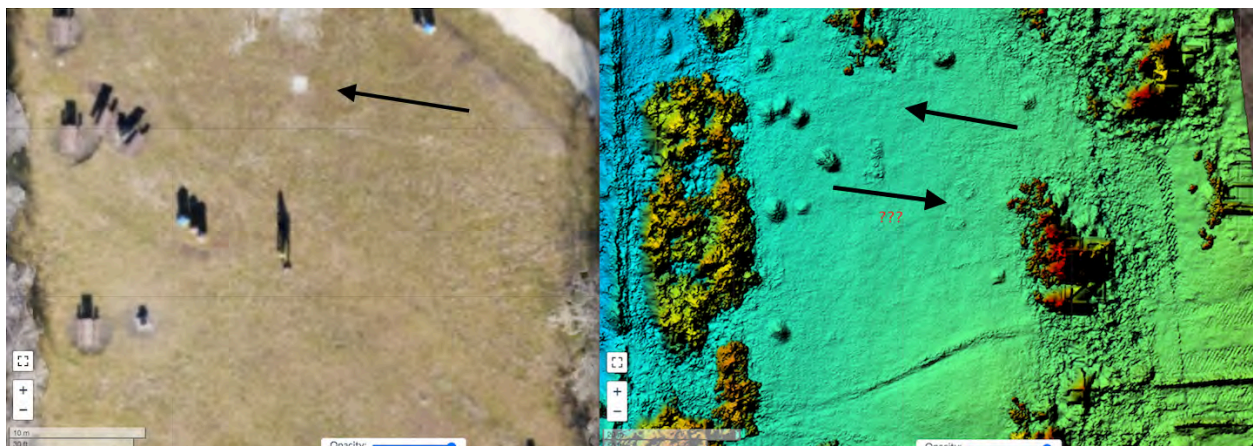


Figure 7. Comparison of the same features at EaLf-1 using RGB in Figure 5 (zoomed in) versus DSM in Figure 6.

development within this urban area. *Figure 7* shows the benefits of rapid mapping for archaeological prospection, demonstrating superior resolution quality over traditional satellite maps. Importantly, there is a good quality of accuracy represented by this map sufficient for general reconnaissance, but this map has some obvious georeferencing issues and warping to the south where the bridge is misaligned (*Figure 5*). The features detailed in *Figure 6* and *Figure 7* demonstrate the capabilities of the Mavic Mini for feature identification during rapid site-mapping missions.

3.3 Case Study 2: Fort Ellice 1 (EcMh-3)

Fort Ellice 1 (1831-1862) was an HBC fur trading post situated on top of an escarpment bank overlooking Beaver Creek, about 4.6 km upstream from its junction with the Assiniboine River in what is the modern-day RM of Ellice Manitoba. The HBC previously occupied the general locality with Beaver Creek Post (1817-1824), and then re-established in the locality with Fort Ellice 1 (FE1) to protect the southern flank of Rupertsland from American fur trade competition

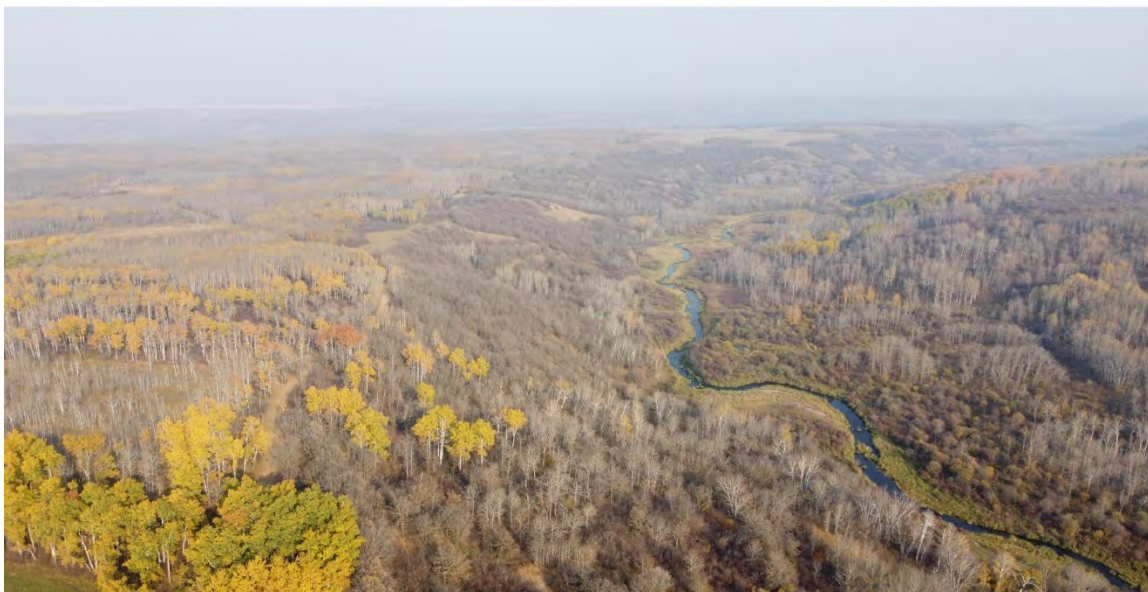


Figure 8. Drone capture of valley near beaver creek from overtop of FE-1 using a DJI Mavic Mini.

(Hamilton 1978:35). Fort Ellice 1 was investigated at the same time as Fort Ellice 2 to support planning of outdoor heritage exhibits at the latter. While no development is anticipated at Fort Ellice 1, we took the opportunity to generate baseline data about this largely unknown site. *Figure 8* reveals the strategic positioning of the Fort Ellice 1 site looking southeast where boat merchants and travelers heading west would inevitably encounter the fort along the Carlton Trail.

Hamilton (2022a) summarizes 19th and early 20th century observations about Fort Ellice 1 and notes a general consistency between the archival sources and his UAV mapping output. This includes observations about the post's location at the top prairie level of the north bank of Beaver Creek (*Figure 8*), with a spring breaking from the valley wall about 100 to 150 yards southwest of the fort location, and with the remnants of the main trail west from FE2 to Fort Qu'Appelle passing a short distance to the north of Fort Ellice 1. The fort was described in 1857 by Captain J. Palliser who recounts buildings composed of wood and surrounded by pickets, likely referencing the palisade format of most of the Hudson Bay trading posts (Palliser, 1863). Palliser also reported that Fort Ellice 1 was once lucrative as a fur trade post, but its principal value at the time of his visit was for trading provisions.

On October 7, 2021, Dr. Scott Hamilton, and fellow professional heritage specialist Mireille Lamontagne, and I visited FE1 site to undertake aerial mapping. Weather conditions were clear with modest wind, thereby optimizing aerial survey and ground truthing. Fort Ellice 1 was comparatively easy to relocate and document because surface indications of the palisade and some of the building features remain visible, but no scaled map and georeferenced map of the site has ever been produced. The investigation sought to remedy this situation.

A GEODE 2 GNSS receiver (Juniper Systems), was used to determine coordinates for ground control points (GCPs) consisting of orange pylons placed over large, galvanized reference

spikes that were labeled FE1-10-15. These points are important as they allowed for refinement of georeferencing of the aerial images. Flights with a Mavic mini and a Mavic 2 pro were conducted to compare the DEM consistency and resolution of the respective output.

Hamilton and Kuncewicz both conducted flights at Fort Ellice 1. Kuncewicz used a Mavic Mini deployed on a rapid mapping mission, while Hamilton used a Mavic 2 Pro using semi-autonomous flight planning software. The biggest difference in these two drones is the resolution capabilities of the RGB camera sensors. The way this affects the final digital product is through GSD, whereby lower resolution cameras will result in a greater GSD value. That is, each pixel element in a photograph will encompass a larger area of ground, resulting in comparatively less clarity and resolution of surface features than cameras generating a smaller GSD. Although the current Transport Canada regulations do not require licensing to operate mRPAS lighter than 250 grams, the regulations were conformed to during the Mavic Mini flight. Kuncewicz used the flight planning software Dronelink to complete flight missions at both FE1 and FE2 successfully generating DEMs and colour orthophotos for both site locations. Hamilton used a Mavic 2 Pro, with semi-autonomous flight planning software to pre-program the mission specifications. The results of the DEM show that on board GPS using a consumer grade drone is enough to identify intra-site features such as pits, middens, cellars, gardens building foundations, and palisade walls, while also illustrating inter-site context of the surrounding area.

The primary goal of the tests at FE1 is to demonstrate the value of consumer and prosumer drones (Mavic Mini and Mavic 2 Pro) as accurate mapping and georeferencing tools for site documentation. This is shown in the results section where the map output using GCPs is compared with the map output without GCP correction of both drones. The DJI Mavic 2 Pro demonstrated greater accuracy than the Mavic Mini when no ground control points (GCPs) were used. However,

when GCP corrections were applied, the Mavic Mini produced a more geospatially accurate and higher-resolution map. This finding highlights the significant impact of GCPs on both horizontal and vertical accuracy, with an increase in GCPs correlating directly with improvements in absolute geospatial precision. Additionally, GCP corrections may enhance the resolution of the output model by refining elevation accuracy along the Z-axis. Interestingly, the clarity and resolution of the Mavic Mini output looks sharper than the resolution of the Mavic 2 Pro output even though the Mavic Mini has a lesser quality 12 MP resolution sensor while the Mavic 2 Pro boasts a 20 MP resolution sensor. Notably, the choice of processing software in this research varied across different experiments. In some cases, the open-source platform WebODM was used, while others employed the photogrammetry software 'Maps Made Easy'. During the planning and organization of case studies, the implications of using different software, particularly regarding variations in map quality and reporting, were not fully considered. In retrospect, even minor differences in algorithms, parameter-setting capabilities, and operability of graphical user interfaces (GUIs) can noticeably influence the styling and overall quality of output products. Maintaining consistency in software choice would have supported greater uniformity across the research outcomes.

3.4 Case Study 3: Fort Ellice 2 (EcMh-10)

The Fort Ellice 2 site (1862-1890) (EcMh-010) is located roughly 5 km northeast of the Fort Ellice 1 post and represents a strategic relocation intended to continue provisioning and trade operations from a more advantageous position atop the Assiniboine River valley (*Figure 9*). This new iteration of the post was established with significantly scaled-down fur trade operations, signaling a shift in both logistical strategy and regional priorities. Fort Ellice 2 became an important administrative centre for HBC operations during its early occupation, but gradually declined in importance after the 1870 sale of Rupert's Land to Canada. In 1872 the HBC

commissioned a legal survey to define its land reserve around the post, as well as a plan for the proposed town of Colville that featured the Fort Ellice 2 compound in a large lot in the southeast corner of the town site. This was in anticipation of large-scale homestead settlement of prairie Canada, and speculation that the Canadian Pacific Railway might pass through the area, rendering the HBC property valuable for settlement and retail commerce. The railway main line eventually passed far to the south, ensuring that Colville was never established, and leaving Fort Ellice 2 comparatively isolated and economically less viable. This led to the gradual decline and



Figure 9. Google Earth screenshot showing the location of FE2 overlooking the Assiniboine River

downsizing of the HBC operations until its 1890 sale to a private merchant. The last of the fort buildings were destroyed in a fire shortly thereafter.

Site documentation was undertaken to precisely relocate the fort compound in anticipation of a planned heritage interpretive trail and outdoor exhibits. The objective was to relocate the fort's archaeological footprint using non-invasive methods to ensure that the proposed heritage interpretation did not inadvertently damage the archaeological deposits. This was done by comparing subtle relief changes observed through aerial remote sensing with a range of map resources available through archival sources. On Wednesday, October 6, 2021, a brief inspection

of the survey area was done by Hamilton and Kuncewicz to identify optimal locations for the GCPs, and to confirm the drone flight area.

These flights were mindful of weather conditions since intense sunshine can cast intense shadows and sun glare that can detrimentally affect photogrammetric processing. Ideal circumstances for photogrammetry include little or no wind and overcast conditions, but sunny conditions can be mitigated using camera filters. Strong wind can also be problematic since it can destabilize the drone in flight and sharply reduces flight time. This can contribute to photographic motion blur and image inaccuracies. On October 7, 2021, Hamilton completed two morning flights at different elevations under ideal weather and lighting conditions. Seven GCPs were set at FE2 throughout the roughly 10-acre site. The GCPs were marked with orange pylons and staked into the ground with a bright orange washer and a label number FE2 1-7. The GNSS coordinate of each GCP was measured using a Juniper Systems GEODE GNS2 receiver. The accuracy of this receiver had been tested previously by Hamilton and yielded a best estimated accuracy of ± 16 cm. Flight 1 was logged at 40 m AGL, while flight 2 took place at 50 m AGL. Both flights were completed using a DJI Mavic 2 Pro drone (*Figure 10*) and a DJI Mavic Mini drone (*Figure 11*).

As the Covid-19 pandemic ended and the Manitoba Provincial Archives reopened, Kuncewicz acquired copies of the field notes and plans from the 1872 HBC survey to establish its land holding around the fort site (HBCA A72/7). This and other archival information proved strategic for integration with the UAV imagery. Hamilton (2021) relocated the fort orientation by projecting the 1872 HBC maps within GIS and comparing the surveyed monuments to the enduring features of the subsequent Dominion Land Survey. These results contribute to data analysis presented later in this thesis (Sub Section 5.6 Summary of the Findings).

The initial thesis task at FE2 is to measure the capabilities of each drone type in their production of DEMs for aiding feature detection. This involved measurement of the variance in resolution and visual feature detection in each model. Professional drone equipment is subsequently introduced at this site to understand the utility of multiple forms of remote sensing for anthropogenic feature identification. In this case study the DEM from the Mavic Mini is



Figure 10. RGB Orthophoto of FE2 captured using a Mavic 2 Pro

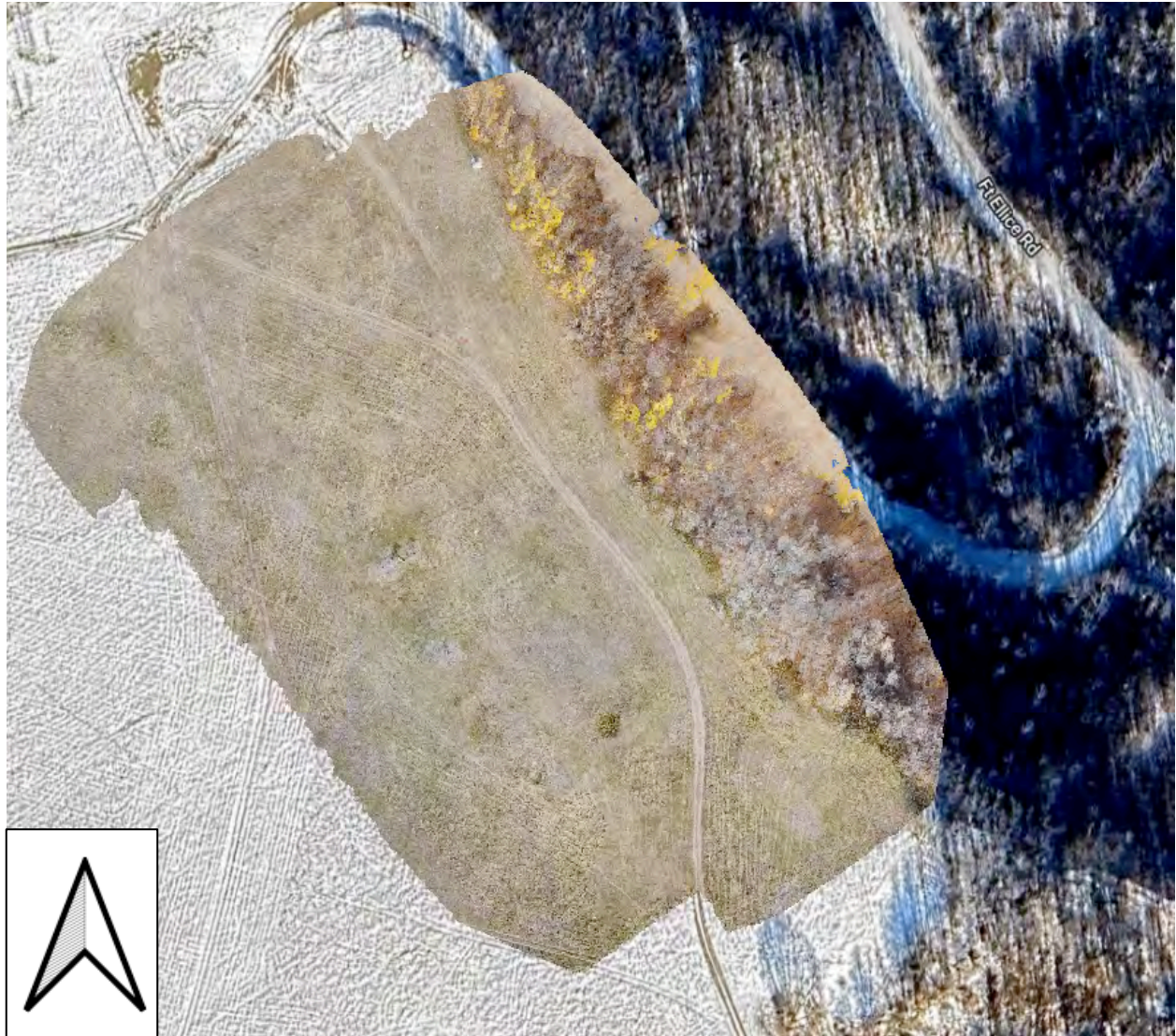


Figure 11. RGB orthophoto of FE2 captured using a DJI Mavic Mini

compared with the DEM from the Mavic 2 Pro, but also DEMs are compared with two other forms of remote sensing to see if certain types of remote sensing offer advantages over others.

3.5 Undisclosed cemetery

Over the course of two field seasons (2022-2023), investigations were conducted at an undisclosed cemetery location that is historically linked to Peguis First Nation. To protect this culturally sensitive site, Kuncewicz and Peguis First Nation agreed to maintain anonymity of the site as a condition for its inclusion as a case study in this thesis. Investigations involved multiple

flights to test diverse sensors and their ability to identify presently unmarked graves. The purposes of this study were twofold: 1) to identify un-used burial plots to allow repatriation and reburial of Indigenous ancestral remains that were accidentally intercepted and recovered through archaeological excavation during construction the previous year; and 2) to supplement existing Peguis First Nation cultural histories through the precise geolocation of now unmarked burials within the unnamed cemetery.

Aerial investigations consisted of two photogrammetric flights, two multispectral flights, three thermal flights, and two LiDAR flights. These flights were conducted at varying altitudes



Figure 12. RGB orthophoto of undisclosed cemetery captured using a DJI Matrice 300 RTK drone equipped with a Zenmuse L1 LiDAR sensor

and at different times of the day dependent upon weather and diurnal cycles. One of the multispectral flights was unsuccessful in producing data using WebODM for unknown reasons,

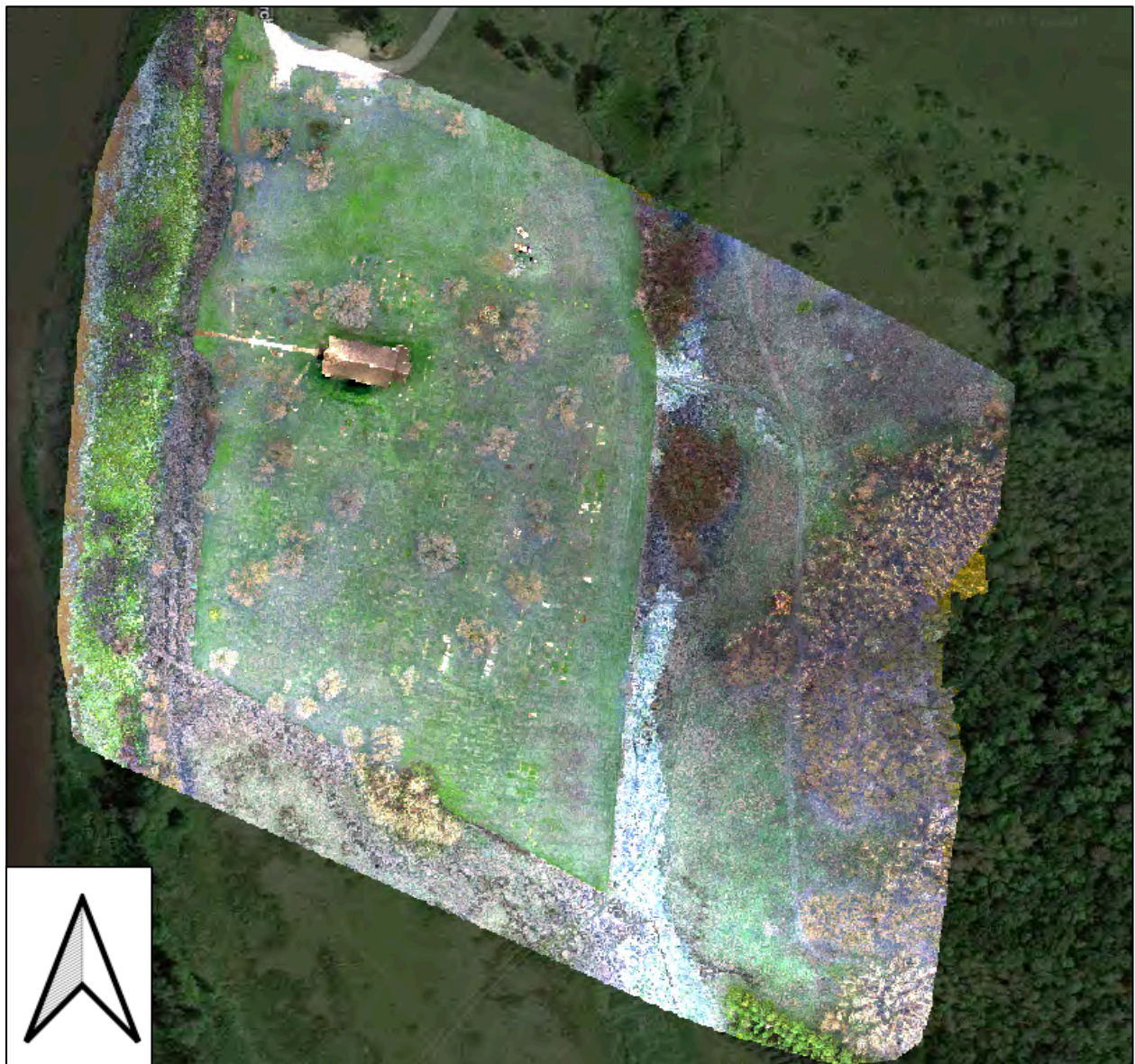


Figure 13. Undisclosed cemetery location showing multispectral orthophoto captured using a DJI M300 RTK drone and a MicaSense RedEdge-MX multispectral camera sensor

while one of the LiDAR flights failed to generate a useful model due to georectification issues caused by accidental disturbance of the DJI D-RTK2 base station during the flight.

WebODM software was used to process the photogrammetry (*Figure 12*) and multispectral datasets (*Figure 13*), while DJI Terra software was used to process the LiDAR and thermal data. Once the raw data was transformed into digital models, they were further processed using QGIS,

Cloud Compare and WebODM interfaces. The most significant of these processes involves transformation of the LiDAR data (or raw .LAS file) after its production in DJI Terra. The raw .LAS file contains all of the data returns within the dense point cloud, including points representing the vegetation canopy. This must be removed via a ground filtering algorithm that classifies points as either "ground" or "non-ground". In this case, the algorithm utilized for ground filtering was accessed through FOSS Cloud Compare. Cloud Compare uses a specific type of filtering algorithm called the cloth simulation filter or CSF (Zhang et al. 2016). The CSF must be adjusted through a multi-iterative process to remove enough extraneous data to approximate the 'bare earth' surface. This version was then used to draw attention to the known and unmarked graves within the cemetery boundary using the VAT algorithm within QGIS. The CSF algorithm requires slight adjustments over multiple parameters, depending on the altitude of the drone during capture. This is because varying altitudes will produce different results for GSD resolution.

Of these investigations, the most promising results come from the thermal and the LiDAR imagery. Datasets were assessed separately by multiple archaeologists working with Peguis Consultation and Special Projects (PCSP) to address potential operator bias in interpretation. Archaeological features believed to be graves within the bounded space of the cemetery were then documented using the QGIS measuring tools to determine length, width, area, orientation of individual graves, and the distance between known graves.

Finally, this case study focuses solely on the use of a professional drone setup using the DJI M300 and undermount optical remote sensors to understand the capabilities of each remote sensing type separately and together as a combination for enhancement and verification. This case study culminates in both the visual assessment of anomalies using professional remote sensing

equipment and also the discreet approach of using qualitative metadata to support anomalies identification and predictions.



Figure 14. LiDAR VAT model of cemetery built using CloudCompare and GIS software

This cemetery investigation demonstrates the potential of aerial remote sensing to detect subtle anomalies in vegetation and terrain that correspond with known and suspected burial features. The effectiveness of these methods in this context is especially significant given the site's similarities to other locations associated with the Indian Residential School System, including comparable burial practices, time periods, geographic region, and cemetery settings. These parallels suggest that the tools and methods tested here may be transferrable to similar investigations elsewhere. Multi-modal aerial remote sensing therefore emerges as a promising, respectful, and non-invasive approach to supporting the search for missing children and unmarked graves. By integrating thermal, multispectral, LiDAR, and high-resolution RGB imagery, this method enhances the detection of subtle ground disturbances, vegetation stress, and spatial patterns that may indicate burial sites, all while minimizing disruption to the land and aligning with the priorities of descendant communities.

Chapter 4.0 Methodology

4.1 Introduction to the methodology

The case studies described in this thesis involved collection, processing, analysis, and interpretation of aerial remote sensing data to assess its utility for archaeological prospection. There is currently no governing legislation or regulation regarding the use of drones in heritage documentation, nor are such methods widely used at an operational level in Canada. The methods employed rely upon previous tests and academic studies relating to the optimal conditions and settings for image acquisition.

4.2 Research design and approach

An implicit goal underlying the research was creation of workflows for collecting, processing, and interpreting digital output. This is a necessary prelude to assessment of the value

of aerial remote sensing to aid archaeological feature identification. Key elements of the research design reflect the technical requirements of drone equipment itself, while the flight parameters vary to ensure appropriate data acquisition to serve unique project objectives. This involved finding a cost-benefit balance between equipment capability, field data collection methods, and time and resources deployed in data processing. It is also dependent upon aerial expanse to be surveyed, the size of anticipated features, ground cover, lighting and weather conditions, and other factors affecting flight altitude and speed, and degree of image overlap. These factors directly affect flight time (and battery management) and have major implications for data processing time and data storage considerations. Clearly, these trials involve consideration of many variables that impact quality of output and efficacy of aerial remote sensing. The initial experiment used the DJI Mavic Mini to test the effectiveness of *ad hoc* mapping missions using dronelink (<https://www.dronelink.com>). This application utilizes a software development kit (SDK) that allows the drone to connect to the application installed on a modern cellular telephone. A flight plan map was created for both FE1 and FE2 using GPS waypoints acquired by the drone immediately prior to undertaking the mapping mission. The GPS accuracy of the DJI Mavic Mini is only 2-5 meters, constraining such missions to those tolerant of such modest geospatial accuracy. This georeferencing accuracy can be enhanced using ground control points (GCP) that have been assigned geographic coordinates using more accurate GNSS receivers. If GCP coordinates are available, they can be uploaded into digital modelling software along with image datasets to refine the georeferencing associated with the photogrammetric output. This process is also known as post-process kinematics or (PPK). Note that for the photogrammetry flights in case studies 2 and 3, ground control points (GCPs) are used to correct the geospatial accuracy of the data and resulting output. The GCPs used for this thesis are orange pylons placed strategically around the area of

investigation with the centermost point being measured by a global navigation satellite system (GNSS) rover.

The Lockport test case did not employ GCPs, while both Fort Ellice test cases utilized GCPs using a GNSS receiver with accuracy capacity between 18 to 30 cm. While not exhibiting sub-cm accuracies associated with survey grade GNSS receivers, this instrument allows significant improvement over that offered by the GPS installed on the Mavic Mini. Conversely, the flights over FE2 and the cemetery location used the RTK method with a DJI RTK2 as the base station.

The primary software program used for image processing for each case study in this thesis is called WebODM (open drone map). WebODM is a FOSS that uses a photogrammetric technique also known as structure-from-motion (SfM). SfM is possible since the X, Y, and Z position of each photograph is known through the GPS integrated into the DJI Mavic Mini. These coordinates form part of the metadata associated with each photograph taken as the drone moves through space during its mapping mission at a standard elevation and degree of overlap with each successive image.

4.3 Data collection, processing, materials, and instruments

Prior to executing data acquisition flight operations, it is important to organize ground control points if georeferencing accuracy beyond the capabilities of the on-board GPS is important to the project outcomes. While experimenting with the data from these case studies, it became clear that there is a point of diminishing returns when considering the number of GCPs used to maximize accuracy of results. The GCPs are laid out at key geographic tie-points and measured using a GNSS receiver capable of gathering sufficiently accurate geocoordinates. This is achieved by triangulating time and distance between the rover, the satellite, and base station(s). The semi-autonomous flight plans help guide the drone using parameters set by the pilot-in-command (PIC).

For much of the data collected in the case studies, flight altitude was set to 60 m AGL and the flight speed was set to the minimum when possible, with image overlap varying with the conditions of each test case locality.

After completion of the semi-autonomous flight, data is first downloaded from the SD card installed on the UAV, with images organized into computer folders and then processed using specialized software. Each folder should be labeled to specify discrete flights to reduce the risk of error when selecting data for processing. Removal of unwanted images from the dataset also ensures that upload to the processing software is not interrupted. Each batch of images is uploaded to webODM via the webODM dashboard command "create new file." The options for data processing in webODM are "Default," "High Resolution," "Fast Orthophoto," "DSM +DTM," "Forest," "Point of Interest," "Buildings," "3D Model", "Volume Analysis," and "Multispectral." Once the model option has been selected, these options can be further customized by editing the tasks. Since webODM runs similarly to a software development kit (SDK), the tasks are edited by "point-and-click" rather than manually entering the code using a computer language. It should be noted that the software makes use of the computer terminal to execute functions by running command lines. This is how the software was initially coded onto the system using a GitHub repository. These software commands connect the computer via localhost and provide encryption via the loopback network interface. This guarantees that the raw primary data sent to the local host does not leave the machine and is, therefore, considered secure against network interception (<https://letsencrypt.org/docs/certificates-for-localhost/>). In addition to the benefit of encryption, webODM also requires the registration of a username and password. Archaeological professionals should remain cautious when using most free open-source software, being mindful of potential security risks involving sensitive data. This is particularly important when such work includes

documentation of Indigenous traditional ecological knowledge (TEK), including sacred sites, toponyms, and other culturally significant data. This is in recognition of cultural sensitivity of such data and mindful of Indigenous data ownership, access and rights. Similar issues of data ownership exist when utilizing data downloaded from government sources where, for example, the Government of Canada retains Crown copyright (Gupta et al., 2020).

4.4 Hardware

The two RPASs used in the October 2021 investigations by Hamilton and Kuncewicz were a DJI Mavic 2 Pro and DJI Mavic Mini rotary UAVs. A total of 5 flights were conducted by Hamilton over three days, while Kuncewicz conducted two flights over two days. Overcast lighting conditions generally yield the best conditions for photogrammetry because it eliminates most shadows deriving from intense sunlight. In feature detection via photogrammetry, unpredictable shadows can often lead to false positives or the deformation of features (Pepe, Fregonese, & Scaioni, 2018). During at least one of the flights, Hamilton attempted to use a filter to reduce the shadowing effects from the sun. Aside from weight, the most significant difference in hardware between the two UAV systems is arguably the camera resolution. The larger and heavier DJI Mavic is better able to resist buffeting by the wind- a major problem for the Mavic mini in even moderate winds. The DJI Mavic Mini camera boasts a 1/2.3" complementary metal oxide semiconductor (CMOS) sensor capable of 12 megapixels (MP), while the DJI Mavic 2 Pro camera has a 1" CMOS sensor capable of 20 MP. While the larger sensor on the DJI Mavic 2 Pro is considered more effective in low-light conditions, the DJI Mavic Mini still does an exceptional job at creating high-resolution orthophotos capable of producing accurate digital models.

The two drones were controlled with two different computerized hardware devices attached to the flight controllers. Hamilton used an iPad with the Mavic 2 Pro, and Kuncewicz used an

iPhone 7 with the Mavic mini. The iPad operated without issue, but Kuncewicz noted that the iPhone 7 occasionally ‘froze’ when attempting to run the dronelink software with the DJI Mavic Mini.

Hamilton supplied the ground control equipment for flights during the October 2021 operations. This process began by establishing GCPS with metal spikes that are visible from the air with numbered small fluorescent orange pylons. The coordinates of these GCP points were then collected using a Juniper Geode GNSS RTK receiver capable of obtaining 18-30 cm accuracy, indicated by the manufacturer's specifications. During data collection care was taken to monitor estimated accuracy of coordinate solution, and to repeat the process if poor satellite geometry results in accuracy estimates greater than 35 cm. These coordinates were recorded and used as part of the post-processing of UAV output to refine its georeferencing accuracy.

The use of GNSS receivers to refine georeferencing accuracy is becoming more common for digital mapping because it is far superior to what is possible when only using the onboard GNSS currently installed in consumer market drones. Modern drones are capable of receiving signals from multiple global satellite systems, such as GPS, GLONASS, Galileo, and BeiDou, but their onboard positioning is still limited in accuracy without correction. The specifications for GNSS accuracy on the DJI Mavic Mini is anywhere from 2-5 meters, while that for the Mavic 2 Pro is rated to within 1-2 metres. These receivers, although technically GNSS-capable, do not apply differential correction, which is required for greater accuracy.

Once positional data is collected, either through a drone-mounted GNSS receiver or more typically via a high-precision external GNSS unit for recording GCPs, mapping output can be refined using differential correction methods such as post-processing kinematic (PPK) or real-time kinematic (RTK). This process uses triangulated signals from satellites, combined with corrections

from a base station or local network, to refine the positional data. PPK refinement was employed in this thesis research and is presented in case study 2 highlighting two very important considerations. First, the model detail (GSD) cannot be directly influenced by PPK, since the resolution is determined by sensor quality and flight altitude. However, PPK can have an indirect effect on GSD during the refinement of positional accuracy along the Z-axis. Specifically, the corrected altitude values introduced by PPK influence the spatial geometry of the reconstructed model, which may subtly alter the distance measurements between pixels. This, in turn, can affect how GSD is expressed within the model and lead to slight distortions. These minor shifts not only influence spatial fidelity but can also enhance relative accuracy by improving internal alignment between features, even though the original image resolution remains unchanged. Second, the application of PPK in combination with GCPs can produce exponential refinement of absolute accuracy. This is demonstrated in case study 2, where images containing multiple GCPs, and

repeated captures of the same GCPs were deliberately selected for cross-georeferencing. After manually identifying the centermost point of each GCP in each image using the webODM GCP

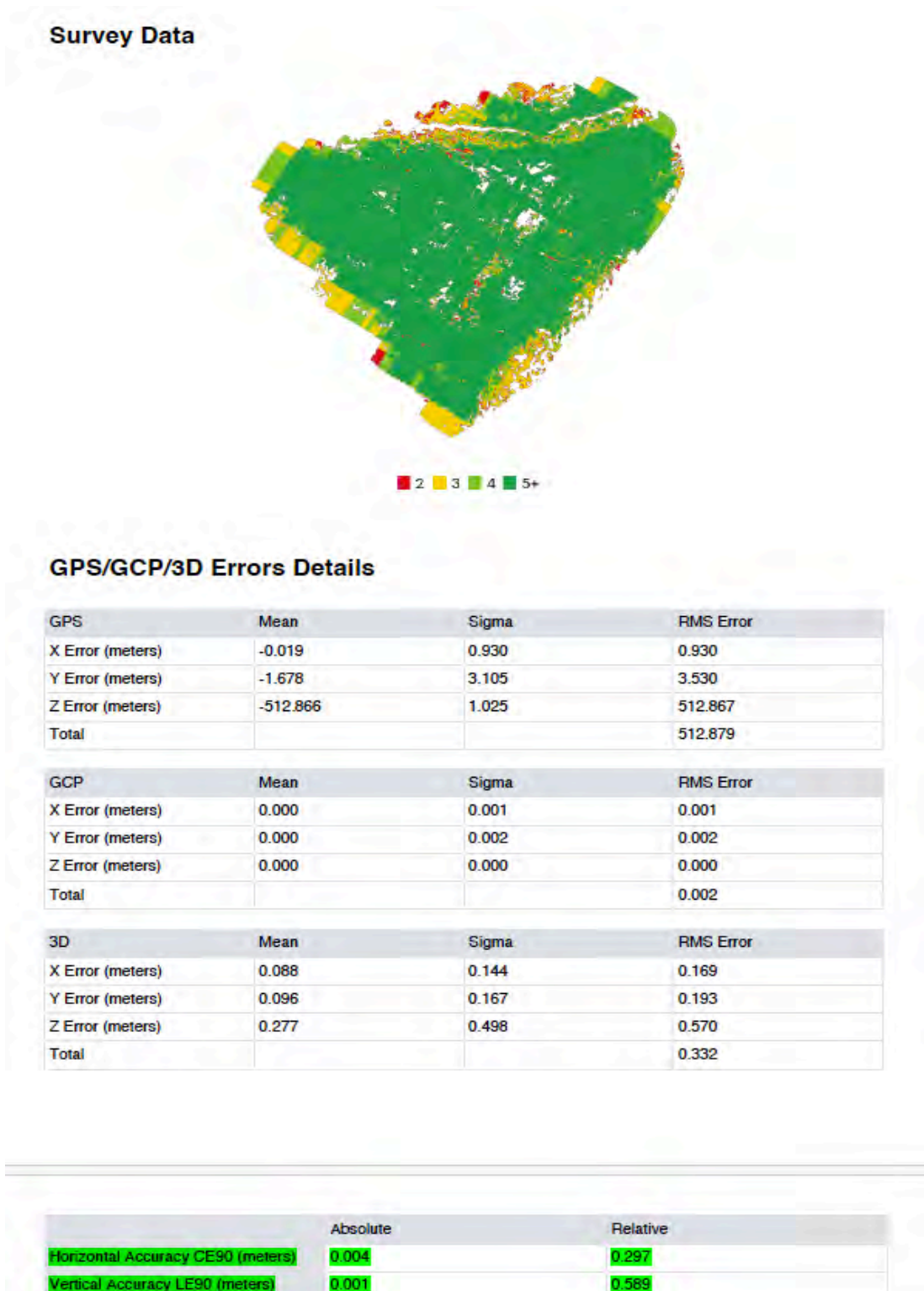


Figure 15. WebODM quality report. Note highlighted accuracies

editor tool, these images were uploaded for PPK model reconstruction using the corrected coordinate values. Approximately 30 GCP-tagged images were used, some of with multiple GCPs, and the results of this experiment produced an impressive 0.004 m horizontal absolute accuracy. However, these values represent the internal alignment of the model to the input GCPs, not true global accuracy. Since the GCPs were collected using a Juniper Geode 2 GNSS rover with a maximum reported positional accuracy of approximately 16 cm at best, the model's true absolute accuracy is limited to that range. Thus, while internal reprojection errors are low (suggesting excellent relative alignment and spatial consistency within the model), the actual global accuracy should be interpreted as ± 16 cm, with the internal variation of ± 4 mm occurring within that broader tolerance. If the same method was applied using peak survey-grade RTK equipment, near absolute accuracies could be attained, but at a considerably higher equipment cost.

In the absence of GCPs, reported absolute accuracy values from WebODM reflect internal consistency relative to uncorrected GNSS metadata, not verified positional truth. To evaluate real-world alignment, orthomosaics were manually compared with georeferenced base layers in QGIS using visual analysis to verify that the models were not largely inconsistent and inaccurate. Discrepancies between visible features (i.e., road edges) and their known mapped positions can be measured, providing an independent empirical check on absolute positional error beyond WebODM's internal estimate.

4.5 Software

Each phase of the archaeological investigation process using aerial tools for archaeology requires software to function: data collection needs flight planning software (DJI flight interface, Dronelink), data processing needs photogrammetry and point cloud software (DJI Terra, WebODM Cloud Compare), data analysis relies on geospatial software and measurement tools

(QGIS, ThermalMetrics, NDVI, NDRE), and interpretation relies on plugin-tools and algorithms for enhanced visualization (CSF, RVT, VAT). These investigative phases and the electronic tools deployed are highlighted below.

While all three UAV systems used to collect data for this thesis can initiate autonomous flights, each uses a different approach. The Mavic Mini can undertake semi-autonomous flights only by using 3rd party software solutions through use of SDK. In contrast, the Mavic 2 Pro and M300 can either communicate with standard software from DJI or by using SDK applications. The Mavic Mini used in case studies 1, 2, and 3 executed flight operations using dronelink software, while the Mavic 2 Pro and the M300 used the DJI interface. Note, the Mavic 2 Pro was also used in conjunction with software called Maps Made Easy for third-party semi-autonomous flight planning and execution. While all flight software types were effective, the DJI interface is designed to be utilized with the DJI smart controller for more in-field applications, while drone link provides a desktop flight planning solution. Unfortunately, there is no SDK offering by dronelink for the M300 at this time.

To keep costs low, free open-source software (webODM) was used for processing RGB photogrammetry and multispectral data. This software was uploaded from a GitHub container (a document containing code). It was entered into the terminal application of a 2012 Macbook Pro with an updated SSD hard drive with 8 GB of RAM. Once the terminal commands are entered, the computer can connect to webODM via a local host and standard web browser. The application webODM could only be interpreted by the computer through a third-party application called Docker. Docker allows the script supplied by GitHub to be interpreted and controlled through the terminal. Due to the age of the computer, and the amount of RAM required to run tasks in webODM, Docker allowed adjustment of memory allocation to suit the mapping tasks, including

image processing, higher resolution elevation models, contour lines, and 3D models. WebODM also offers the ability to upload GCPs in the .csv format so that data can be processed with greater accuracy as demonstrated in case study 2 at the Fort Ellice 1 site.

There are many geographic information system platforms to consider for analysing and presenting geographic data. Most notably, ArcGIS by ESRI is the leading industry standard for desktop systems. This subscription-based commercial software is widely used within corporate and academic environments and is a stable, but expensive option. Since the research for this project focused on evaluating low-cost archaeological prospection strategies, FOSS GIS software (QGIS) provided the backbone for data input and conversion of coordinate systems. QGIS acts as the prime source for data analysis in each of the case studies. It optimizes analysis with tools for reading thermographic data and reflectance values associated with some optical remotely sensed data, as well as dimensional measurement tools for analyzing feature anomalies. Another way QGIS successfully aids digital data analysis is by first converting LAT/LONG geodata to UTM coordinates that are necessary for the projection of points in the webODM system. GIS is important because it can help track and trace ground control points. The export of comma-separated value (CSV) files becomes vital for the quick organization and import of georeferencing data such as LAT/LONG, UTM, and mapping projections such as WGS84 (World Geodetic System).

QGIS is also relevant in data interpretation since it is compatible with plug-ins that are software developed to execute commands without using 'command line' code. This makes it easier and less error-prone for users to interface with maps, models, and digital data for interpretation. For example, a plug-in software kit known as the "relief-visualization toolkit" (RVT) for QGIS can transform DEMs with various relief applications such as slope and lighting filters as seen in case studies 3 and 4 (appendix 5). An algorithm tool featured by the RVT plug-in for QGIS is

called "visualization for archaeological topography" (VAT) and demonstrates how features can be highlighted through algorithmic mimicking of real-world conditions. Tools for interpretation such as the VAT algorithm are considered feature enhancement techniques. Some examples of these functions are slope gradient, hill shading, contouring, openness, and sky-view factor. Appendix 5 illustrates how these filter algorithms can be blended into a VAT model to benefit archaeology. Minor topographic changes can indicate otherwise unidentified features using common aerial orthophotography. This method known as VAT was used in case studies 3 and 4 to demonstrate the effectiveness of this tool for archaeological feature identification including subsurface features such as walls, pits, and burials (see *Figure 14*).

Ultimately, each step in the workflow of digital model generation is reliant upon the former. Since new developments in GIS and image recognition software can aid archaeological observation, the quality of the analysis, interpretation, and processing rely upon the quality of the data collection.

4.6 Sampling strategies

The sampling strategy for quick aerial reconnaissance at the Lockport east site in case study 1 was deployed after adjusting the input parameters for optimization of data collection after experiments at Fort Ellice. On November 9, 2021, a rapid-mapping mission over Lockport east (EaLf-1) was designed with the following input parameters: 60 m over 1.3 ha with 90% forward overlap and 80% side overlap at a max speed of 6 km/hr. This resulted in a total flight time of 20 minutes, 19 seconds, while collecting 253 images. This was sufficient for the photogrammetric process using webODM that took only approximately 30 min. to render a quick orthophoto and DEM. Kuncewicz analyzed the data over approximately 3 hours of the same evening. This demonstrates that it is possible to execute a rapid-mapping mission for aerial reconnaissance in

approximately 4 hours. This could permit next-day ‘ground truthing’ of map output, representing a sharp efficiency improvement over traditional processes of map production and validation.

On October 7, 2021, two test flights were conducted at Fort Ellice 1 with the DJI Mavic Mini mRPAS. This sought to understand the ideal flight settings for maximizing quality and efficiency of image acquisition. This approach required a balance between field time requirements and map output detail. The first test flight was designated the alphanumeric name FE1 A (for Fort Ellice 1 flight A) and the second flight was named FE1 B. At the time of these test flights, the user had not used dronelink; and was unfamiliar with the requirements of the software. The first goal was to understand software operation for both rapid-mapping potential and on-the-fly adjustments. The input parameters for FE1 A were approximately 40 m altitude over 0.4 ha with 80% forward overlap and 70% side overlap at a max speed of 29 km/h. This speed was much too fast to capture sharply focused images unaffected by motion blur. The mapping mission only took 2 minutes, 13 seconds, and generated only 34 images. This was insufficient to produce a quality photogrammetric product. To reap the benefit of terrain visualization filters, a GSD equal to or better than the expressed relief is considered optimal because of the variation between single pixels. For example, if a user wants to represent changes in the relief change of less than 1 cm, then 1 cm GSD or less is optimal. Similarly, the input parameters for flight FE1 B were 50 m altitude over the same area and with the same overlap of FE1 A, but with a max flight speed of 5 km/hr. While the reduction in flight speed eliminated motion blur, the increase in altitude over the same area resulted in fewer images (20) and increased total time duration of flight to 3 minutes, 30 seconds, still rendering it insufficient to produce a useful photogrammetric model.

Although the data amassed in both trial flights FE1 A and FE1 B, technically could have been enough to render digital models, the required flight parameters proved less than optimal either

due to flight times exceeding battery capacity or generating insufficient photogrammetric detail. For example, FE1 A would have generated a GSD of 1.37 cm/px, but the estimated flight duration would have exceeded the three-battery limit of the UAV used for this experiment. The same type of error occurred with flight test FE1 B. The decision was made to shift the flight path from a grid (criss-cross) pattern to a linear (lawnmower) type pattern. However, this resulted in too few images per flight with less-than-optimal image overlap. These trials demonstrate some limitations of associated with consumer-grade hardware and free open-source software. In contrast, the flight planning software used by Hamilton with the DJI Mavic 2 pro (a subscription-based application with more capacity) did not face the same kinds of issues. This is mostly because most flight planning software, including the ones used in this research, are optimized for useability and will generally notify the user when input parameters will not be sufficient for data capture for photogrammetry.

After deliberating over the problems encountered during the October 7, 2021 test flights, the first full flight of Fort Ellice 2 (FE2 A) was conducted on the morning of October 8, 2021, using the adapted flight plans from FE1 A and FE1 B. The following are the input parameters used for flight FE2: altitude (50 m), overlap (80% front, 70% side), flight speed (5.0 km/h), pattern type (grid), gimbal pitch (-90 degrees, nadir), minimum capture interval (2.0 sec.). These parameters resulted in a flight time of 31 minutes, 13 seconds, and generated 184 images to encompass an area of 1.9 ha.

In the afternoon on October 8, 2021, Kuncewicz, Hamilton, and LaMontagne returned to the Fort Ellice 1 site to execute flight FE1 C with the following parameters: altitude (60 m), overlap (90% front, 80% side), flight speed (5.0 km/h), pattern type (grid), gimbal pitch (-90 degrees, nadir) minimum capture interval (2.0 sec.). Note that slight differences in altitude and image

overlap are evident between flights FE2 A and FE1 C. This is deliberate to assess the differences in output after data processing, and which flight parameters are most important to improve the overall quality of the DEM.

The strategies for sampling data from other remote sensors (thermal, multispectral, and LiDAR) are more complex than the photogrammetric sampling that took place at the Lockport and Fort Ellice sites, and these other remote sensing types require more deliberate planning and preconceived strategy in their deployment. While these other methods still rely on core input parameters like those used in photogrammetry such as flight speed, altitude, and image overlap, these parameters must be carefully adapted to suit the specific requirements of each remote sensing method and the environmental context of the site. For example, LiDAR data quality is dependent on the frequency of laser pulses and point cloud density, which in turn are influenced by flight speed, altitude, camera angle, and flight path. Additional features such as terrain-following can be used to maintain consistent point spacing and Z-axis accuracy over variable topography. Thermal and multispectral imaging, on the other hand, demand slower flight speeds due to shutter speed and sensor specifications required to capture distinct spectral bands. These elements must be understood and optimized in advance to ensure the success of a given survey. For example, methods for multispectral data collection at the cemetery location in case study 4 were optimized with parameters that account for reflectance calibration and bit-depth of image collection. These parameters are input using the MicaSense website instead of directly on the DJI controller. Additionally, when using the MicaSense Rededge-MX sensor and the DJI H20T sensor, the focal length and aperture make a difference regarding the sensitivity to the intensity of light permitted by the camera sensor. The DJI Zenmuse L1 LiDAR sensor is even more complicated to calibrate in that both the IMU needs to warm up pre-flight and needs to re-calibrate with every pass of the

drone flight path, but also factors such as point cloud density, and pulse-frequency will impact the final product.

4.7 Data analysis methods and techniques

The test at east Lockport focused on rapid mapping for archaeological reconnaissance, where the priority was not on high-resolution detail but rather on establishing general site orientation and identifying the presence or absence of heritage features of interest. RGB photogrammetry was used as the primary remote sensing technique to enable visual interpretation. The objective was to generate a basic model in WebODM, export it as a GeoTIFF file, and import it into QGIS to facilitate site-level interpretation.

Tests at Fort Ellice 1 and 2 employed two different consumer-grade drone models, both using semi-autonomous flight planning software. Each drone contains components to manage the flight and collect important metadata. This includes built-in compasses, a radio transmitter and receiver, collision avoidance sensors, GPS and IMU. The results were then post-corrected using geodata from a roving RTK unit to generate coordinates from each GCP. In this experiment, the platform was the DJI Mavic Mini with a 12 MP resolution CMOS camera sensor. DJI specifies the operational Hovering Accuracy Range as Vertical: ± 0.1 m (with Vision Positioning), ± 0.5 m (with GPS Positioning), Horizontal: ± 0.3 m (with Vision Positioning), ± 1.5 m (with GPS Positioning).

At issue is what degree of accuracy is necessary to appropriately record and analyze archaeological sites and features. In archaeology, precision in geospatial data enhances the ability to document cultural resources, but the required level of accuracy can vary depending on the purpose of the project. For preliminary reconnaissance and survey, lower-resolution mapping may

be sufficient. However, in projects requiring excavation, determination of mitigation or site avoidance, or in several academic research applications, higher accuracy becomes essential.

This distinction framed the experimental design in case study 2 at Fort Ellice 1. Here, the goal was to evaluate how the number of GCPs, combined with PPK correction in WebODM, could improve absolute model accuracy. The experiment compared a photogrammetric model using multiple GCPs against one relying solely on the onboard GNSS from both the DJI Mavic Mini and the Mavic 2 Pro.

At Fort Ellice 2 (case study 3), a different approach was used. This site tested the comparative quality of DEMs generated by the Mavic Mini versus the Mavic 2 Pro. In addition to photogrammetry, thermal and LiDAR datasets were collected using a professional grade DJI Matrice 300 to evaluate the benefits of integrating multiple sources of remotely sensed data. These methods offered a broader perspective on how different sensor types contribute to archaeological interpretation.

Methods at the cemetery location in case study 4 consist of a variety of visual and statistical factors drawn from and combined over the various optical remote sensing techniques outlined in this thesis to maximize interpretive value. The Infrared and Near-infrared spectra of the Micasense Rededge-MX were calibrated using a special calibration panel coupled with the camera hardware and triggering of the camera was set using a timed-interval. This information was collected to produce NDVI and NDRE models for analyzing plant health, growth and vigour, and to apply these data to detect archaeological features. The DJI H20T thermal sensor was deployed at low altitude (45) m at dusk when entropy is higher, and with the maximum degree of overlap (90% forward and 90% side) to compensate for the lower optical resolution of the FLIR sensor compared to the RGB cameras used in all the case studies. The lower altitude coupled with

slower flight speed serve to improve the resolution of the final thermographic model. Last, the DJI Zenmuse L1 was deployed over the cemetery location with the highest pulse-frequency possible and using triple return at 45 m altitude in order to maximize the penetration possible through tree canopy, scrub brush, and tall grasses. These settings allowed for the camera to collect laser pulse returns with point cloud density of $\sim 17,000$ points per meter squared. When used with ground filtering software algorithm CSF via Cloud Compare and with the VAT model presented earlier in this thesis, the resulting model drastically improves archaeological visualization and enhanced interpretation.

4.7.1 Ground Sampling Distance

Ground sampling distance (GSD) measures the linear distance between each sample taken of the ground. With raster data, this is most readily imagined as the distance between the centres of adjacent pixels, each representing discrete data points. GSD relies on camera resolution capabilities and the distance between the camera and the ground (altitude) during the time of capture. Since GSD is an empirical property of the dataset, determined by camera resolution and flight altitude, it remains consistent within the digital model. However, how the data is visualized depends on the resolution of the display medium. For example, viewing the same model on a high-resolution monitor allows for greater perceptual clarity than on a lower-resolution screen, even though the GSD itself has not changed. Additionally, while zooming in or out does not alter the model's inherent resolution, it does impact how users interpret spatial details, making display quality and scale important factors in analytical contexts. While GSD is a measurement calculated during photogrammetric reconstruction, this metric can also be recorded, tested, and verified manually if relative accuracies are good. Since georeferenced files like TIFFs contain X, Y, and Z EXIF metadata, it is possible to draw linear measurements between pixels derived from a Cartesian

Coordinate Reference System (CRS) such as WGS84 in GIS. By identifying two known points in a CRS using the centre of each pixel for reference, it is possible to manually calculate the linear distance between them, thereby determining the GSD with a high degree of accuracy. This approach can be especially useful when software outputs do not provide GSD directly or when validating the results of quality reports from WebODM. Manual measurement of GSD in GIS also offers a valuable solution when analyzing multi-modal data that may not align perfectly due to collection inconsistencies or sensor limitations. In such cases, measuring pixel spacing directly within each dataset can assist in identifying and correcting variance between models, supporting improved interpretation, validation, and feature matching. This method provides an added layer of quality control, ensuring that spatial inconsistencies do not propagate through to final outputs or hinder interpretations.

GSD is particularly important when studying DEMs and point clouds, as these digital products are designed to highlight subtle variations in slope, terrain, and ground surface morphology. The embedded height metadata within each pixel or point is used in the calculation of derivative products such as slope maps, hillshades, openness models, and other visualization-enhancement algorithms in QGIS and similar platforms. Some of these are shading-based, relying on simulated light sources, while others emphasize geometric relationships or topographic exposure. In addition, software like CloudCompare allows users to manually define or adjust the grid size to control the coarseness or fineness of the model, depending on the investigative needs and the scale of features being targeted. This user-defined manipulation supports better interpretation across a range of spatial scales, especially when working with VAT models or comparing multi-modal datasets.

4.8 Validity and reliability of the study

A central theme underlying debates about the utility of aerial remote sensing for archaeology revolve around issues of data scale and resolution. This simultaneously considers the spatial expanse to be investigated coupled with the data resolution required to detect and characterize archaeological features that are often quite subtle and localized. With this in mind, workflow design for data collection must consider the following: A) what are the desired outcomes? and B) of all the possible outcomes, what is the scale needed to delimit such information. Using a basic ecological example, imagine that a large river system is the subject of a digital remote sensing investigation. In this example, there can be a multitude of inquiries about the data, but let's examine two straightforward research questions. First, what are the area dimensions and the location of the river in reference to other ecological landscape features; and second, what is the direction of water flow within the river.

Addressing both of these questions using digital data requires information at sufficient resolution to enable interpretation. Landscape features such as rivers can be of variable size. To represent this accurately, image data must be of sufficiently high resolution to document this variability accurately. This would require flight parameters that are sufficiently low elevation to capture the necessary detail. On the other hand, if the priority is to document the geospatial position of the river relative to other landscape features, a much smaller scale map product might serve that encompasses both the river and its surroundings. Since lower image resolution is required, the flight parameters can be structured around documentation of a more expansive area from a higher elevation. These two very different objectives can be realized by varying flight elevation, speed and degree of image overlap when doing flight mission planning. Addressing the direction of flow of the river might require different input parameters. Determining the water flow direction using

still images is a complicated process within structure-from-motion (SfM) software. While the details of such analysis are not relevant here, determination of stream flow would require higher resolution imagery that derives from lower elevation flights or higher resolution sensors (or both). Such information might also be generated through analysis of lower resolution photogrammetric output by documenting the dendritic nature of tributaries, or by considering the detail of the stream gradient or evaluation of the surrounding terrestrial surface elevation model. What is important in both examples is understanding the necessary image scale required to address the research question. Another important flight planning consideration is that higher resolution image processing requires greater computing power and larger storage digital capacity.

These concepts are also critical when addressing archaeological remote sensing objectives. This might involve planning to collect data that is appropriate for intra-site versus inter-site documentation. Documenting the relationship of the archaeological site within its broader landscape context might be addressed with lower resolution data over a more expansive area (high elevation flights that are more efficient in terms of flight time, battery endurance and data volume). Intra-site documentation of small and subtle characteristics will require much higher resolution data collected with low elevation flights at slower speed and higher image overlap (with associated cost in terms of longer flight times, more care in battery management, and larger data processing and storage demands).

In case study 2 and 3 at Fort Ellice, this is akin to saying what inter-site characteristics for documenting 19th century site selection criteria by ensuring documentation of the fort compound relative to the surrounding ‘culturally-mediated’ landscapes. This might be addressed with comparatively coarse resolution public domain satellite imagery or coarse-resolution LiDAR imagery, or orthoimagery deriving from high-altitude manned aircraft. While very useful, such

data may be insufficient to detect intra-site details important for archaeological prospection and interpretation. This might include patterned variation in vegetation, micro-topographic detail, or extant structural remnants. Such detailed intra-site imagery also become valuable for generating derived attributes (contour lines), or as a backdrop upon which to include thematic data such as artifact scatterplots, or site features observed through conventional excavations such as walls, foundations, hearths, grave shafts, and other features. Most archaeology has traditionally been concerned with documenting and interpreting intra-site details, and deploying UAVs can appropriately support such analyses. That said, with rapid technological improvement, UAVs with sufficient capacity and flight endurance are now also capable of supporting inter-site analyses.

Remote sensing technologies can help us understand environmental phenomena that are beyond conventional sensory capacity. Humans have comparatively narrow visual sensory capacity that might be overcome with sensors that detect beyond the RGB spectra. This includes multispectral sensors capable of detecting light wavelengths from multiple bands (measured in nanometers) beyond human capabilities. The multispectral camera used in case study 4 demonstrates that it is possible to use Red, Near-infrared, and Red-edge bands to identify changes in plant health and vigor via nitrogen uptake. There have been several studies previously conducted on the effects of nitrogen on plants and plant health via biological decomposition and the release of Nitrogen back into the surrounding soils. Theoretically, if mapped at a sufficient large scale and high resolution, this might be visible and enable non-invasive detection of human graves. These possibilities are explored more fully with Case Study 4.

Similar possibilities exist when considering thermography as a tool to support archaeological aerial remote sensing. In this circumstance, solar radiation might be differentially absorbed by or reflected from the ground surface depending upon the physical character of the

sediment, its water content, or its degree of vegetation cover. Some of this variability may derive from anthropogenic sources. By mapping this patterned variation of heating/cooling using thermal sensors might also offer considerable potential for archaeological prospection. Again, the efficacy of such methods is dependent upon local conditions and by careful flight planning that considers issues of data scale and resolution. These issues are addressed in Case Study 3 and 4.

Approaches to archaeological site interpretation using remote sensing will soon undergo explosive development as innovations in AI and machine learning algorithms become more fully developed and undergo technology transfer. Computers are now capable of having human-like sensory experiences such as the concept of computer vision. One such example of this is the Scale-Invariant-Feature-Detection (SIFT) algorithm that is the basis of photogrammetry. This is a critical factor for digital archaeological applications since the SIFT algorithm, and others like it, provide evidence for the detection of anomalous features in minor ground undulations. Taking this notion a step further, computers that are capable of vision are theoretically more inclined to delineate features that are natural from features that are human made more efficiently than human archaeologists.

Chapter 5.0 Results

5.1 Introduction to the results

The results from the case study experiments are presented here. This includes both empirical data validated by statistical analysis, and more subjective qualitative data evaluated through visual assessment. The analyses of each case study demonstrated that several evaluative approaches might be used in archaeological prospection using aerial remote sensing. For example, in case study 4 both qualitative and quantitative information suggested the identification and location of anomalies that might be unmarked graves. Quantitative evaluation of multispectral data involved examination of output coinciding with marked graves compared to that associated with possible unmarked graves. The former acted as ‘controls’ to document distinctive ‘signatures’ associated with the marked graves that was then used to evaluate the suspected unmarked graves. Data analysis also sought to refine appropriate levels of relative and absolute georeferencing accuracy, optimal data resolution and how to balance database ‘size’ with computer requirements to process, analyze and store it. A recurring theme emerging from the analysis was the value of demonstrating replicability of spatial ‘patterns’ that might appear in output from various sensors deployed in different flight configurations. While the origin and function of these patterns might not be immediately clear, their consistent appearance aided cross-validation of air remote sensing as a prospection tool and served to identify candidate areas warranting more comprehensive ‘ground truthing’.

5.2 Examining workflow and making analytic inferences

The experiments were conducted to evaluate the archaeological utility of different UAV and sensor types to detect archaeological features at diverse sites. This involves testing both equipment technical capacity, and the effect of flight planning and data processing parameters on

the eventual output. Test cases 1 and 2 focused on generating and evaluating photogrammetric output collected using comparatively inexpensive consumer drones. This considered RGB camera capacity, and the utility of 3rd party semi-autonomous flight planning and photogrammetry software. This also assessed the relative accuracy and image resolution important for documenting archaeological environments. These evaluations focused on georeferenced orthophotographs and elevation models, and the analytic value of such digital products for archaeological remote sensing.

It became clear that simple visual evaluation of output was not particularly robust for systematic analysis over large sites or where an abundance of features are apparent. This was particularly the case when considering output from sensors that detect phenomena beyond the visible light spectrum. In these cases, strategies were sought to identify quantitative means of evaluating output. Each experiment yielded analytically useful results for identifying anomalies that are arithmetically distinctive from surrounding landscape. For multispectral analysis, NDVI and NDRE formulae were calculated and used to detect possible human graves based on relative plant vigor, perhaps reflecting localized abundance of biological breakdown products such as Nitrogen. For thermographic analysis, mean temperature values of the resulting model were used to understand the variance between anomalies and surrounding soil conditions. When considering the LiDAR data, local relief was assessed by considering the mean, median, mode, and RMSE of area dimensions of ground anomalies.

5.3 Qualitative data analysis, themes, and visualization

Two important themes emerge from these data-driven experiments: 1) natural environmental conditions (localized variability in soil, microclimate, topography and vegetation) complicate interpretation and the ability to detect anomalies of possible anthropogenic origin; and 2) despite these potential disruptions, under the right conditions remote sensing techniques also

detect anthropogenic features. The challenge is development of robust strategies to differentiate natural from anthropogenic features. It is also clear that localized anomalies detected using one technique often appear in output from others. This replicability across methods helps address data inconsistencies and focus attention upon specific anomalies or unconformities for further analysis. Thermographic results showed the greatest sensitivity to localized environmental fluctuations due to complex interactions between surface conditions, weather patterns, ambient temperature, and diurnal cycles. All examples of thermographic data in this thesis were collected during the fall season and some in different years. This proved effective since during the late summer and early fall there are generally more dramatic contrasts in solar heating between day and night. As the ground is heated throughout the day, the earth tends to absorb and retain heat in ways reflecting the local ground conditions. These patterns of heat retention persist until the ambient temperature begins to cool, whereupon the accumulated heat begins to dissipate into the cooling air. This usually begins around dusk when the ambient temperature changes and the emissivity of the soils enables heat exchange into the air. This process of heat dispersal is not uniform and some surfaces are more vulnerable to heat accumulation, meaning they will have more heat to disperse into the cooling evening air. Other surfaces either reflected more solar radiation during the day, or were insulated from it, and therefore will release comparatively less heat into the air. This patterned variability in heat dispersal into the evening air might reflect a range of underlying natural or cultural circumstances affecting the ground surface. The importance of collection of

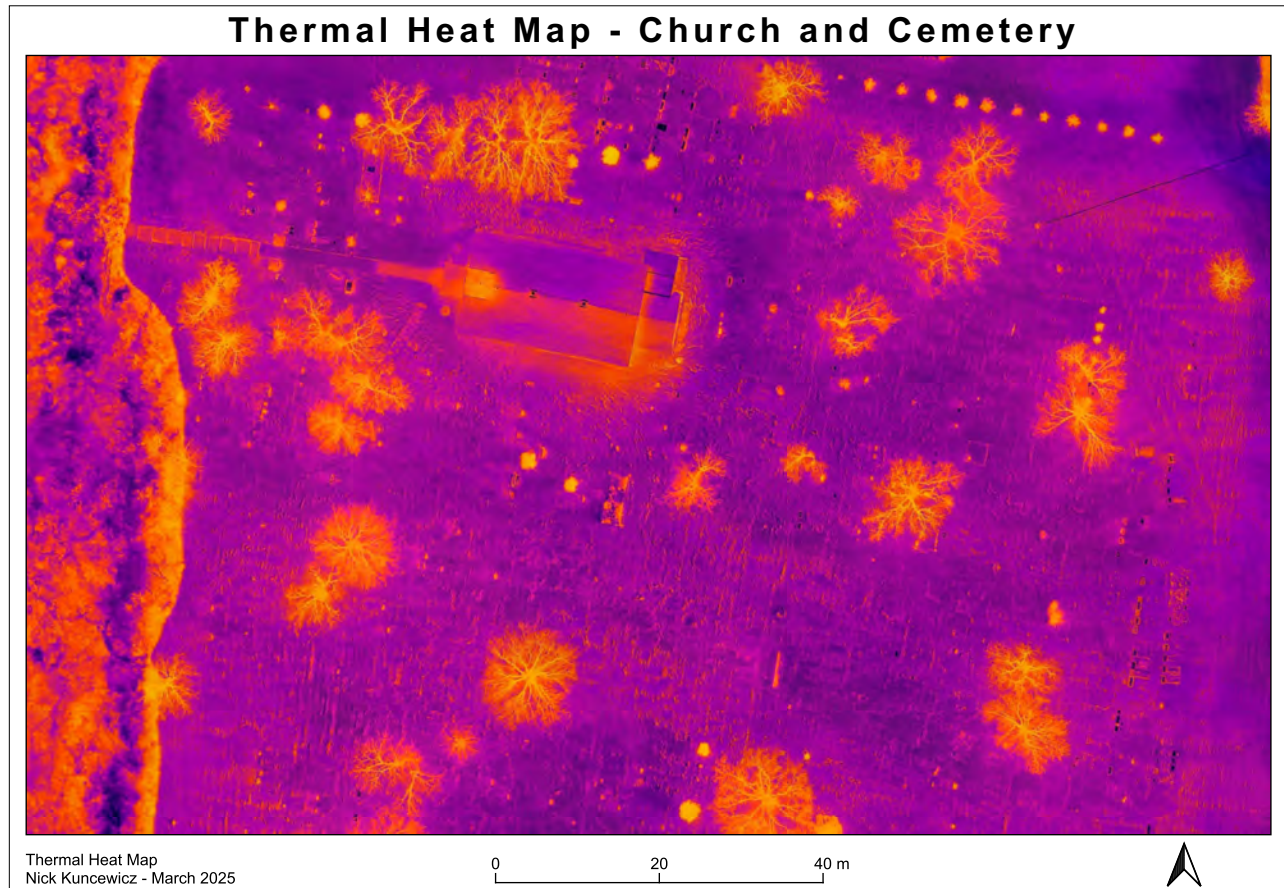


Figure 16. Thermal heatmap of cemetery capture with a DJI M300 RTK drone equipped with a DJI H20T thermal camera sensor

thermographic data at dusk is evident in *Figure 16*. This contrasts with efforts at thermographic data collection during the early afternoon on a hot summer day near FE2. This yielded poor results since there was insufficient thermal contrast between the ground temperature and the ambient air temperature.

While all remote sensing methods in this study produced relevant information, their outputs varied in terms of data richness and analytical robusticity. Thermographic sensing enabled visualization of temperature variations and environmental changes, making it effective for pattern recognition but less suited for statistical modeling. In contrast, photogrammetry and LiDAR generated DEM and VAT models that yielded significantly more quantitative metadata to support statistical analysis, including elevation, point density, and terrain modeling. Multispectral imaging,

however, offered a unique advantage by utilizing multiple spectral bands to generate derived indices such as NDVI and NDRE, allowing for deeper insights into vegetation health, soil conditions, and potential subsurface features. The ability of multispectral approaches to convert reflectance data into measurable indices highlights their potential for predictive modeling and computational analysis, further expanding the scope of archaeological prospection.

5.4 Data interpretation

Case Study 1 (experiments in rapid mapping missions at EaLf-1) did yield valuable insight into the efficacy of RGB orthophotos and DEMs as tools for rapid reconnaissance missions. In this context, detail and georeferencing accuracy were sacrificed in favour of expeditious data collection, demonstrating that quick reconnaissance workflows can still aid archaeological investigators by facilitating site visualization, refinement of feature orientation and spatial distribution. The ability to rapidly generate a basic site overview allows researchers to navigate and contextualize archaeological landscapes efficiently, making it a useful first step before more detailed analysis.

Case study 2 and 3 highlights investigations at Fort Ellice 1 (FE1) and 2 (FE2), where two separate tests were conducted to use photogrammetry to understand the level of detail and relative accuracy required for detecting and measuring archaeological features and basic site characterization. Both tests compared data output produced by the software WebODM where the input data was derived from a batch of RGB images collected via the DJI Mavic Mini drone.

The first test examined a single dataset collected at FE2 in late summer 2021, subjecting the data to two different processing workflows in WebODM. This dataset consists of 184 images that were subjected to two different workflows to compare outcomes. The first was titled 'FE2 A DTM Quality Report' and second titled 'FE2 A Quality Report'. The key difference between these

workflows lies in how WebODM links the images together during processing. The Quick Orthophoto preset is designed to maximize speed and efficiency- something of value when using a computer with limited computational capacity, or when the analyst requires a quick evaluation of output. It identifies and connects fewer common points between images, resulting in a faster data processing but a less detailed model. The Quick Orthophoto preset took 17 minutes and 5 seconds using a 2012 MacBook Pro equipped with 8 GB of RAM.

The DTM/DSM option, on the other hand, searches for and connects as many matching points as possible, creating a more detailed and accurate representation of the landscape. These connection points, known as tie points, are essential in photogrammetry because they allow the software to align images correctly and build a 3D model with better absolute and relative accuracy, but the model takes much longer to generate. In the situation of this comparatively small mapping mission (only 184 images), the time and processing ‘costs’ are still minimal. Most mapping missions for detailed archaeological investigation require far more than 184 images, resulting in the DTM/DSM function requiring several hours to complete. This can be problematic since the processing sequence is quite taxing from a computational perspective, sometimes causing the computer system to become ‘overloaded’ to the point that it ‘crashes’. This happened multiple times while attempting to process datasets with a larger number of RGB images each batch. These failures are typically due to insufficient RAM to process the model to completion. During early stages of this research a MacBook Pro 2012 equipped with 8 GB of RAM proved to be insufficient, requiring an upgrade to 16 GB of newer and more efficient RAM. This sharply improved capacity in processing larger batch datasets, but makes the point that equipment demands to support analysis are an important consideration as flights get larger and one uses UAVs with higher capacity cameras. See *Table 2* for WebODM RAM requirements.

Table 2. Showing the RAM processing requirements for WebODM

Minimum RAM needed for N images	
Number of images	RAM or RAM + Swap
40	4
250	16
500	32
1500	64
2500	128
3500	192
5000	256

These problems aside, the DTM/DSM function outperformed the quick orthophoto option in *relative* accuracy. (Horizontal CE90, and Vertical LE90) The quick orthophoto only yielded results of 0.174 m horizontal accuracy, but the DTM/DSM function yielded greater results of 0.036 m. horizontal accuracy. Interestingly, both options produced the same results for *absolute* vertical accuracy of 0.828 m, while the quick orthophoto produced greater *absolute* horizontal accuracy of 1.262 m compared to the DTM/DSM function which produced a lesser *absolute* horizontal accuracy of 1.901 m. The DTM/DSM product would have likely outperformed the quick orthophoto in all categories aside from an error during the upload process identified after the models were produced; the error being that the quick orthophoto option did not make use of one of the images in the batch process allowing for only 183 images of the 184 that were uploaded for the reconstruction.

Aside from georeferencing accuracy, the detail of features, resolution, and integrity of reconstructed points are also important considerations because these factors contextualize digital models, providing insight into site characterization. Both reports document the median number of detected and reconstructed features. It is important to clarify that the term 'features' in these reports does not refer to archaeological features, but rather to distinct points identified in the imagery that

WebODM uses for model reconstruction. Detected features represent key points that the software recognized and tracked across images, which improve alignment and structure-from-motion

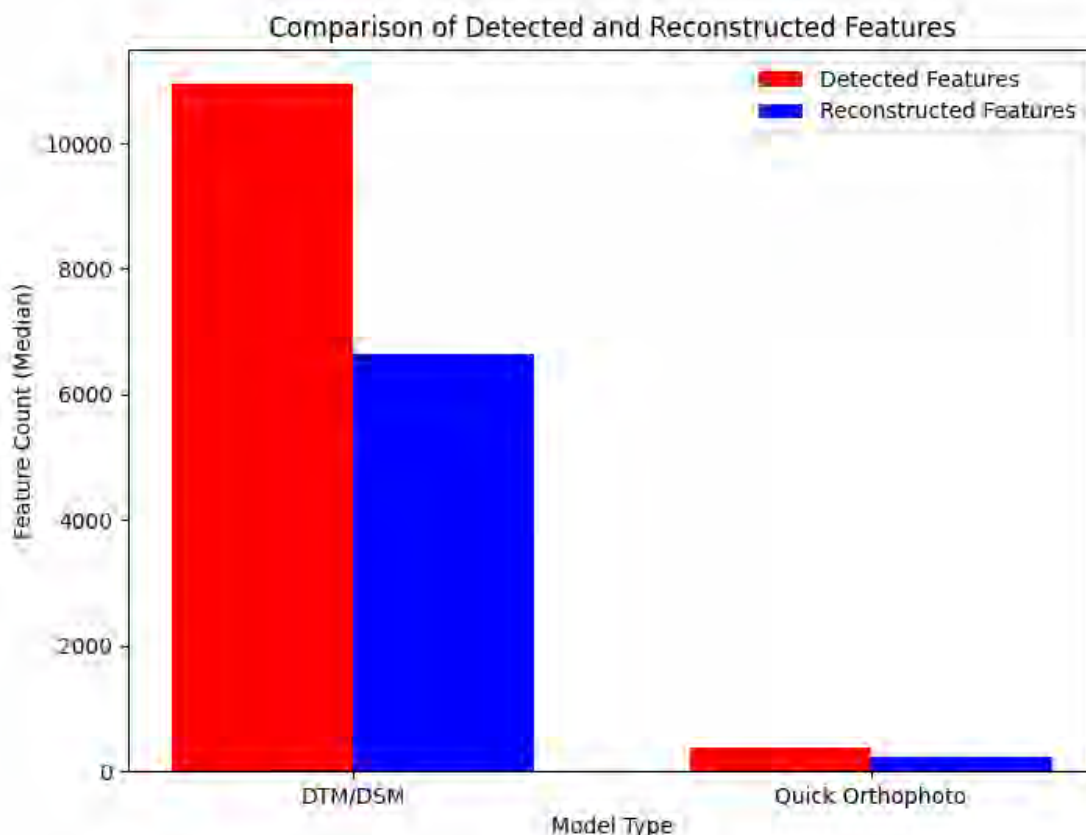


Figure 17. Bar chart showing reconstructed features versus detected features for two different processing options in WebODM

calculations. Reconstructed features refer to these points that were successfully matched across multiple images and therefore were incorporated into the 3D model. A higher number of reconstructed features indicates a more complete and accurate representation of the surveyed area thereby providing more detail to assist with archaeological interpretation of sites and site features.

In this analysis, the DTM/DSM model significantly outperformed the quick orthophoto model. The quick orthophoto model produced a median of 372 detected features and a median of 223 reconstructed features, while the DTM/DSM model produced a median of 10,946 detected features and a median of 6,637 reconstructed features. The quality of the output model being

derived from the number of tie points, detected features, and reconstructed features, directly affects the GSD. The GSD between the two models demonstrated a difference of 13.5 cm with the DTM/DSM option yielding superior results. This test begs the question whether it is better to have greater accuracy with a larger ground sampling distance, or a lesser accuracy with a smaller GSD. In both cases the median for both detected and reconstructed features for the DTM/DSM option is approximately 30 times greater than the quick orthophoto option. Inferences can be made about this test to understand which digital model is most appropriate for the given task.

The second test used two versions of the same dataset from FE1 to compare differences in accuracy based on the use of GCPs. This test is different from the accuracy test just described. It focuses specifically on georeferencing accuracy and not the detection and reconstruction of features or discrete characteristics. This second test considers absolute georeferencing accuracy of the ortho model generated from photogrammetric processing. Without GCPs, the photogrammetric output relies solely on geographic coordinate ‘tags’ associated with each image (generated by the drone's GNSS hardware technology) to georeference the resultant imagery. As the onboard GNSS receiver offers ‘accuracy’ within 1 or 2 metres that varies with satellite geometry and visibility among other factors, this can significantly impact accuracy and replicability of results. When GCPs are utilized, these reference points are associated with more accurately determined coordinates and can be used to adjust the photogrammetric output to improve overall georeferencing accuracy. This offers advantage in terms of improving replicability of results and contributes to greater efficiency and success in relocating remotely sensed features when ground truthing using other GPS systems (see for example Hamilton 2020). In test number 2 a significant difference in *absolute* accuracy is apparent between results depending upon whether GCPs were used or not. When GCPs were used, WebODM reports 0.004 m Horizontal Accuracy CE90 and 0.001 Vertical Accuracy LE90. When

the same data was processed without using GCPs the results report 1.033 Horizontal Accuracy CE90 and 1.946 Vertical Accuracy LE90 seen in number 1) of the appendix. The former result is an extraordinary measure of accuracy that was obtained through the use of repeated identification and acknowledgement of the GCP X, Y, and Z coordinates using WebODM's Ground Control Point Interface.

It is important to note that ground sampling distance (GSD) is often mistaken for raw image resolution, but it is more accurately a measure of scale that represents the real-world distance covered by each pixel in an orthophoto. Like Ordnance Survey mapping scales discussed previously, GSD defines how much ground is represented per pixel. For example, 25 cm GSD means each pixel corresponds to 25 cm on the ground. The GSD is determined by UAV altitude and camera specifications, including camera resolution. The lower the drone elevation at the time of image capture, the smaller the GSD (each pixel representing a smaller area), thereby allowing more information to be captured in each image. The trade-off, of course, is that low elevation flights capture a smaller area in each photograph, requiring longer flight times and larger dataset



Figure 18. GCP interface in WebODM allowing for PPK

for processing. Additionally, the resolution capabilities of the camera, such as a 20 MP versus a 48 MP sensor, also influence GSD by determining how finely the sensor can capture details at a given altitude.

When ground truthing anomalies, GSD is less critical than accuracy, as the primary goal is to verify whether features identified in the digital model can be reliably relocated in real space. In this context, intrasite details such as the shape, texture, or material composition of individual features contribute to characterization but are not as relevant for effective ground truthing. Instead, intersite details, which relate to the spatial positioning of features within a site, are more dependent on the level of absolute accuracy to correctly place features in geographic space. Absolute accuracy refers to how well a digital model aligns with real-world coordinates on Earth's surface, while relative accuracy determines whether features maintain their proper relationships and contextual integrity within the model. Verifying these spatial relationships using remote sensing enables a more comprehensive approach to archaeological reconnaissance, where spatial patterns may serve as a proxy for interpreting site organization, identifying unconformities, and guiding further investigation. The ability to measure and assess absolute cartesian accuracy of conventional maps has been traditionally constrained by technological capacity of the available instrumentation and the scale of map representation. Even with modern GNSS systems absolute accuracy reflects a degree of inaccuracy reflecting technical capacity of the instruments, the satellite geometry and visibility, and weather conditions. In some circumstances sub-centimetre absolute accuracy is required, requiring deployment of more sophisticated instrumentation. When high levels of absolute accuracy are not required, less complex and expensive instruments are suitable. Relative accuracy, on the other hand, measures the precision of spatial relationships between features within the model itself, with less concern for placing that model with absolute geographic accuracy on

Earth's surface. Additionally, CE90 stands for circular error not below the 90th percentile, thereby measuring the horizontal error via a circle, whereas LE90 stands for linear error below the 90th percentile and is concerned with vertical errors. This is important because it is potentially the most precise way of measuring accuracy within digital models currently.

For case studies 3 & 4 multispectral flights were conducted at the FE2 site and at the undisclosed cemetery. Because of complications with the integration of the MicaSense camera with the DJI equipment, a failed attempt occurred at the FE2 site. Experimentation with the FE2 imagery resolved these problems, allowing generation of usable results at the cemetery location in case study 4. This multispectral dataset revealed positive results for the identification of human

graves using two (2) different vegetation indices known to correlate with plant health, plant abundance, chlorophyll, and nitrogen levels (see *Figure 19* and *Figure 20*).

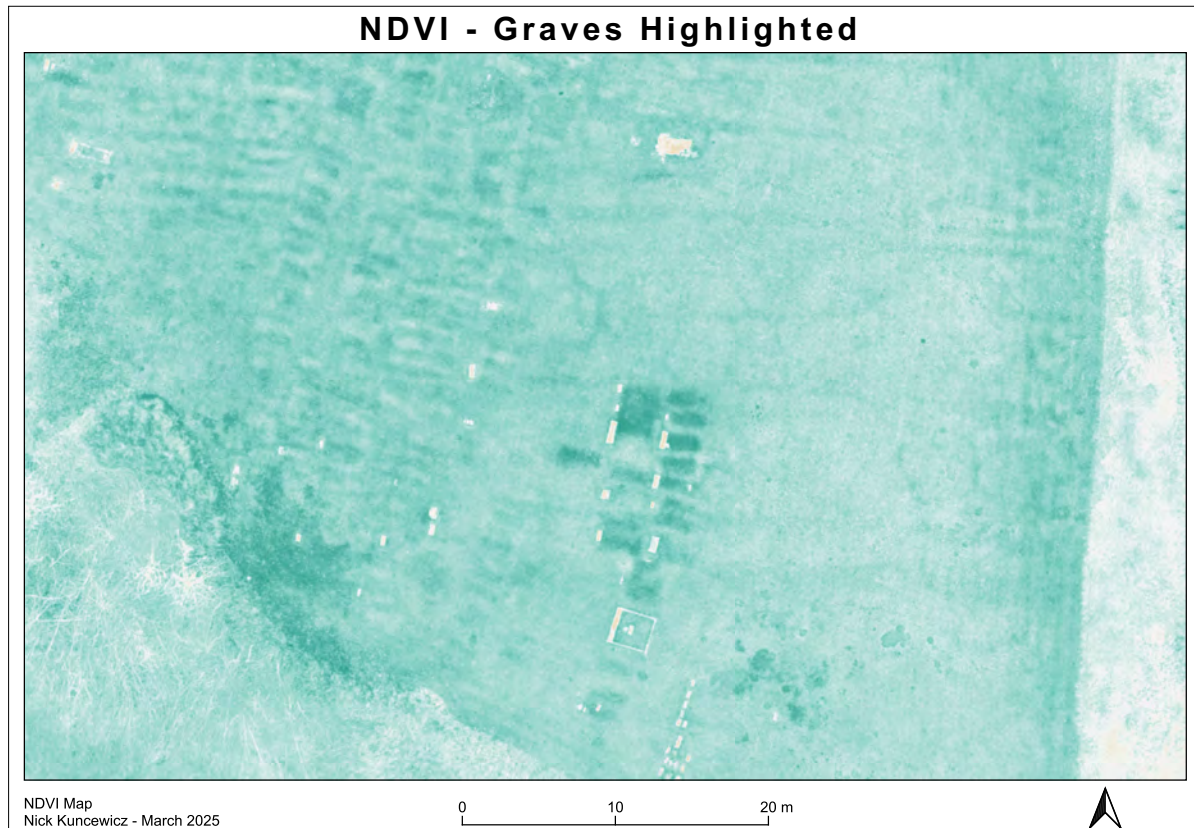


Figure 19. NDVI model of isolated graves area showing high spectral reflectance

This experiment used NDVI and NDRE processing to compare the Red, Near-infrared, and Red-edge light spectra. This process required first identifying the coordinates of already known graves and then examining the multispectral signature(s) of those known graves. The known graves often yielded elevated values that are associated with increased levels of chlorophyll and Nitrogen in plant foliage compared to the surrounding flora. This is thought to reflect plant vigour deriving from soil nutrient enrichment, including that deriving from human body decomposition. These NDVI and NDRE signatures associated with known graves were then used as references to consider other localities in the cemetery where graves are suspected but where no markers remain.

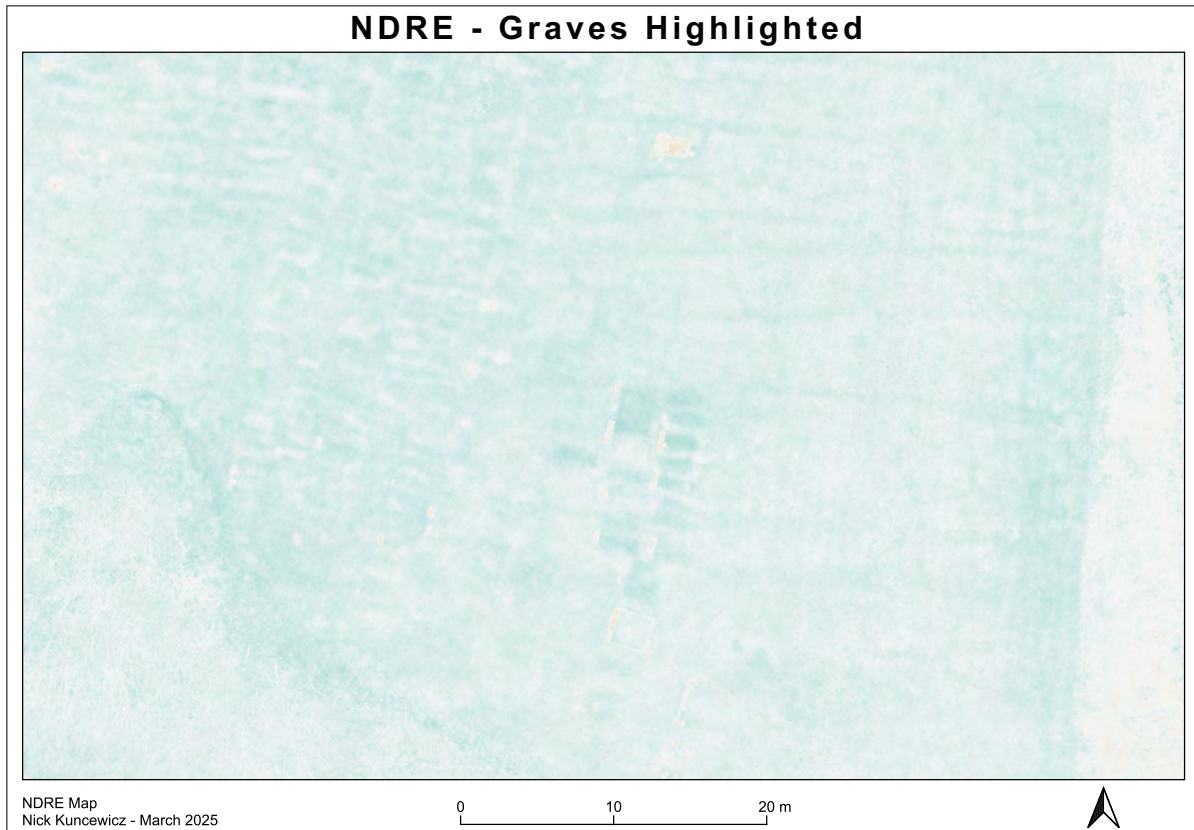


Figure 20. NDRE model of isolated graves area in the cemetery of case study 4 demonstrating high spectral reflectance signatures, likely indicating increased plant health, chlorophyll, and nitrogen

Tables in appendix 3 show NDVI and NDRE values for both marked and unmarked graves inside the cemetery bounds.

A visual assessment identified the darkest-colored known graves in both the NDVI and NDRE orthomosaics to capture the most intense reflectance signature within each marked grave. One pixel was selected from the darkest area within each grave at an appropriate zoom level. These values were then entered into an MS Excel spreadsheet and processed to determine the mean and median. This provided a range of values thought to reflect the strongest plant response to nutrient enrichment within the graves and was then used to identify other similar patches of luxuriant plant growth elsewhere in the cemetery. This approach captured the most accurate depiction of the range

of reflectance values associated with the known graves and enabled a semi-automated process of finding similar values elsewhere in the mapped space.

The data from NDVI and NDRE tables in the appendix conclude that the mean NDVI value for *marked graves* inside the cemetery is 0.629465575 and the mean NDVI value for *unmarked graves* inside the cemetery is 0.572595, while the mean NDRE value for *marked graves* inside the cemetery is 0.187599575 and the mean NDRE value for *unmarked graves* inside the cemetery is 0.16458341. All this data is based on forty (40) marked graves (inside the cemetery and marked with headstone) and forty (40) unmarked graves (inside the cemetery) (see tables in appendix number 3). This difference in means of the NDVI values is 0.056871 while the difference in means of the NDRE values is 0.02301616. The most striking difference is between NDVI mean values and NDRE mean values of both marked and unmarked graves inside the cemetery where the difference of means of NDVI and NDRE is 0.441866 for marked graves and 0.408011 for unmarked graves respectively. It is important to note that NDVI and DNRE are derived measures (varying from -1 to +1) that consider arithmetic comparison of the light spectral bands described above. As such, numeric representation to 6 decimal points reflects the nature of these indices. The precision with which these spectral signatures are associated with known human graves is the critical issue. That is, what is the range of indices variation within such graves in contrast to non-graves, and how much ‘overlap’ is there with vegetation patches with similar indices values that are not related to graves. Clearly, continued collection and analysis of cemetery data is important to refine our expectations before consideration of automatic classification algorithms for the identification of unmarked graves is fully viable.

Taking this data further, histograms are presented in *Figure 21* and *Figure 22* showing the pixel value on the x axis and the frequency of that value appearing in the dataset on the y axis.

Approximations of marked grave size using the LiDAR VAT data captured at the same site, indicate an average grave size of 1.4905 m² measured with a ground sampling distance of roughly 5 cm. Since a GSD of 5 cm represents an area of 25 cm² per pixel within the multispectral dataset, this suggests that each grave shaft might encompass about 596 pixels. The histograms for NDVI and NDRE show the frequency of pixel reflectance values within the cemetery dataset in case study 4. Since we know the approximate number of pixels that make up a single grave (596 pixels in this dataset), we can estimate the total number of graves by dividing the total pixel frequency by this baseline number. This assumes an even distribution of pixel groups, which may not always be the case but provides a useful approximation of grave numbers in the dataset. When referencing the histogram for NDRE it's evident that both marked and unmarked grave measured pixel reflectance each show up with a frequency of about 160,000 times in the dataset. Since we now have a baseline for approximately how many pixels on average make up one (1) grave in the dataset, dividing the frequency by the number of pixels in a single grave results in about 268 graves of each type on average (160,000 / 596 pixels = 268). This result is interesting in comparison to

Table 3. Showing 10 individual graves (marked) and 10 individual graves (unmarked) measured from a LiDAR VAT model. Note, there is a discrepancy where the Inside Cemetery and Outside Cemetery headings were incorrectly labelled, and they should instead read marked (for inside) and unmarked (for outside)

Inside Cemetery			Outside Cemetery	
<i>Anomaly #</i>	<i>VAT Anomaly Area (m²)</i>		<i>Anomaly #</i>	<i>VAT Anomaly Area (m²)</i>
1	1.439		1	1.629
2	0.631		2	1.814
3	1.819		3	0.914
4	2.188		4	0.618
5	0.824		5	1.371
6	2.453		6	1.887
7	1.974		7	1.779
8	2.262		8	2.1
9	0.731		9	1.717
10	0.584		10	1.224
MEAN	1.4905		MEAN	1.5053
MEDIAN	1.629		MEDIAN	1.673
MODE	0.584		MODE	0.618
		RMSE = 0.824		

the NDVI dataset where frequencies are much lower, and the reflectance values are much higher. For example, NDVI marked grave pixels have a frequency of about 3500 while the unmarked grave pixel values have a frequency of about 6000. When estimating the number of graves based on our calculations for the NDVI dataset, marked graves = 6 and unmarked graves = 10. This is far less than the NDRE predictions for the number of graves and far underestimated in comparison to the visual assessment and historical documentation of the cemetery. The NDVI-based estimate significantly undercounts graves compared to NDRE. This suggests that NDVI may be less effective in distinguishing grave-related spectral variations, whereas NDRE appears to provide a

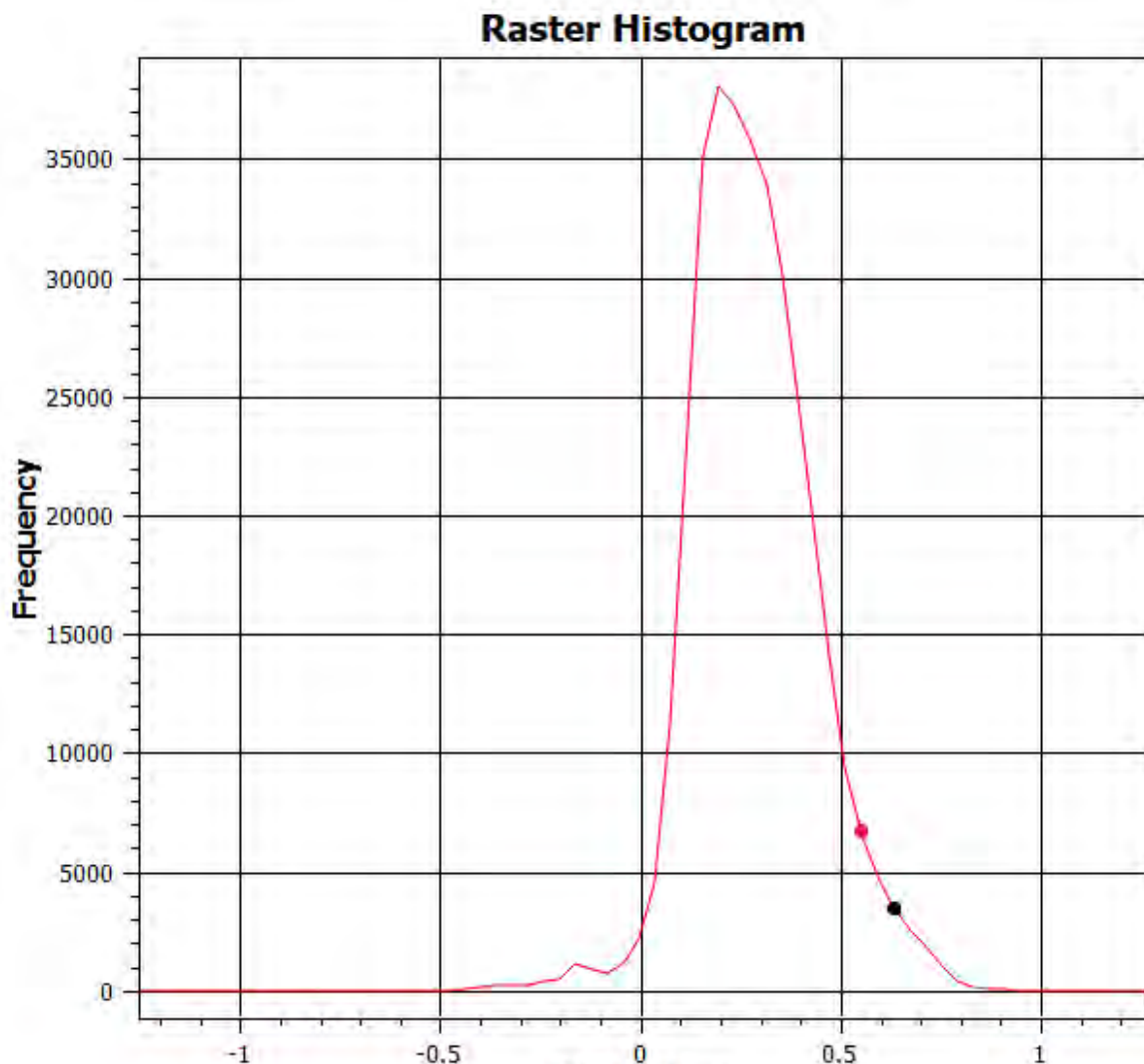


Figure 21. Raster histogram showing low frequencies of NDVI pixels using the mean of marked graves (black) and unmarked graves (red)

more reliable estimate based on frequency distributions. By identifying precise NDVI and NDRE reflectance values correlated with known graves, we can establish spectral thresholds for future automated analysis. This could improve multispectral and hyperspectral remote sensing methodologies for detecting unmarked graves, particularly when combined with machine learning approaches to recognize patterns in spectral data.

A focused statistical comparison was conducted between NDVI and NDRE values over a set of ten (10) identified grave plots in a recently used burial area of the cemetery. Of these, two

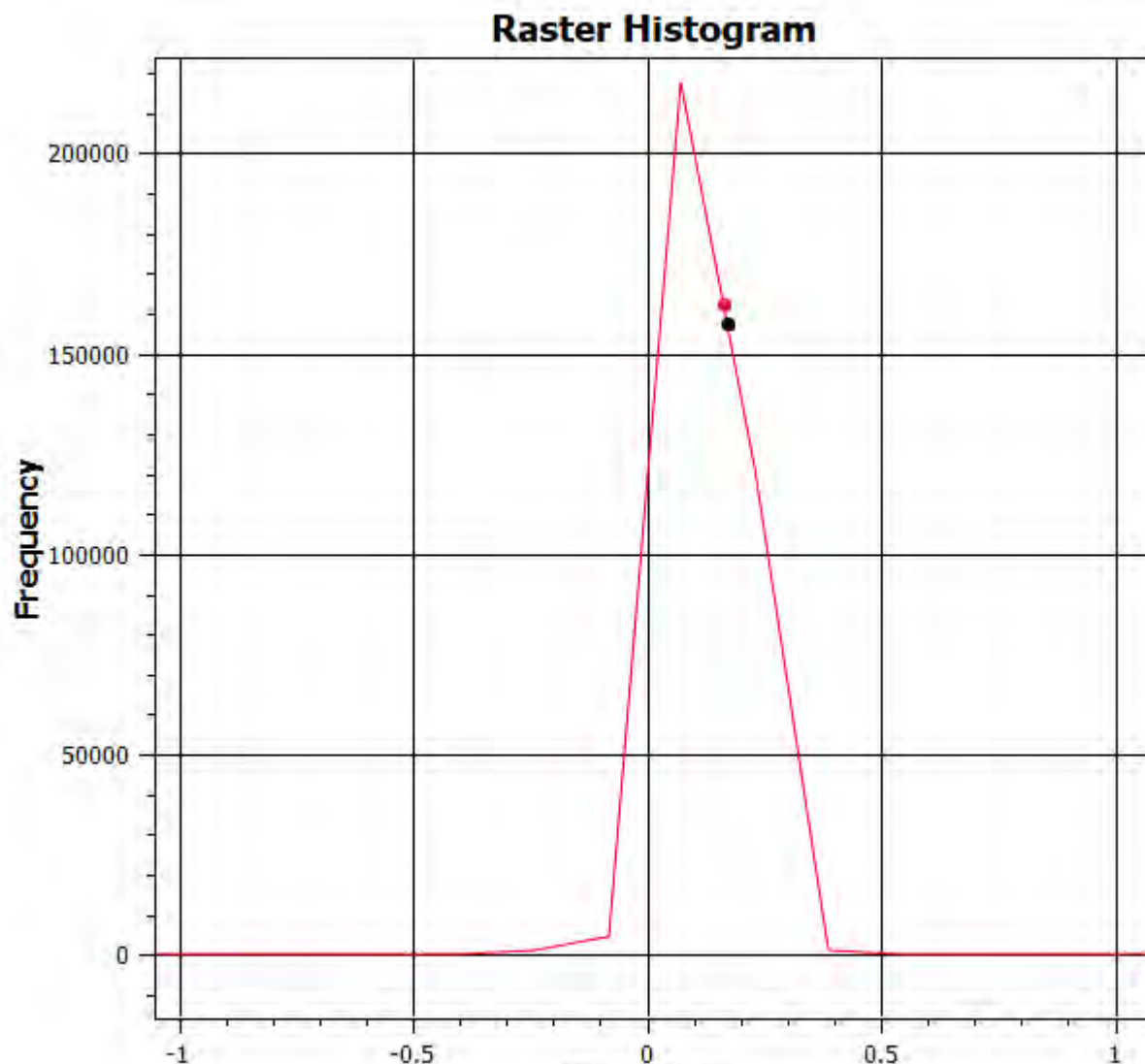


Figure 22. Raster histogram showing high frequencies of NDRE pixels using the mean of marked graves (black) and unmarked graves (red)

(Graves 7 and 8) are unmarked with no headstones, but are suspected to have been buried in the same general time frame as the surrounding marked graves based on spatial clustering and cemetery layout. The intent of this comparison was to determine whether spectral reflectance values, particularly variation within a range of reflectance signatures, could support automated or semi-automated grave detection methodologies, especially in the case of unmarked burials.

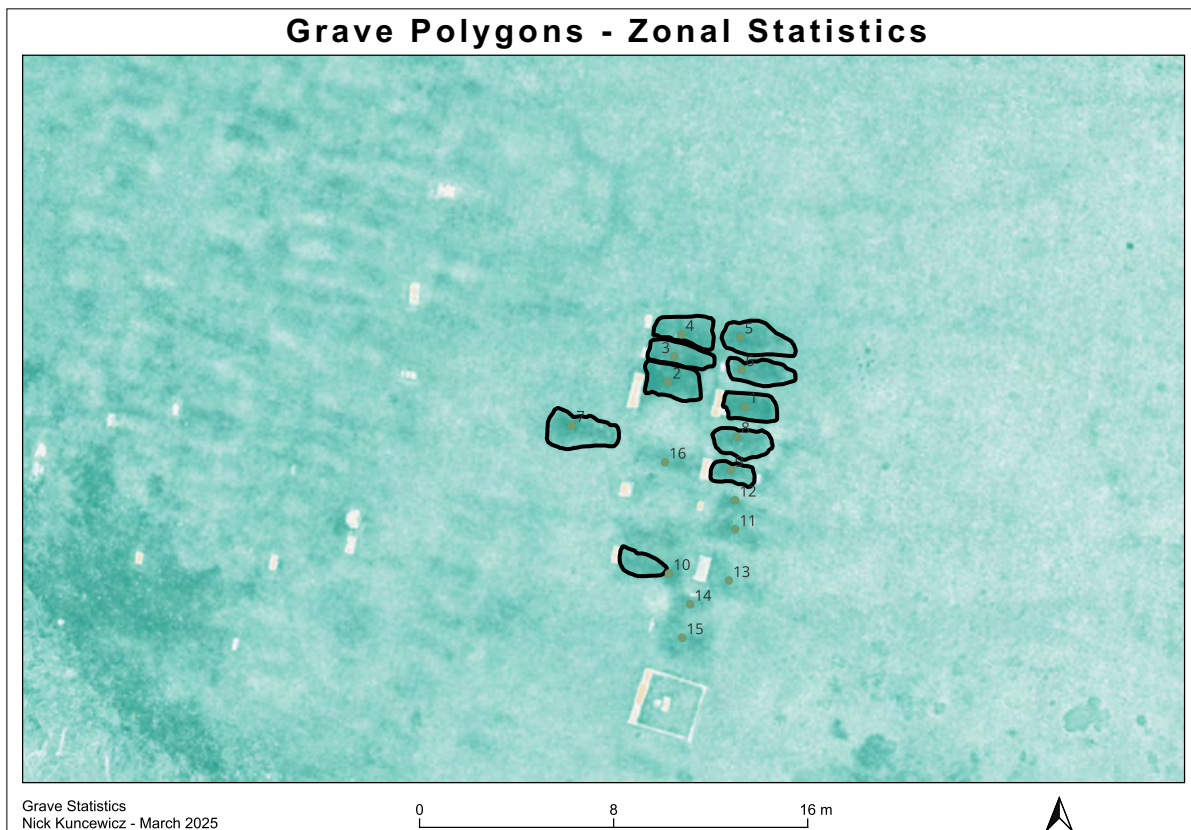


Figure 23. 10 graves selected for zonal statistics to analyze multiple pixels within a grave

Data was collected in the fall season, a time when changing environmental conditions can influence spectral reflectance due to seasonal plant decline. NDVI and NDRE are both influenced by vegetation vigour, but NDRE is more closely linked to chlorophyll content and nitrogen levels; two factors that may be enhanced by human decomposition, subtly enriching surrounding soil and increasing plant uptake in ways that affect reflectance signatures.

Each polygon (grave) was statistically analyzed for mean, minimum, maximum, and standard deviation of reflectance in both indices. The primary focus was placed on standard deviation, which offers insight into within-grave variability, a potential indicator of mixed vegetation, soil disturbance, or spectral anomalies that could correlate with burial features.

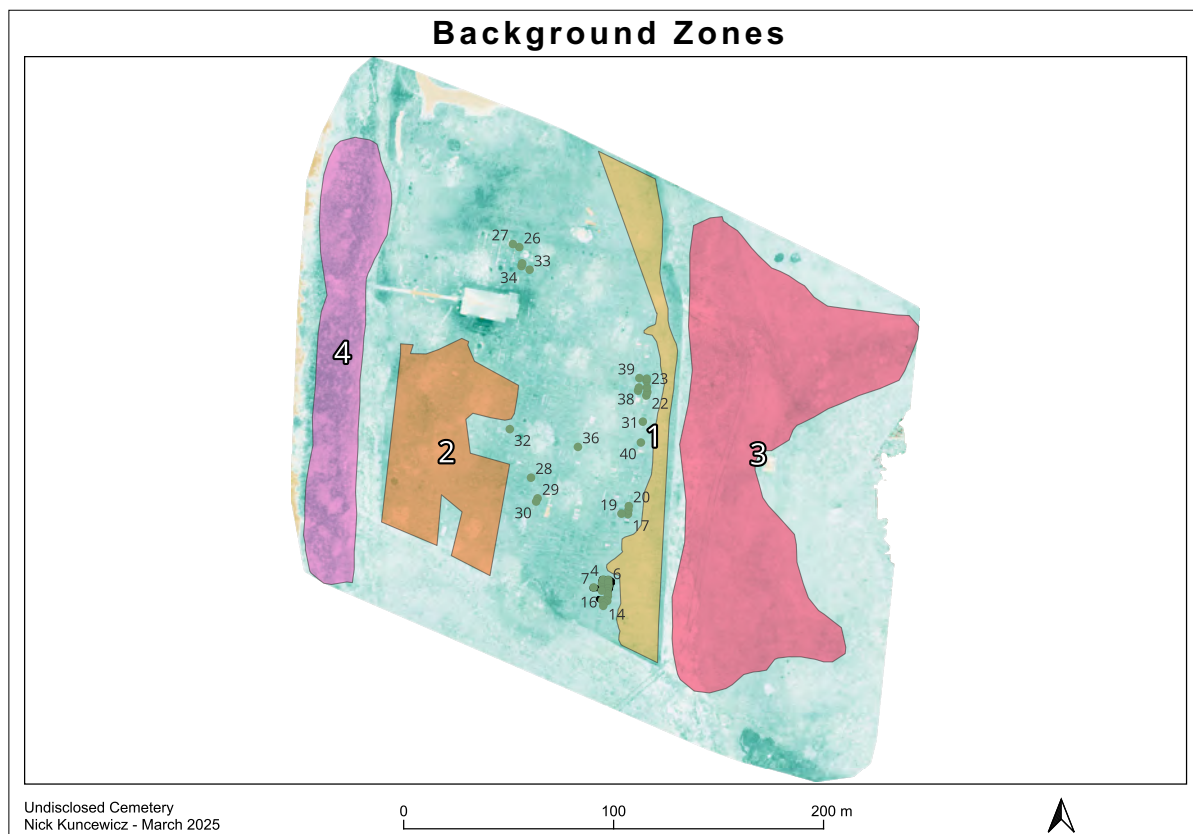


Figure 24. Backgrounds for zonal statistics to understand surrounding environment in comparison to the spectral values of graves

To help interpret the reflectance values of the grave plots, four surrounding areas were also analyzed, two inside the cemetery and two in the natural environment outside its boundaries. These background zones included maintained lawn areas, as well as patches of forest, shrub, and dense riverside grasses. Across all zones, NDRE data showed that graves had lower internal variability (standard deviation) compared to the surrounding environment. This consistency in NDRE may be due to uniform regrowth of vegetation or subtle changes in soil conditions related

to burial. In contrast, NDVI values were more scattered and showed high variability both in grave areas and natural vegetation, making it harder to distinguish burial sites from their surroundings. Interestingly, the two unmarked graves in the dataset had NDRE values similar to the marked ones, suggesting that NDRE can still detect differences associated with burial even when no headstone is present. Overall, while NDVI was visually useful, NDRE proved more reliable for statistical analysis, offering clearer separation between graves and background vegetation, even in less maintained or heavily vegetated areas.

In any of the remote sensing approaches that attempts to detect graves, especially unmarked ones, there is always the potential for false positives (Type I errors) and false negatives (Type II errors). A false positive would occur when an area is identified as having spectral characteristics of a grave, but in fact no burial is present. A false negative would mean a true burial site was missed because its spectral signature did not meet the detection threshold criteria.

To address this issue directly, a comparative analysis was conducted between known grave plots and a range of background environments both within the cemetery (maintained grass, open lawn) and outside of it (forest, shrub, tall prairie grasses). This included unmarked graves, marked graves, and natural, undeveloped land. The results showed that NDVI reflectance values were highly variable across both grave and background environments, with wide standard deviations and significant spectral overlap. This confirms that NDVI, while useful for visual mapping, carries a high risk of false positives, especially in natural or overgrown environments where vegetation is inconsistent or unrelated to burial. In contrast, NDRE demonstrated strong statistical separation between graves and all background areas, with much lower internal variability (standard deviation) within grave plots, and consistently lower NDRE mean values in

non-burial environments. This was true even in densely vegetated zones outside the cemetery where false positives were most likely to occur. Based on this analysis, the risk of grave false positives using NDRE was significantly reduced in all background contexts, and where ± 1 standard deviation appears to eliminate Type I error altogether. NDRE mean values in the 0.17–0.22 range were strongly associated with known graves, while all background zones to ± 1 standard deviation fell below this threshold. Furthermore, the spectral consistency within NDRE grave plots, including the unmarked burials, suggests that NDRE is not only sensitive to burial-related vegetation change, but also resistant to being misled by unrelated natural vegetation.

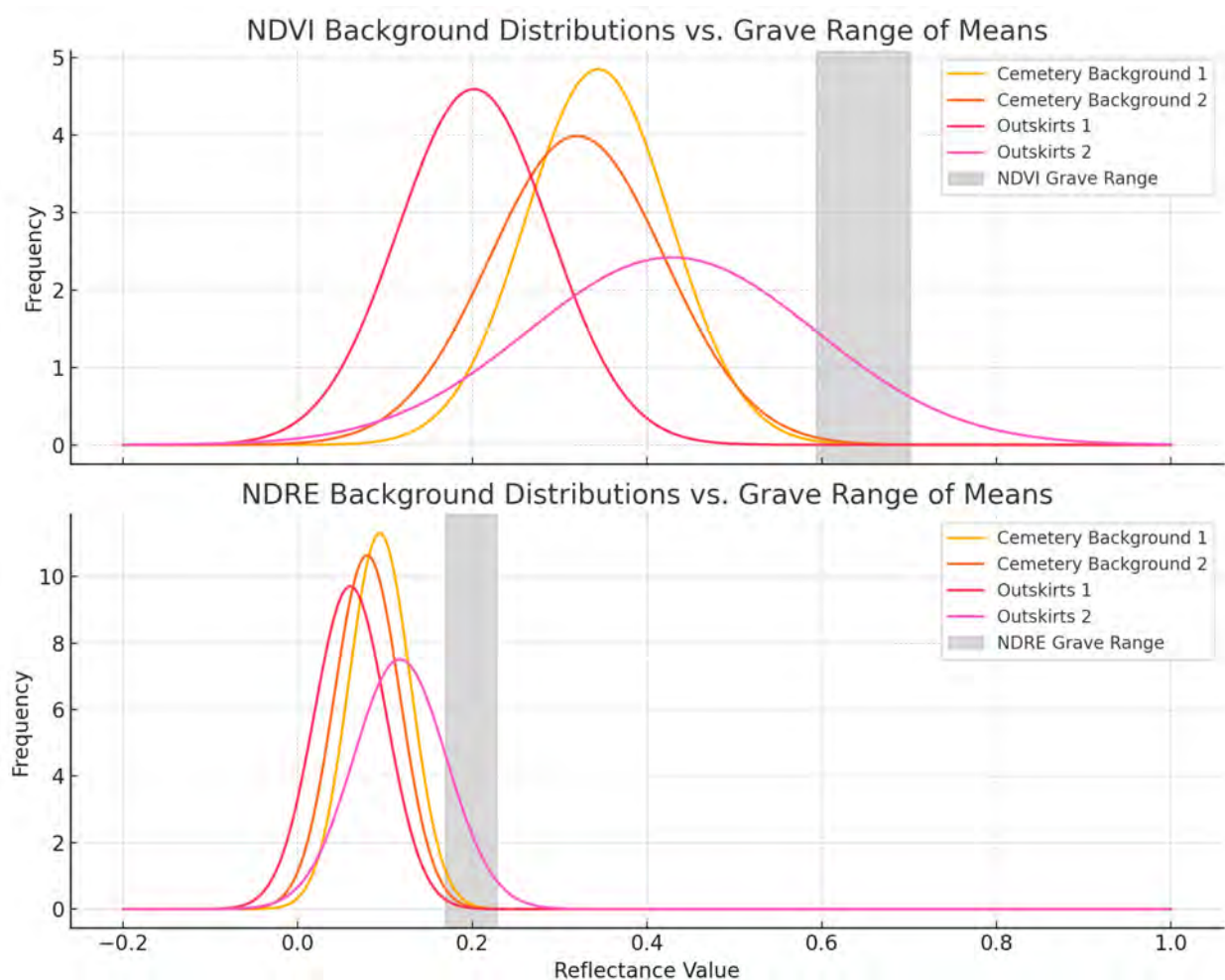


Figure 25. Frequency histograms with implied value showing the range of means for NDVI compared to NDRE. Note the standard deviation for backgrounds and graves using NDVI are much wider, versus the narrow distributions of the NDRE data.

This comparison provides strong support for the reduction of Type I errors using NDRE as a proxy for grave identification that is not found in NDVI. The risk of Type I error is valid in theory, since no remote sensing method is without limitations, yet the evidence here supports NDRE as a statistically reliable and significantly more accurate tool for spectral analysis of burial sites. It is important to note that the background zones used in this analysis contained far more pixels than the individual grave plots, often by several orders of magnitude. This introduces a potential sample bias: even if a small percentage of background pixels fall within the NDRE range typical of graves, their absolute number could be high simply due to scale. While the summary statistics (mean, standard deviation, and range) indicate that such values are statistically rare and not affecting the overall distribution, this analysis did not assess the spatial arrangement of those pixels. Therefore, while no evidence of NDRE value clustering in the background zones was observed, the possibility that small-scale spectral clusters may exist cannot be ruled out. However, the consistently low mean NDRE values and moderate standard deviation suggest these are isolated outliers rather than structured false positives, reinforcing the statistical strength of NDRE in this context. A more detailed pixel-based spatial clustering analysis would be a valuable next step to further validate these findings.

After running inferential statistics on the thermographic datasets from case studies 3 & 4, there is a strong indication that soil redeposition influences thermal entropy and exergy and is visible using the infrared spectrum detected with the DJI H20T thermal camera. To demonstrate this effect, the experimental plugin *ThermalMetrics* for QGIS was used to evaluate the mean, median, and mode for temperatures in degrees Kelvin. It is evident when comparing data collected in the summer of 2022 versus the fall of the same year, that the extent of the visual heat contrast varies with seasonality. For example, thermal data acquired from FE2 occurred shortly after sunset

on Friday, June 24, 2022, while other thermograms were captured at dusk on October 31, 2022 from the cemetery location. The high temperature recorded on June 24, 2022 in St. Lazare, MB, a community near FE2, was 22 degrees Celsius. The higher-than-average temperatures observed consistently throughout the flight mission at FE2 represent greater heat dispersion as the ambient temperature cools the surrounding earth and vegetation after sunset (*Figure 26*). Invariably, on

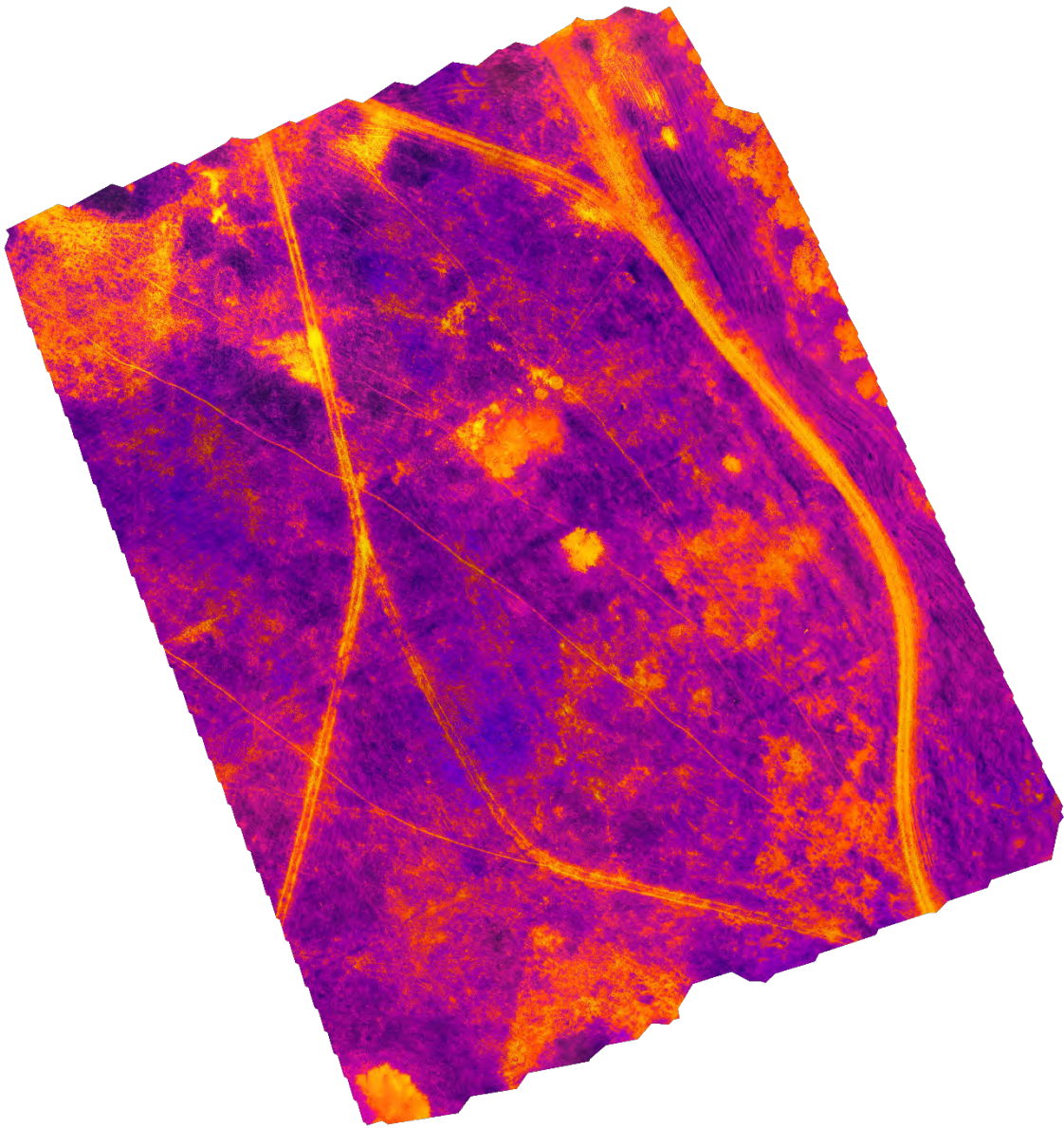


Figure 26. Thermal heatmap showing remnants of the FE2 palisade walls and other feature anomalies.

days with cooler ambient temperatures, results will show less heat dispersion post-sunset since surface and subsurface features have had less opportunity to absorb thermal energy than they would on a hotter day. A flight at the beginning of November before snowfall at the cemetery location (case study 4) illustrates this phenomenon (*Figure 16*). The average ambient temperature during this mission ranged between 8-10 degrees Celsius after a mostly overcast day. While the thermal results from FE2 reveal crisper and clearer delineation of cold/hot spots making it easier to distinguish features from non-features, the cemetery results in case study 4 (with cooler days/nights) are still impressive and indicate the potential for thermographic archaeology even in cooler weather/climates (Walker, 2020). While it's still very important to visually assess the thermographic data, a quantitative approach to the data is also important and is demonstrated in the results section using a software tool for measuring ground temperature.

The DJI Zenmuse H20T thermal camera used in this study captures thermal images in a proprietary R-JPEG format. These images embed raw sensor data in absolute temperature units (Kelvin) rather than Celsius or Fahrenheit. To analyze the data in software like QGIS, it must first convert the R-JPEGs into a more accessible format, such as TIFF, which still contains temperature information. Tools like the *ThermalMetrics* plugin for QGIS facilitate this process by enabling the calculation of various metrics from the thermal image metadata. After conversion, the temperature data is often stored in units where each pixel value represents the temperature in degrees Celsius multiplied by 10. This scaling is often used to preserve precision without resorting to floating-

point numbers or having to convert for negative values. To obtain the actual temperature in degrees Celsius, the pixel value must be divided by 10 as demonstrated in Table 3.

Metric analysis tools are also a demonstrably useful approach for data interpretation. For example, temperature and thermal resonance are useful to locate and identify anomalies, but the thermal signatures can also be used to define feature size, shape, and area. In turn, this information can be used as a validation technique. *Figure 27* shows a modern ground feature (20th century

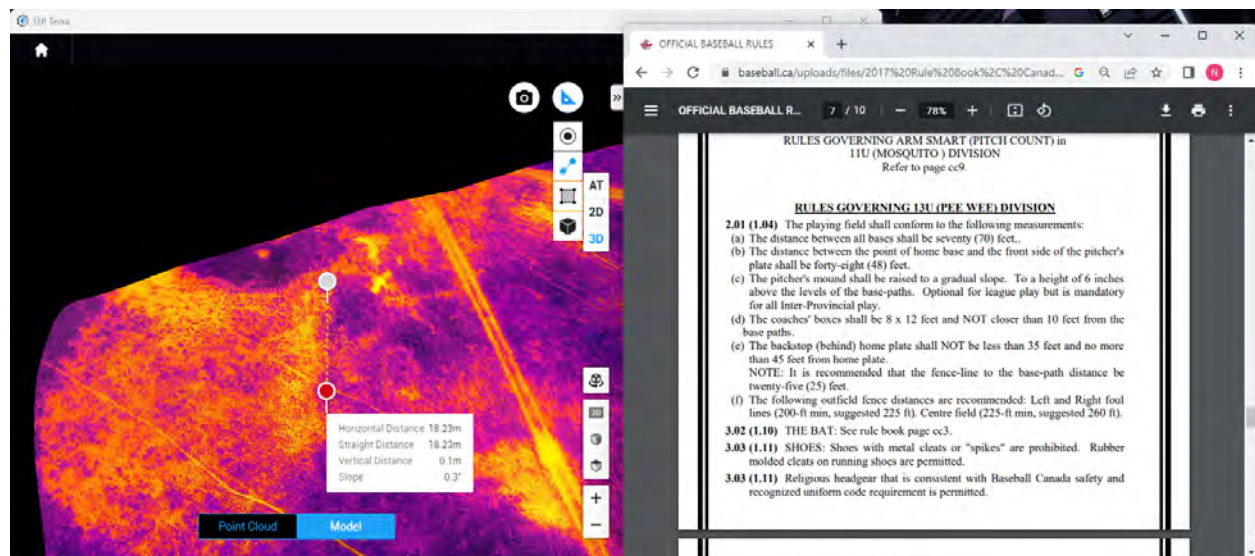


Figure 27. Thermal heat map of FE2 showing the remnants of an old baseball diamond. Measurements are consistent with the rules and regulations for noted baseball activity at this site during the same time.

baseball diamond) at FE2 coupled with the standard regulations for baseball diamond layout.

The results of the LiDAR experiments were once again drawn from inferential statistics where dimensional measurements were manually tallied from VAT models of both the FE2 site (case study 3) and the undisclosed cemetery (case study 4). The data from case study 4 summarize the mean, median, and mode in table 2 and show that the average grave size is 1.49 m^2 . The measured grave dimensions played a crucial role in verifying how many pixels constitute a single grave in in case study 4 where there is likely a mix of both adult and child graves, and where multispectral analysis was used to estimate the number of graves across the dataset. By establishing an average grave size of 1.49 m^2 from LiDAR-derived VAT models, this value served as a baseline

for approximating the number of pixels per grave in multispectral imagery. This step was essential for frequency-based estimations, where spectral reflectance values in NDVI and NDRE datasets were analyzed to assess the potential distribution of marked and unmarked graves. The ability to correlate spectral anomalies with known grave dimensions reinforced the utility of multispectral remote sensing in combination with LiDAR for burial detection.

Beyond numerical analysis, VAT-based visual representations of LiDAR anomalies provided an additional layer of interpretation, acting as a visual aid for assessing burial site patterns within a broader archaeological context. The VAT method enhances site interpretation by revealing microtopographic variations, which may not be visible in standard DEMs or hillshades. These visual outputs allow researchers to distinguish depressed features, subtle earthworks, and grave alignments more effectively. Moreover, VAT operates as a subset of algorithms that can be customized to highlight specific terrain characteristics. Adjusting parameters such as slope gradient, hillshade, sky-view factor, may more effectively enable the identification and visualization of subtle variations in the landscape. This may unveil features that would otherwise remain undetected in conventional surface models (Kokalj & Somrak, 2019; Zakšec, 2011). When applied alongside other remote sensing output, VAT-derived models provide an invaluable multi-modal approach for detecting and interpreting archaeological features in a way that is both quantitative and visually intuitive (Doneus, 2013; Khelifi et al., 2021).

5.5 Summary of results and key findings

Testing multiple remote sensing techniques using both consumer and professional-grade drones demonstrated the efficacy of this approach, and also important differences in accuracy and precision that varies with equipment class. Even the sub 250g drones are considerable research capacity since they are equipped with onboard GPS and cameras capable of 12 MP or higher RGB

imagery. They can effectively assist with archaeological reconnaissance when working within tree canopies or when assessing rugged terrain that requires pedestrian access. The very small size and weight of this maneuverable drone makes it a viable tool for generating high resolution aerial imagery under such conditions, particularly when absolute georeferencing accuracy is less important. These instruments are also valuable because they enable purpose-built construction of digital information and reference datasets. Even if archaeological features are not immediately recognized using currently existing processing and analysis tools, these datasets can offer a basis for future work using new investigative techniques and computer software as they become available. Additionally, the results demonstrate that utilizing several remote sensing tools in tandem work better than single sensor approaches to site evaluation. Specifically, anomalies are often identified in the RGB, multispectral, and thermal data based on visual characteristics within their respective datasets. In contrast, LiDAR anomalies are primarily defined by numeric analysis of spatial properties and terrain variation. The results of the multispectral analysis are interesting since the difference of averages of each vegetation index for marked graves versus unmarked graves shows minimal change (i.e. less than a 2% change in reflectance values). However, there was a significant disparity in overall reflectance levels between vegetation indices, with NDVI values being more than 40% higher than NDRE values for both marked and unmarked graves. This suggests that in general the Red and Red-edge bands were more effective at demonstrating changes in plant vigor. These findings are important because they indicate that there is no substantial difference in spectral reflectance ranges between marked and unmarked graves. Importantly, the unmarked grave signatures appear to be more subtle, perhaps indicating these burials are older and that the nutrient enrichment that enables greater plant luxuriance is fading with the passage of time since burial. Furthermore, the large difference in reflectance between

indices suggests that NDVI is more suited for visual interpretation but failed to produce meaningful results when analyzed through frequency-based estimation methods. In contrast, NDRE proved to be more effective for statistical modeling and quantitative analysis, making it better suited for research applications involving computational detection methods. Additionally, it was determined that using mRPAS can achieve survey-grade accuracy within digital models using high-precision survey-grade GPS equipment.

The results presented in this chapter demonstrate the strengths and limitations of various remote sensing techniques for archaeological prospection. Across four case studies, a combination of photogrammetry, multispectral imaging, thermography, and LiDAR revealed meaningful patterns in anomaly detection, spatial relationships, and site characterization. The findings indicate that while each method suffers constraints, the integration of datasets deriving from diverse sensors allows for improved validation and cross-verification of results.

Table 4. Showing the temperature conversions at two different site locations after using data collected with a DJI H20T thermal camera sensor and in conjunction with an analysis tool called TermalMetrics

<u>Site</u>	<u>Degrees Kelvin</u>	<u>R-JPEG Conversion to Degrees Celsius</u>	<u>Real Degrees Celsius</u>
<i>Fort Ellice 2 (EcMh-10) *June 2022</i>			
Mean temperature [in Kelvin and in °C]:	423.3871 K	150.2371	/ 10 = 15.02 °C
Max temperature [in Kelvin and in °C]:	432.5098 K	159.3598	/ 10 = 15.94°C
Min temperature [in Kelvin and in °C]:	418.3449 K	145.1949	/ 10 = 14.52°C
<i>Undisclosed Cemetery *October/November 2022</i>			
Mean temperature [in Kelvin and in °C]:	189.7102 K	-83.4398	/ 10 = -8.34 °C
Max temperature [in Kelvin and in °C]:	206.6205 K	-66.5295	/ 10 = -6.65 °C
Min temperature [in Kelvin and in °C]:	183.4426 K	-89.7074	/ 10 = -8.97 °C

Notably, the NDRE spectral analysis provided a more reliable estimate of unmarked grave distribution than NDVI, reinforcing the importance of precise spectral reflectance values for future machine learning applications. Likewise, accuracy assessments in photogrammetry highlighted the trade-offs between processing efficiency and model detail, emphasizing the role of resolution and GCPs in geospatial accuracy. Thermographic analysis further demonstrated the impact of seasonal and diurnal temperature variations, offering valuable insights into soil properties and subsurface anomalies, while LiDAR-derived VAT models provided statistically significant measurements of grave dimensions and terrain variations.

Ultimately, these results underscore the utility of remote sensing as a powerful tool for archaeological reconnaissance, especially when used in combination. By leveraging the unique advantages of each method, future research can refine data collection strategies, enhance interpretive accuracy, and improve the detection of cultural features, including unmarked graves, with greater confidence. Across all case studies, the integration of multiple sensor types and UAV platforms revealed clear trade-offs between accessibility, resolution, and interpretive utility. Consumer-grade RGB systems such as the Mavic Mini offered logistical and financial advantages for site surveying but the spatial and spectral sensitivity required to detect fine-scale archaeological features is hindered by the camera specifications, IMU/GPS, and single-mode capability. In contrast, professional-grade UAVs like the Matrice 300 RTK, equipped with LiDAR, multispectral, and thermal sensors, consistently produced higher-resolution data capable of supporting detailed site analysis, including the detection of potential unmarked graves. These findings underscore the importance of matching sensor capability to the complexity of archaeological questions being asked. *Table 5* synthesizes these results by comparing sensor-platform combinations across resolution, performance, and operational constraints.

Table 5. UAV platform and sensor types used at each case study site location.

Case Study	UAV Platform	Sensor Type	Resolution (GSD)	Key Observations	Cost, Licensing, etc.
Lockport Site (EaLf-1)	Mavic Mini	RGB	13.3 cm	Useful for general mapping, low detail on subsurface features.	Low cost, no licensing required.
Fort Ellice I Site (EcMh-03)	Mavic Mini	RGB	19.8 cm	Mid-resolution imagery provided basic spatial context.	Low cost, limited precision.
Fort Ellice I Site (EcMh-03)	Mavic 2 Pro	RGB	2.0 cm	Detected subtle terrain depressions linked to historic features.	Moderate cost, requires basic pilot certification.
Fort Ellice II Site (EcMh-10)	Mavic Mini	RGB	16.8 cm	Provided basic spatial context, Identified large features like foundations.	Low cost, limited precision.
Fort Ellice II Site (EcMh-10)	Mavic 2 Pro	RGB	1.4 cm	High-resolution imagery provided enhanced visibility.	Moderate cost, limited in windy conditions.
Fort Ellice II Site (EcMh-10)	Matrice 300 RTK	LiDAR (L1) Thermal (H20T)	2.1 cm 5.3 cm	Offered clear surface detail and improved topographic context, thermal somewhat obscured by semi-modern features.	Expensive, requires advanced certification
Cemetery	Matrice 300 RTK	LiDAR (L1) Thermal (H20T) Multispectral RedEdge MX RGB	1.0 cm 6.7 cm 4.2 cm 5.0 cm	Detected potential graves via height rasters, thermal heat maps and vegetations indices. RGB provided site context.	High cost, complex post-processing.

5.6 Comparison with existing literature

The existing literature addressing efforts to assess archaeological features via aerial remote sensing reveals distinct differences from the results presented in this thesis. There is also something of a literature void when it comes to the practical application of these technologies in professional archaeology with exceptions being Agudo et al., (2018); Altaweel et al., (2022); Campana, (2017a); Carmona et al., (2020); Casana et al., (2017); Dawson et al., (2022); Fernández-Hernandez et al., (2015); Hamilton (2020; 2022a; 2022b); Hamilton & Kuncewicz (2024); Hill (2019); Khelifi et al., (2021); Krasinski (2016); Rocke & Ruffell (2022); Silván-Cárdenas (2021); Thomas (2018); Walker (2020); and Woywitka & Michalchuk (2021). This may reflect slower uptake of new technology given regional variability in physical geography, climate and vegetation and its impact upon diversity of archaeological site types. These issues are compounded by rapid technological development. Rapid transformation of drone and camera sensor capabilities and cost rapidly ensure rapid obsolescence, causing uncertainty when to invest in emerging technologies. These rapid transformations also have a profound effect on data interpretation protocols, with a constant cycle of upgrading of computers, software and data storage demands. While few studies focus on the accuracy results using RTK and PPK approaches to data collection and georeferencing, these studies are either too broadly focussed on the functionality of the equipment and not as concerned with digital representations of the data, like in Ekaso et al. (2020) or Roosevelt (2014). While these studies are important contributions to the archaeological body of work regarding microtopography and drones, the methods and equipment are now considered to be somewhat outdated. Further, in 2020, Hamilton addressed the need for GCPs, and the difficulty associated with consistent repeatability of absolute accuracy and precision of X, Y, and Z

coordinates over a multi temporal frame. This becomes important when considering site revisits, ground truthing, and change analysis.

Chapter 6.0 Discussion

6.1 Introduction

This section discusses the relevance of this study compared with the existing literature, offers explanations and interpretations of the results, and underscores important future research directions in digital archaeology and remote sensing. Most of this discussion centers on the development of new remote sensing technology, refinement of the current technology, limitations in archaeological application, and future directions. This includes wide-ranging issues including computer science, data integration, systems management, cyber security, digitization, advanced remote sensing and GIS.

6.2 Restatement of the research objectives

At the outset of this thesis, the investigation was guided by three central research questions aimed at evaluating the role of aerial remote sensing in non-invasive archaeological applications. Specifically, the study examined whether consumer and professional-grade UAVs could provide more comprehensive tools for archaeological site characterization; whether these technologies could help overcome the physical and financial challenges often associated with archaeological fieldwork; and what technical and regulatory barriers might limit the routine integration of UAVs into archaeological investigations. During the course of this research it became increasingly apparent that a multitude of factors must be considered when using aerial remote sensing techniques. One important aspect is the orderly phasing of non-invasive archaeological research investigations. Six (6) phases were used to build out this research: understanding the research question (regarding non-invasive archaeological approaches), data acquisition, processing, interpretation, analysis and results validation. The thesis research results support the proposition that optical remote sensing technologies can be used for archaeological site prospection and hold

value as an interpretive tool for non-invasive archaeological sites assessments. This potential is tempered by barriers to access to technology, and the investment in training and experience necessary to fully employ these tools. However, these constraints are diminishing in light of rapid technological advancement, the growing support for FOSS, and online educational and informational opportunities including forums and access to online training. While considerable potential for aerial remote sensing applications in archaeology exist, it is less clear whether such approaches can be conducted independent of traditional archaeology, particularly to aid validation of remotely sensed insight.

6.3 Comparison with existing literature and theoretical frameworks

Deploying digital methodologies in archaeology is not new, as computer-driven data collection, storage, processing, and dissemination have been routinely integrated into the field for at least four decades (Huggett, 2018). As reviewed in Chapter 2, the existing literature addressing remote sensing in archaeology indicates a more recent history closely tied to rapid development of increasingly sophisticated electronics coupled with innovations in computing science. GIS and remote sensing tools have long enhanced how archaeologists conduct surveys and analyze landscapes. These methods have traditionally required manual interpretation, with human analysts identifying features and patterns from digital models. While computational tools have steadily improved the accuracy and efficiency of these workflows, the true paradigm shift is emerging with semi-automated and fully automated computer-aided analysis. This revolution will affect many fields, with AI in combination with machine learning is capable of transforming the nature of the archaeological discipline.

This thesis research demonstrates some practical applications of such computer-assisted processing using WebODM and Python-based GIS scripts for digital data manipulation. The

analysis of RGB data, thermal unconformities, spectral vegetation indices (NDVI/NDRE), and LiDAR-based microtopography (VAT models) exemplify how high-resolution datasets can be processed through systematic filtering and analysis to identify potential archaeological features. These results align with existing literature demonstrating the utility of remote sensing in archaeology, while also highlighting the increasing need for computer-aided methodologies to manage the sheer scale of modern datasets.

One of the ways AI and computational models are already reshaping archaeology is by supporting new interpretations of the past through data-driven reconstructions. The latest developments in computer vision and feature extraction allow for highly detailed digital environments that closely replicate real-world conditions. For example, machine-learning algorithms for feature detection and automated anomaly recognition are enabling archaeologists to process larger datasets with greater speed and accuracy than ever before. These advances, while still in their early stages, point to an increasing shift where AI-assisted analysis augments human interpretation rather than replacing it.

A particularly well-documented example of machine-assisted archaeological discovery is the application of LiDAR in Central and South America, where dense jungle vegetation previously obscured ancient cities and ceremonial centers under the cover of the Amazon Rainforests (Chase et al., 2011; Chase et al., 2017; Krasinski, 2016; Prümers et al., 2022). Since the utility and benefits of LiDAR are seen differently through the characterization of local ecology and the source of the LiDAR data itself, it remains to be determined how the outcomes of LiDAR and other aerial research methods will help to define heritage investigations in North America, but more specifically Canada. As of recently, there has been a significant increase in sentiment around drones in the industry. Recent studies in Canada utilize LiDAR data from public sources for broad

archaeological assessments, often applying terrain classification and geomorphology as a proxy for archaeological potential (Woywitka & Michalchuk, 2021). However, comparatively few studies have examined the efficacy of low-altitude drone-borne LiDAR from private sources for site and feature identification at a local scale. While similar applications have been explored in forested environments, the nuances of local ecology, soil composition, and ground conditions introduce regionally specific challenges that must be addressed (Krasinski et al., 2016).

This research builds upon previous studies but also highlights the limitations of manual classification approaches, suggesting that future advances in AI-driven pattern recognition will be necessary to handle the growing complexity of large-scale remote sensing datasets. While AI and machine learning are increasingly recognized as critical tools for future archaeological research, the findings of these experiments suggest that current remote sensing workflows still rely heavily on human interpretation and statistical validation. The growing availability of high-resolution data and machine-learning-based pattern extraction tools will likely transform the discipline within the next five years, enabling fully automated anomaly detection, predictive modeling, and automated classification of archaeological features. These implications will be further explored in the Conclusion chapter, where the broader trajectory of AI-driven archaeological interpretation will be discussed in relation to the findings of this thesis.

6.4 Explanation and interpretation of the results

This thesis focuses on addressing the usefulness of aerial remote sensing methods in archaeology using comparatively low-cost tools. The DJI Mavic Mini produced horizontal and vertical relative accuracies with millimeter-level error. These high-accuracy models have the potential to reach near absolute accuracy when combined with high-quality GNSS equipment, making the approach outlined in this thesis consistent with survey-grade expectations. These

results are well beyond what would be considered a necessary level of accuracy for most archaeology projects, primarily because they are typically focussed on location and reconnaissance. Compared with the results from other tests conducted with the upgraded DJI Mavic 2 Pro drone data, the accuracy of the models and identification of features are very similar. In some instances, the DJI Mavic Mini yielded superior results.

With constant flux and change within applied and academic archaeology related to technology and legislation, aerial remote sensing and digital data processing is rapidly becoming a necessary skill for archaeologists. While CRM budgets in Canada can vary, they often must balance technological innovation with competitive bidding operations. While initial purchase cost might be perceived as an impediment, the speed, efficiency and data quality possible from use of remote sensing tools offer informed decision-making and cost efficiency when considering that associated with conventional methods. Advancements in remote sensing and GIS-based analytical techniques have significantly improved the accuracy and efficiency of archaeological reconnaissance. This research demonstrated how RGB photogrammetry, multispectral vegetation indices, thermal imaging, and LiDAR-based microtopographic modeling each contribute to detecting buried or obscured archaeological features. The effectiveness of NDVI and NDRE spectral indices in identifying possible human graves, for example, underscores the potential for vegetation-based anomaly detection as a reliable non-invasive approach. Similarly, the integration of LiDAR-derived VAT models allowed for enhanced visualization of subtle terrain modifications, reinforcing the role of GIS-based spatial analysis in refining archaeological interpretations. These advancements provide a robust foundation for further refining automated feature detection in archaeology, expanding the utility of remote sensing in cultural heritage research. Table 5 shows the types of UAV technology used at each site. This information can be used to establish a bar

minimum of the aerial remote sensing data quality required for each type of investigation, in addition to the associated cost.

6.5 Implications for theory and practice

As new methods in applied archaeology continue to evolve, it is essential to consider the broader ethical and theoretical frameworks that guide archaeological practice, particularly regarding process automation and informed decision-making.

Informed and responsible decision-making is not only beneficial for archaeological practice but it is also essential to fulfill ethical commitments to descendant communities whose ancestors are the subject archaeological enquiry (Colwell, 2016). Scientific methods and digital geospatial data should be used to inform archaeological assessments, yet at the same time, caution should be taken not to rely solely on these approaches, and to consider as many reliable sources of information as possible, enabling the most comprehensive and ethical approach to site evaluation.

Although this thesis primarily examines the processes, benefits, and accuracy of remote sensing technologies, it also raises critical issues regarding digital data rights and the transformation of legacy data. These concerns lead to fundamental questions about the future of archaeology: Who will control access to the highest quality data, and how will it be used? As technology advances, will archaeologists rely entirely on digital methods, rendering traditional archaeological approaches obsolete?

The integration of computer science into aerial remote sensing for archaeology has revolutionized the way large-scale datasets are processed and analyzed. Advances in machine learning algorithms, computer vision, and automated classification techniques allow for the rapid identification of anomalies and data unconformities that would otherwise be difficult to detect through visual inspection alone. For instance, deep learning models such as convolutional neural

networks (CNNs) can be trained to recognize spectral patterns indicative of buried features in multispectral and thermal imagery, or metric patterns like marked and unmarked graves in RGB imagery, LiDAR point clouds, and height models reducing the reliance on purely manual interpretation (Knöbelreiter et al., 2018). The ability to automate feature detection significantly enhances the efficiency of archaeological prospection, providing a scalable and repeatable methodology that reduces human error while increasing the accuracy of site characterization.

Two barriers to entry are causing major implications for the deployment of the new practices outlined in this thesis. These barriers are economic variability and technical skill level. While drones and remote sensing equipment become increasingly less expensive, newer, better technologies will quickly become available and have the potential to render current technologies obsolete. Industry professionals should be obligated to uphold data integrity and exercise digital safety and security measures while also providing the highest quality data possible. This is financially significant since the newest to market options will always retain a higher cost than their outdated counterpart technologies, presuming that they offer greater technological capabilities and features.

6.6 Limitations and future research directions

One of the primary limitations associated with this work are economic barriers to entry hindering the capabilities to conduct non-invasive aerial survey. This problem is multifaceted and may include the cost of drone equipment, training, and hiring personnel to operate and maintain these technologies, as well as investment in digital infrastructure for data storage, security, and analysis.

Free and Open-Source Software (FOSS) also present some limitations in terms of data security and sovereignty, but these are mostly manageable if operating localized systems that are

not public facing or externally reachable by the broad internet. Some examples of unnecessary risk exposure considered during these experiments were the allocation of additional resources and storage through cloud-based servers and virtual machines, and the enabling of port-forwarding via WiFi router to access outside sources. While FOSS offers accessibility and cost benefits, it also raises concerns about where and how sensitive data regarding heritage is stored and accessed. As aerial remote sensing and GIS applications in archaeology become increasingly data-intensive and reliant on external services like cloud-based processing, concerns over cybersecurity are becoming increasingly urgent. The transmission and storage of sensitive archaeological data, particularly when working with protected information regarding cultural heritage sites, raises ethical and security considerations. This is especially true if utilizing non-localized storage or processing options. Data encryption, restricted access protocols, and offline data storage solutions are necessary to safeguard sensitive site information from unauthorized access or cyber threats from hackers. Furthermore, as machine learning algorithms are integrated into predictive modeling for site detection, ensuring the transparency and integrity of training datasets will be essential in preventing algorithmic bias or misclassification errors in automated archaeological prospection. This problem is already apparent in 'black box' services and software like DJI Terra, presenting challenges to understand how data is handled and processed by third parties.

Looking toward the future, advancements in AI and machine learning hold significant promise for archaeological site detection and classification. One possibility is the use of hyperspectral imaging and spectroscopy to detect human graves with extreme precision, particularly by isolating spectral bands associated with Nitrogen-15 (N^{15}) isotopes. Since N^{15} is a stable isotope that remains in human skeletal structures post-mortem, its presence in soil and vegetation could serve as a non-invasive indicator of human burials (Philben et al., 2018). This

concept suggests that, in the future, AI-driven remote sensing tools could be used to identify burial sites through spectral analysis of plant nutrient uptake. However, major challenges remain; the exact spectral resonance of N^{15} , the accuracy of its reflectance interpretation, and the complexities of isotope fractionation in different environmental conditions must be better understood before such technology can be reliably implemented.

Despite these limitations, the integration of digital archaeological methodologies into CRM and academic research is rapidly evolving. If approached ethically and collaboratively, these tools have the potential to strengthen sovereignty over cultural histories, heritage, and archaeological data, enhancing site protection, and advancing non-invasive archaeological techniques while respecting traditional systems.

Other optimistic theories for future research using remote sensing applications for archaeology involve the use of Bayesian statistics for predictive modelling and probabilities. Elementary approaches to Bayesian statistics outlined by Schmitt (1969) suggest that it's possible to use average ground temperature as a *prior* and additional data on thermal properties as a *posterior* such as the emissivity of different soil types and material composition of artifacts. The continual addition of posterior data will increase the accuracy of probability outcomes such that statistical analysis of this form could accurately identify and predict artifact and feature distribution/location with a high degree of probability. Data is acquired using the *ThermalMetrics* tool in case studies 3 and 4 and is available in the appendix (Ellsäßer, 2021).

LiDAR also offers promising future capabilities as the level of accuracy and point cloud density becomes stronger and more efficient. Eventually with advancements in LiDAR technology, it should be possible to penetrate even the densest of tree cover and tall grasses in forests and mixed woodland ecosystems. This will make LiDAR an even more valuable tool for

enhanced site characterization. In combination with near-surface geophysical techniques, and dependent upon the level of penetration depth and laser capabilities, these enhanced forms of LiDAR could hold future value for defining subsurface characteristics. This new LiDAR could also produce capabilities of penetrating through other mediums like snow, where these capabilities are still considered somewhat ambiguous.

Lastly, a brief note on other forms of remote sensing is warranted since this thesis focussed solely on optical remote sensing. Other technologies currently exist that can produce maps and models via remote sensing by smell. A product called Sniffer4d is available to market and is compatible with the DJI M300 drone used in this thesis. The product is an air pollutant mapping system using a sensor to register volatile compounds in the air. While this product is currently designed and optimized for the oil and gas industries and environmental monitoring, there is some future potential for this system to be used in conjunction with archaeology, at least conceptually. For example, Historic Human Remains Detection Dogs (HHRDD) can detect graves exceeding 100 years old and up to 6 feet DBS (Baxter and Hargrave, 2015). The study by Baxter and Hargrave (2015) explicitly states the composition of chemical compounds responsible for human bone odour. If these chemical compounds can be isolated and read by remote sensing machines such as the Sniffer4d, then with increased geospatial accuracy and the evolution of drone equipment capabilities, this remote sensing technology could provide another avenue to the successful detection of human graves.

6.7 Workflow

One of the greatest challenges in non-invasive archaeological research is the integration of multiple remote sensing datasets into a cohesive analytical framework. LiDAR, thermal, multispectral, and RGB photogrammetric data each offer distinct insights into the landscape, but

their combined interpretation requires careful spatial alignment, calibration, and standardization. The use of geospatial data integration platforms, such as QGIS allows researchers to overlay datasets and compare results, reinforcing findings through cross-validation. For example, areas where thermal anomalies overlap with vegetation stress signals in NDRE models may indicate subsurface disturbances related to past human activity. The synthesis of multiple data sources ensures that interpretations are robust, repeatable, and empirically grounded, strengthening the validity of remote sensing methodologies in archaeology.

The design of aerial research missions using drone-borne remote sensing requires a very specific set of pre-thought stages that demand precise execution and functionality that when combined become a systematic workflow for digital output. This thesis had a heavy focus towards producing a variety of digital products to demonstrate the range of output deliverables that modern drone-borne remote sensing systems are capable of creating. The workflow for each method of remote sensing data creation is structured based on its essential components: hardware, software, or a combination of both. Managing hardware can be complex, especially when working with interchangeable equipment and intricate physical systems. At the same time, software management can be overwhelming, particularly due to the specific and independent nature of different remote sensing tools and their unique data processing requirements. Many software programs, especially proprietary ones, do not easily interact with each other, as they are often designed for single, specialized tasks. For example, CloudCompare is primarily used for point cloud filtering, making it well-suited for that purpose but not directly compatible with other types of data processing.

Efficient systems management is critical in handling the large volumes of data produced by aerial remote sensing missions. The processing of high-resolution orthophotos, point clouds, and spectral indices demands significant computational resources, sometimes in the realm of many

gigabytes or terabytes, necessitating structured workflows for data storage, retrieval, and processing. Computer hardware requirements of this magnitude often limit workflows, forcing users to adhere to strict specifications including brand, type, and size of CPU, GPU, and RAM. Implementing network-attached storage (NAS) solutions, such as the Synology system used towards the end of this research, provides a professional, scalable way to store and access project files while ensuring data redundancy and security. Additionally, workflow automation tools, such as batch processing in WebODM or Python scripting for spectral analysis and VAT processes, streamline the transformation of raw data into actionable insights. Proper systems management ensures that data integrity is maintained across projects, facilitating long-term analysis, healthy data curation, and multi-temporal comparisons.

The key to successful digital model production relies on selecting the appropriate hardware and software that cooperate with one another. An excellent example of hardware explicitly designed with software is the DJI line of UAV for autonomous flight mapping, planning, and data processing. These drones are optimized for use with DJI Terra so that there is a seamless workflow of the phases of data production. Not only will the workflow change based on the differences and similarities between hardware and software, but the workflow may also be different between remote sensing techniques. For example, the workflow for data collection using multispectral and photogrammetric RGB capture might use the same concepts of photogrammetry; however, the content within the metadata of the captured imagery is different, and therefore the analytics, processing requirements, and post-processing styling will vary between these two techniques. So far, DJI is the fastest, most reliable, most cost-efficient way to achieve professional-level results. Hill (2019) discusses the general workflow for photogrammetry across disciplines, and while there are many similarities to the approach taken with case studies in this thesis, the complete workflow

for photogrammetry and orthophoto collection and rectification was different. Due to the increasing quality of onboard GPS, the methods suggested by Hill (2019) regarding the use of ground control point (GCP) referencing for post-processing accuracy become redundant unless precise georeferenced accuracies are required. The requirements for geospatial accuracies are a continual theme throughout the core of this thesis. It is worth exploring the necessity of precision and accuracy for archaeological investigations in the CRM industry, including site monitoring, exploration, and documentation. There is a varying necessity of scale for archaeological projects within the discipline and across disciplines and industries. Intradisciplinary examples of the necessity of scale could focus on anything from broad site identification to the minutiae of archaeology, including material identification using cluster analysis (Sánchez-Romero et al., 2021) and Bayesian modeling using lithic-scatter and debitage locales increases the likelihood of site identification. A precise level of scale could also be significant in contributing to the identification of unmarked graves via small changes to the earth's surface topography. Additionally, suppose an archaeological site was to be mapped and revisited regularly or semi-regularly to confirm changes to the archaeological sites and site features. In that case, a hyper-precise level of geospatial accuracy and change analysis might be necessary to monitor erosion, site degradation, and looting (Dawson et al., 2022; Parcak, S. 2019). In the traditional practice of archaeology, destruction is inherent and permanent, meaning there is only one chance to properly excavate the earth so that cultural material exhumation and collection may be appropriately documented. Hill (2019) notes the increasingly common use of drones for survey and assistance with archaeological research tasks, such as excavation recording. Most modern drones geotag each image as EXIF (Exchangeable Image File Format) metadata. This capability not only ensures images are correctly recorded for photogrammetry and digital model construction but also allows for the capture of

important contextual details in single images during excavation (Hill, 2019; Nex & Remondino, 2014).

Throughout the data collection component of case studies in this thesis, some data was captured and processed using nothing more than the onboard GPS unit of the drone itself. The case studies presented from the Lockport site consist of DEM digital elevation models generated without post-processing the data for greater georectification accuracy.

Three photogrammetric workflows were used in each case study of this thesis and are all nearly identical. The first workflow is the Direct Georeferencing (DG) of GPS resulting from the drone onboard GPS and Inertial Measurement Unit (IMU). This device is usually combined with a gyroscope and communicates to the drone's intelligent systems measuring space and time. The onboard GPS unit in the DJI Mavic Mini is capable of vertical $\pm 0.1 - \pm 0.5$ m and horizontal ± 0.3 m - ± 1.5 m. This is unusual since most UAV studies indicate that vertical accuracies generally tend to be 1.5 times greater than horizontal accuracies. The accuracy results shown in *Figure 15* align with the common conception that vertical accuracies are greater than horizontal accuracies. They are represented by absolute and relative accuracies of Linear Error (LE) and Circular Error (CE). Relative accuracy is the accuracy given of a point relative to other points in the same map. Relative accuracy then measures the relationship between and within things considering their dimensions.

Conversely, absolute accuracy measures the relationship between things on a map and their spatial orientation according to a fixed coordinate system in the real world. For example, the coordinate system applied in most geographic regions of Manitoba corresponds with the geodetic code system NAD 83, 14 N. While the accuracies in are nowhere near survey grade, they are still impressive, given no post-correction processes using GCPs. For some archaeological survey and

inspection purposes, 1.591 meters absolute accuracy might be enough to assist archaeological discovery, reconnaissance, and field methods such as field-walking and ground truthing. This method of direct georeferencing was used in Case study 1 of this thesis at Lockport east. It was an effective method of reconnaissance for this site given time constraints and the complexities of an ongoing infrastructure development project at this location. Using DG within areas of obvious general points of reference is an effective method of quickly capturing and processing data for exploration.

In Case studies 2 and 3, Fort Ellice, the method of processing georeferenced points after flight and data collection known as PPK was used. PPK stands for Post-Process Kinematics and is a way of geo-rectifying digital information such as maps, models, and images using known ground control points that have been previously georeferenced. Once these GCPs are recorded and identified manually within the software, their coordinates are entered into the Ground Control Point Interface of WebODM, the digital information will adapt to reflect the changes. This is time-consuming but can result in the best accuracy for georeferencing. Images captured at the Fort Ellice 1 site were used to generate a DEM yielding sub-centimeter absolute horizontal accuracy. To achieve this, a low-altitude flight with post corrective information was uploaded to the application webODM, and individual images containing GCPs were identified using the GCP coordinates displayed in QGIS for faster identification. Of the 6 GCPs used, there were approximately five images used per each ground control point totaling roughly 30 additional points of reference along with the drone onboard GPS. These GCPs consisted of orange pylons with an open center, and when zoomed in on the image, the exact near center could be selected to represent the point recorded with the GNSS rover Juniper Systems Geode 2. The centermost pixel identification in each already georeferenced image could have helped to correct the entire model to millimeter

accuracy and should be a regular addition to photogrammetric workflows where at least sub-decimeter accuracy is sought. The last physical workflow method for data capture is demonstrated in Case study 4 at the undisclosed cemetery location and was made possible by using Real-Time Kinematics (RTK). This method requires using a base station or station-rover combo and an RTK-equipped drone. The DJI Matrice 300 series enterprise drone was used in this case study with the DJI D-RTK2 Base Station and a Leica Systems GNSS rover GS14. This rover can achieve 1 – 3 cm accuracy. Once this accuracy measurement is recorded, it is time to sync the drone using these coordinates to receive complete real-time corrections. These coordinates are given in Latitude/Longitude. When tests were compared on the remote control using the DJI DRTK 2 base station in comparison with the corrected coordinates from the rover, the base station accuracy would fluctuate between 0.0001 0.00001 decimal degrees of a coordinate equating to changes anywhere from 11.1 m – 1.1 m. Contrary to what was previously said about the necessity of scale for archaeological investigations, the top end of this error level would be considered unacceptable in map production and even for reconnaissance purposes, as errors ranging in the tens of meters and beyond would pose a significant challenge to ground truthing. Incorporating the three methods of geographically correcting data is critical to an effective and efficient workflow for digital model production and mapping purposes through geographic information systems (GIS). Photogrammetry is the only possible remote sensing method for DJI Mini drones. However, this might change as the need for rapid mapping grows, and technology improves. These are the two defining factors that are working to propel the use of microdrones in the surveying industry. Otherwise, the level of quality when using multiple remote sensing methods is far superior to photogrammetry alone.

6.8 *Contribution of results from case studies*

The case study results add to an ever-growing body of research on remote sensing applications. Qualitative data will help other researchers with visualization of workflows and outcomes, while the quantitative data results offer some contribution to the potential development of new filters and algorithms for data analysis and interpretation.

The RGB photogrammetry studies from Lockport, FE1, and FE2 using the Mavic Mini demonstrated how to significantly reduce error and refine accuracy using GCPs and a GNSS rover.

The MicaSense RedEdge-MX™ (MSRE) multispectral camera used at the undisclosed cemetery location aided interpretation of grave statistics and was found to offer utility as a possible estimator for predicting the number of graves in a dataset. A refined version of this workflow can and should be adapted for use in the search for missing children from Indian Residential Schools. The full workflow and formula are highlighted in the appendix.

Thermal analysis using the DJI M300 and H20T produced thermograms and thermographic models that aided visual interpretation of subsurface features including walls, pits, and graves, and yielded significant empirical results from the *ThermalMetrics* tool demonstrating generalized temperature ranges and variances of archaeological sites. The importance of thermal metrics in archaeology is highlighted in section 6.6 on future directions. When coupled with predictive models such as Bayesian statistics, thermography can offer strong support for archaeological interpretations with added probability.

Last, the results from the LiDAR studies increase the small pool of studies dedicated to the effect of flight parameter settings on feature identification and digital model. The workflow used to develop a VAT model is only one of many varied approaches to build a visual relief model. The

unique settings of the ground filtering algorithm are identified in the appendix and are used in combination with VAT to display graves based on physical dimensions and other attributes.

The transition from traditional archaeological methods to digitized, data-driven approaches represent a fundamental shift in how archaeological landscapes are documented and analyzed. High-resolution digital elevation models (DEMs), LiDAR-derived point clouds, multispectral visualizations and measurements, and radiometric thermal mosaics allow for a level of detail and precision that was previously unattainable with conventional survey methods. The results from the case studies in this research highlight how digitization enhances site interpretation, particularly in contexts where excavation is not possible or cultural sensitivities necessitate non-invasive approaches. By digitizing archaeological landscapes, future researchers can revisit and re-analyze sites without requiring new field investigations, ensuring that data remains accessible, reproducible, revisable, and open to future innovations in analytical techniques.

Chapter 7.0 Conclusion

7.1 Recap of the study

This thesis demonstrates the effectiveness of aerial remote sensing as a powerful tool to support archaeological investigation. By integrating mRPAS equipped with high-grade GNSS technology and data collected using various forms of remote sensing, this research showcased how high-resolution, geospatially accurate survey data can be efficiently collected for archaeological assessments. These technologies provide cost-effective and scalable solutions for mapping landscapes, identifying subsurface features, and documenting archaeological sites with a level of precision that traditional methods alone cannot achieve.

A key contribution of this study is the exploration of multi-modal remote sensing approaches, emphasizing the importance of cross-validation between different datasets. By combining multiple forms of aerial remote sensing, this research highlights how overlapping data sources enhance interpretation, improve feature detection, and increase the overall reliability of archaeological site assessments.

This study applied remote sensing techniques across three unique areas of investigation, each representing different archaeological contexts. These four case studies demonstrated the practical application of rapid reconnaissance, geospatial accuracy, detailed site characterization, and forensic archaeological prospection, with particular application to the detection and documentation of human grave features. The ability to use remote sensing for non-invasive, high-precision site analysis illustrates its growing importance in modern archaeological practice, particularly in scenarios where traditional excavation may be impractical, restricted, or ethically sensitive.

Ultimately, this research underscores the value of integrating aerial remote sensing within archaeological workflows. These methods are not supplemental to traditional methods, but rather,

standalone investigative procedures capable of transforming archaeological prospection, documentation, and heritage management. As remote sensing technologies continue to advance, their role in archaeology will only expand, offering new ways to interpret landscapes, protect cultural heritage, and support non-invasive site discovery efforts.

7.2 Conclusions and recommendations

Each drone type, with associated sensors, demonstrate utility as site prospection tools for archaeology that offer advantages over traditional surface survey techniques. The Mavic Mini was used to assess its utility for rapid production of site evaluation maps to support preliminary reconnaissance. The imagery was collected and then rapidly processed (overnight) to generate photomosaic and 3D digital models to aid ongoing archaeological monitoring shortly before heavy snowfall prevented any further flights. The speed and efficiency of drone deployment offers strategic advantage in enabling *ad hoc* mapping operations suited to local circumstances. The Mavic 2 Pro data yields some advantage over the Mavic mini in terms of image resolution, but this advantage is minor compared to the dramatically improved capacities of professional level M300 enterprise drone. The results of the Mavic Mini data from FE1 using GCPs indicates greater georeferencing accuracy than the Mavic 2 Pro with and without GCPs; therefore, it's evident that using increased GCPs is more important for accuracy than the step-up in drone type from the Mavic Mini to the Mavic 2 Pro. Last, combinations of remotely sensed data contributed to increased success in identifying anomalous features in the cemetery data from case study 4. Additionally, the use of thermographic and multispectral metadata, and ground filtering and shading algorithms derived from LiDAR provide a useful case for the incorporation of statistical methods and quantitative analysis in the professional workflow.

The future of archaeology in Canada depends on maintaining rigorous standards and guidelines that integrate emerging technologies in a timely fashion to enhance archaeological investigations. The adoption of new digital tools by archaeological practitioners is crucial for ensuring that heritage evaluations remain comprehensive, accurate, and ethically conducted. This technological shift presents opportunities for archaeological development and regulatory reform, reinforcing heritage ownership, strengthening sovereignty and ownership over digital data, and fostering the evolution of digital literacy through educational resources.

The digitization of archaeological environments into useable data holds significant potential, not only for private study and enhancing archaeological insights but also for reshaping public perceptions of material history and redefining traditional geographic space. While aerial remote sensing offers valuable applications for archaeological and environmental monitoring, it also introduces challenges related to data security, surveillance, and land governance. The global expansion of private satellite imaging and micro-drone technology raises concerns about unauthorized data collection, covert surveillance, and potential exploitation of sensitive archaeological and environmental information. These technologies can be used in opaque or unethical ways, including unregulated monitoring of landscapes and heritage sites.

As satellite imagery and aerial remote sensing technologies continue to advance, the widespread adoption of drone technology and digital methodologies should be prioritized in shaping policies and ethical guidelines for archaeological practice in Canada. However, regulatory bodies have been slow to adapt, favoring traditional approaches despite the demonstrated advantages of these emerging tools. While these technologies are rapidly transforming archaeological investigations, institutional reluctance to modernize threatens to hinder progress rather than enhance the discipline.

7.3 Full Contribution of the study

This study provides new approaches for integrating geospatial information into decision-making processes in CRM, demonstrating the versatility of remote sensing in archaeology and beyond. By presenting a structured workflow for both qualitative and quantitative approaches to aerial archaeological prospection, this research outlines a cost-effective and scalable strategy for obtaining high-resolution survey maps using mRPAS, enterprise drones, and various airborne remote sensing tools. The success of these methods led to broader explorations into multi-scale remote sensing applications and their impact on archaeological interpretation. Notably, resolution emerged as a critical factor across all case studies, influencing how different sensory applications capture and define archaeological site features. Non-invasive archaeological approaches using remote sensing hold considerable merit since they minimize site disturbance while providing valuable spatial and contextual data.

The implications of this research extend to both the academic study of archaeology and its professional practice. As drone and remote sensing technology evolve, so too does our ability to identify and assess archaeological sites with greater precision and accuracy. This study contributes to the ongoing refinement of prospection tools in archaeology, reinforcing a cyclical relationship between technological advancements and archaeological methodology. By demonstrating non-invasive approaches for detecting and analyzing archaeological features, this research highlights how remote sensing is reshaping modern archaeological practice and accelerating the discovery and preservation of vulnerable cultural heritage.

One of the most urgent applications of non-invasive remote sensing today is its role in addressing historical injustices and revealing hidden narratives within the archaeological record. In Canada, technologies like those explored in this thesis are helping to identify unmarked graves

and clandestine burials linked to the Indian Residential School (IRS) system. The Government of Canada, along with several Christian denominations, played a central role in this system, which was responsible for the mistreatment, cultural erasure, and deaths of many Indigenous children. Remote sensing offers tool to aid documentation these tragedies while respecting the sanctity of these sites. By providing a non-intrusive means of investigation, these tools help balance the need for truth and accountability with the cultural and spiritual practices of Indigenous communities that oppose disturbing the land.

Ultimately, the most positive outcome of this study is the potential to standardize and expand remote sensing workflows for archaeological prospection, ensuring that these techniques remain accessible, ethical, and effective. This includes its application in ongoing efforts to investigate sensitive historical sites, demonstrating the value of non-invasive methodologies in both forensic and cultural contexts as indicated in the above paragraph regarding IRS investigations in Canada. By showcasing the power of these approaches, this research not only advances archaeological practice but also drives the broader evolution of the discipline. As technology continues to push the boundaries of archaeological exploration, this study advocates for a paradigm shift that fully integrates drones, remote sensing, and digital data processing as foundational pillars of archaeological investigation.

The time has come for aerial archaeology to take precedence, not as a supplement to traditional fieldwork, but as a leading force in archaeological research, preservation, and heritage management. A drone-based, remote-sensing-led, digital archaeological revolution is not just possible; it is necessary. This research affirms that the future of archaeology must embrace technology-driven, data-centric methodologies, ensuring that investigations are not only more

precise, efficient, and scalable, but also more ethical, practical, inclusive, and sustainable for generations to come.

REFERENCES

- Abdollahnejad, A., & Panagiotidis, D. (2020). Tree Species Classification and Health Status Assessment for a Mixed Broadleaf-Conifer Forest with UAS Multispectral I maging. *Remote Sensing (Basel, Switzerland)*, 12(22), 3722–. <https://doi.org/10.3390/rs12223722>
- Access to Information Act, R.S.C., 1985, c. A-1. (2023). *Justice Laws Website*. Government of Canada. <https://laws-lois.justice.gc.ca/eng/acts/a-1/>
- Agudo, P., Pajas, J., Pérez-Cabello, F., Redón, J., & Lebrón, B. (2018). The Potential of Drones and Sensors to Enhance Detection of Archaeological Cropmarks: A Comparative Study Between Multi-Spectral and Thermal Imagery. *Drones (Basel)*, 2(3), 29–. <https://doi.org/10.3390/drones2030029>
- Altaweel, M., Khelifi, A., Li, Z., Squitieri, A., Basmaji, T., & Ghazal, M. (2022). Automated Archaeological Feature Detection Using Deep Learning on Optical UAV Imagery: Preliminary Results. *Remote Sensing*, 14(3), 553. <https://doi.org/10.3390/rs14030553>
- Baxter, C., and Hargrave, M., (2015) Guidance on the Use of Historic Human Remains Detection Dogs for Locating Unmarked Cemeteries (Legacy 12-510). (tDAR id: 475565); doi:10.48512/XCV8475565
- Bewley, R. H., Crutchley, S. P., & Shell, C. A. (2005). New light on an ancient landscape: lidar survey in the Stonehenge World Heritage Site. *Antiquity*, 79, 636–647.
- Boyd, M., Varney, T., Surette, C., & Surette, J. (2008). Reassessing the northern limit of maize consumption in North America: Stable isotope, plant microfossil, and trace element content of carbonized food residue. *Journal of Archaeological Science*, 35(9), 2545-2556. <https://doi.org/10.1016/j.jas.2008.04.008>
- Brabazon H., DeBruyn, J. M., Lenaghan, S. C., Li, F., Mundorff, A. Z., Steadman, D. W., Stewart, C. N., (2020). Plants to Remotely Detect Human Decomposition?, Trends in Plant Science, Volume 25, Issue 10, 2020, Pages 947-949, ISSN 1360-1385, <https://doi.org/10.1016/j.tplants.2020.07.013>.
- Campana, S. 2017a. Drones in Archaeology State-of-the-art and Future Perspectives: Drones in Archaeology. *Archaeological Prospection*, 24(4): 275–296. DOI: <https://doi.org/10.1002/arp.1569>
- Canadian Aviation Regulations, SOR/96-433. (2023). *Justice Laws Website*. Government of Canada. <https://lois-laws.justice.gc.ca/eng/regulations/SOR-96-433/FullText.html>

- Carmona, J. Á. S., Quirós, E., Mayoral, V., Charro, C. (2020). Assessing the potential of multispectral and thermal UAV imagery from archaeological sites. A case study from the Iron Age hillfort of Villasviejas del Tamuja (Cáceres, Spain), *Journal of Archaeological Science: Reports*, 31, 102312, ISSN 2352-409X, <https://doi.org/10.1016/j.jasrep.2020.102312>. (<https://www.sciencedirect.com/science/article/pii/S2352409X20301036>)
- Casana, J., Wiewel, A., Cool, A., Hill, A., Fisher, K., & Laugier, E. (2017). Archaeological Aerial Thermography in Theory and Practice. *Advances in Archaeological Practice*, 5(4), 310-327. doi:10.1017/aap.2017.23
- Chase, A. F., Chase, D. Z., Weishampel, J. F., Drake, J. B., Shrestha, R. L., Slatton, K. C., Awe, J. J., & Carter, W. E. (2011). Airborne LiDAR, archaeology, and the ancient Maya landscape at Caracol, Belize. *Journal of Archaeological Science*, 38(2), 387–398. <https://doi.org/10.1016/j.jas.2010.09.018>
- Chase, A. S., Chase, D. Z., Chase, A. F. (2017). LiDAR for archaeological research and the study of historical landscapes. In Masini N. & Soldovieri F. (16) *Sensing the Past* (pp. 89–100). Berlin, Germany: Springer.
- Colwell, C. (2016). Collaborative archaeologies and descendant communities. *Annual Review of Anthropology*, 45(1), 113–127. <https://doi.org/10.1146/annurev-anthro-102215-095937>
- Daakir, M., Pierrot-Deseilligny, M., Bosser, P., Pichard, F., Thom, C., Rabot, Y., & Martin, O. (2017). Lightweight UAV with onboard photogrammetry and single frequency GPS positioning for metrology applications. *ISPRS Journal of Photogrammetry and Remote Sensing*, 127, 115–126. <https://doi.org/10.1016/j.isprsjprs.2016.12.007>
- Dawson, P., Brink, J., Farrokhi, A., Jia, F., & Lichti, D. (2022). A method for detecting and monitoring changes to the Okotoks Erratic – “Big Rock” provincial historic site. *Journal of Cultural Heritage Management and Sustainable Development*, 14(38). <https://doi.org/10.1108/JCHMSD-10-2021-0183>
- DJI. (n.d.). *Zenmuse H20 series: Specifications*. <https://enterprise.dji.com/zenmuse-h20-series/specs>
- Doneus, M. (2013). Openness as Visualization Technique for Interpretative Mapping of Airborne Lidar Derived Digital Terrain Models. *Remote Sensing*, 5(12), 6427-6442. <https://doi.org/10.3390/rs5126427>
- Ekaso, D., Nex, F., & Kerle, N. (2020) Accuracy assessment of real-time kinematics (RTK) measurements on unmanned aerial vehicles (UAV) for direct georeferencing. *Geo-spatial Information Science*, 23:2, 165-181, DOI: 10.1080/10095020.2019.1710437

- The electromagnetic spectrum. (n.d.). *University of Tennessee, Department of Physics and Astronomy*.
<http://labman.phys.utk.edu/phys222core/modules/m6/the%20em%20spectrum.html>
- Eve, S. (2013) ‘ZEITGEIST: Stuart Eve’, in Morgan, C. (ed.) *Then Dig*. Peer-reviewed archaeology blogging, October 28. Available at: <http://arf.berkeley.edu/thendig/2014/03/zeitgeist-stuart-eve/> (Accessed: August 21 2016).
- Ellsäßer, F. (2021) *QGIS3 ThermalMetrics Plugin version 0.1 URL:*
<https://plugins.qgis.org/plugins/thermalmetrics/>
- Fernández-Hernandez, G., González-Aguilera, D., Rodríguez-Gonzálvez, P., & Mancera Taboada, J. (2015). Image-Based Modelling from Unmanned Aerial Vehicle (UAV) Photogrammetry: An Effective, Low-Cost Tool for Archaeological Applications. *Archaeometry*, 57(1), 128–145.
- Fleming A. Post-processual Landscape Archaeology: a Critique. *Cambridge Archaeological Journal*. 2006;16(3):267-280. doi:10.1017/S0959774306000163
- GitHub—OpenDroneMap/WebODM. Available online:
<https://github.com/OpenDroneMap/WebODM> (accessed on January 21 2022).
- Gompf, H. S., Anaclet, C. (2019) NREM Sleep Regulation From Neuronal Assembly to Ion. In: *Handbook of Behavioral Neuroscience*, edited by Dringenberg, H. C., 30(9), 137-159, ISSN 1569-7339, ISBN 9780128137437, <https://doi.org/10.1016/B978-0-12-813743-7.00009-8>. Elsevier.
- Gupta, N., Blair, S., & Nicholas, R. (2020) What We See, What We Don’t See: Data Governance, Archaeological Spatial Databases and the Rights of Indigenous Peoples in an Age of Big Data. *Journal of Field Archaeology*, 45, S39-S50,
- Hamilton, S., (1978) The Fort Ellice Area: Pre-excavation Research from an Archaeological Perspective. Unpublished report submitted to the Manitoba Historic Resources Branch, Winnipeg.
- Hamilton, S. (2019). Remote sensing at the Sourismouth forts (Manitoba): Archaeological Re-interpretation after nearly 40 years. *Advancing archaeology: Industry and practice in Alberta, 2019*. Archaeological Survey of Alberta Occasional Paper No. 39, 41-79.
- Hamilton, S. (2020). *Assessing UAV-aided photogrammetry: Efficacy for archaeological mapping* (Unpublished manuscript). Department of Anthropology, Lakehead University.
- Hamilton, S. (2021). Assessing UAV-aided Photogrammetry: Efficacy for archaeological mapping. *UAV Mapping Precision and Accuracy*.

- Hamilton, S. (2022a) *Non-invasive documentation of Fort Ellice 1 (EcMh-03), (1862-1890)*. Unpublished report submitted to the Manitoba Historic Resources Branch, Winnipeg.
- Hamilton, S. (2022b). *Non-invasive archaeological investigations at Fort Ellice 2 (EcMh-010), (1862-1890)*. Lakehead University, Department of Anthropology. Unpublished report prepared for the CDC P'tite Fourche, R.M. of Ellice-Archie.
- Hamilton, S., & Kuncewicz, N. (2025). Noninvasive archaeological site characterization: Case studies from Fort Ellice 1 and 2, Canada. *Drone Systems and Applications*, 13, 1-32. <https://doi.org/10.1139/dsa-2023-0119>
- Hill, A. C. (2019). Economical drone mapping for archaeology: Comparisons of efficiency and accuracy. *Journal of Archaeological Science: Reports*, 24: 80-91
- Hill, A. C., Laugier, E. J., Casana, J. (2020). Archaeological Remote Sensing Using Multi-Temporal, Drone-Acquired Thermal and Near Infrared (NIR) Imagery: A Case Study at the Enfield Shaker Village, New Hampshire. *Remote Sensing*. 12(4), 690. <https://doi.org/10.3390/rs12040690>
- Hill, L. (2014). Human geography and archaeology: Strange bedfellows?. *Progress in Human Geography*. 39. 10.1177/0309132514521482.
- Hirschmuller, H. (2008). Stereo Processing by Semiglobal Matching and Mutual Information. *IEEE Transactions on Pattern Analysis and Machine Intelligence*, 30(2), 328–341. <https://doi.org/10.1109/tpami.2007.1166>
- History of ballooning. (n.d.). *National Balloon Museum*. <https://www.nationalballoonmuseum.com/about/history-of-ballooning/>
- Huggett, J. (2018). Computer applications in archaeology. In S. L. López Varela (Ed.), *The encyclopedia of archaeological sciences*. Wiley. <https://doi.org/10.1002/9781119188230.saseas0108>
- Inomata, T., Triadan, D., Pinzón, F., Burham, M., Ranchos, J. L., Aoyama, K., & Haraguchi, T. (2018). Archaeological application of airborne LiDAR to examine social changes in the Ceibal region of the Maya lowlands. *PloS one*, 13(2), e0191619. <https://doi.org/10.1371/journal.pone.0191619>
- Iriarte J., Robinson M., De Souza J., Damasceno A., Da Silva F., & Nakahara F. (2020). Geometry by design: contribution of lidar to the understanding of settlement patterns of the mound villages in SW Amazonia. *Journal of Computer Applications in Archaeology*. 2020; 3(1): 151-169. DOI: 10.5334/jcaa.45
- James, M. R., Robson, S., d'Oleire-Oltmanns, S., Niethammer, U. (2017). Optimising UAV topographic surveys processed with structure-from-motion: Ground control quality, quantity and bundle adjustment. *Geomorphology*, 280, 51-66,
- Johnson, M. (2012). Phenomenological approaches in landscape archaeology. *Annual Review of Anthropology*, 41, 269-284.

- Keane, J. F., & Carr, S. S. (2013). A brief history of early unmanned aircraft. *Johns Hopkins APL Technical Digest*, 32(3), 558-571.
- Khelifi, A., Ciccone, G., Altaweel, M., Basmaji, T., Ghazal, M. (2021). Autonomous Service Drones for Multimodal Detection and Monitoring of Archaeological Sites. *Applied Sciences*. 11(21), 10424. <https://doi.org/10.3390/app112110424>
- Kilby, J. S. C. (2001). Turning potential into realities: The invention of the integrated circuit (Nobel lecture). *ChemPhysChem*, 2(8-9), 482-485. [https://doi.org/10.1002/1439-7641\(20010917\)2:8/9](https://doi.org/10.1002/1439-7641(20010917)2:8/9)
- Knöbelreiter, P., Vogel, C., & Pock, T. (2018). Self-supervised learning for stereo reconstruction on aerial images. *2018 IEEE International Geoscience and Remote Sensing Symposium (IGARSS)*, 4379-4382.
- Kokalj, Z., Zaksek K., & Ostir K. (2011). Application of sky-view factor for the visualization of historic landscape features in LiDAR-derived relief models. *Antiquity*, 8, 263–273.
- Kokalj, Ž., Somrak, M. 2019. Why Not a Single Image? Combining Visualizations to Facilitate Fieldwork and On-Screen Mapping. *Remote Sensing* 11(7): 747.
- Krasinski, K. E., Wygal, B. T., Wells, J., Martin, R. L., & Seager-Boss, F. (2016). Detecting Late Holocene cultural landscape modifications using LiDAR imagery in the Boreal Forest, Susitna Valley, Southcentral Alaska. *Journal of Field Archaeology*, 41(3), 255–270. <https://doi.org/10.1080/00934690.2016.1174764>
- Maass, M. (2015). From U-2s to Drones: U.S. Aerial Espionage and Targeted Killing during the Cold War and the War on Terror. *Comparative Strategy*, 34(2), 218 238. <https://doi.org/10.1080/01495933.2015.1017385>
- MacNeish, R. S. (1958) An Introduction to the Archaeology of Southeast Manitoba. National Museum of Canada, Bulletin 157, Ottawa.
- Marín-Buzón, Pérez-Romero, A., López-Castro, J. L., Ben Jerbania, I., & Manzano-Agugliaro, F. (2021). Photogrammetry as a New Scientific Tool in Archaeology: Worldwide Research Trends. *Sustainability* (Basel, Switzerland), 13(9), 5319–. <https://doi.org/10.3390/su13095319>
- Mavic 2 Specs. <https://www.dji.com/ca/mavic-2/info>. Accessed Friday, April 23, 2021.
- NASA. (n.d.). *Wright Brothers aircraft*. NASA Glenn Research Center. Retrieved May 22, 2025, from <https://www1.grc.nasa.gov/beginners-guide-to-aeronautics/wright-brothers-aircraft/>
- Nex, F., & Remondino, F. (2014). UAV for 3D mapping applications: a review. *Applied Geomatics*, 6(1), 1–15. <https://doi.org/10.1007/s12518-013-0120-x>
- Nicholson, B.A. 1977 A Theoretical Model for the Excavation of Fort Ellice II. Unpublished student paper on file at Brandon University, Brandon.

- Noviello, C., Gennarelli, G., Esposito, G., Ludeno, G., Fasano, G., Capozzoli, L., Soldovieri, F., Catapano, I. (2022) An Overview on Down-Looking UAV-Based GPR Systems. *Remote Sens.* 14, 3245. <https://doi.org/10.3390/rs14143245>
- Palliser, J. (1863). *Exploration—British North America: The journals, detailed reports, and observations relative to the exploration, by Captain Palliser, of that portion of British North America... during the years 1857–1860*. G.E. Eyre and W. Spottiswoode. HBC Archives, accessed September 26, 2021.
- Parcak, S. (2019). *Archaeology from Space: How the Future Shapes Our Past*. New York: Henry Holt and Company.
- Pecci, A. (2020). *Digital survey from drone in archaeology: Potentiality, limits, territorial archaeological context and variables*. IOP Conference Series: Materials Science and Engineering, 949, 012075. <https://doi.org/10.1088/1757-899X/949/1/012075>
- Pepe, M., Fregonese, L., & Scaioni, M. (2018). Planning airborne photogrammetry and remote sensing missions with modern platforms and sensors. *European Journal of Remote Sensing*, 51(1), 412-436.
- Perry, S. & Taylor, J. S. (2018). Theorising the Digital: A Call to Action for the Archaeological Community. In *Oceans of Data: Proceedings of the 44th Conference on Computer Applications and Quantitative Methods in Archaeology*, Mieko Matsumoto & Espen Uleberg, eds. Oxford: Archaeopress, pp. 11-22.
- Philben, M., Billings, S. A., Edwards, K. A., Podrebarac, F. A., van Biesen, G., & Ziegler, S. E. (2018). Amino acid $\delta^{15}\text{N}$ indicates lack of N isotope fractionation during soil organic nitrogen decomposition. *Biogeochemistry*, 138(1), 69–83. <https://www.jstor.org/stable/48720372>
- Pingel, T. J., Clarke K., & Ford A. (2015). Bonemapping: a LiDAR processing and visualization technique in support of archaeology under the canopy. *Cartography and Geographic Information Science*, 42, 18-26.
- Prümers, H., Betancourt, C. J., Iriarte, J., Robinson, M., & Schaich, M. (2022). LiDAR reveals pre-Hispanic low-density urbanism in the Bolivian Amazon. *Nature*, 606(7913), 325–328. <https://doi.org/10.1038/s41586-022-04780-4>
- Rocke, B., & Ruffell, A. (2022). Detection of Single Burials Using Multispectral Drone Data: Three Case Studies. *Forensic Sciences*, 2(1), 72-87.
- Roosevelt, C. H., (2014). Mapping site-level microtopography with Real- Time Kinematic Global Navigation Satellite Systems (RTK GNSS) and Unmanned Aerial Vehicle Photogrammetry (UAVP). *Open Archaeology (Berlin, Germany)*, 1(1). <https://doi.org/10.2478/opar-2014-0003>

- Rogers, S. R., Manning, I., & Livingstone, W. (2020). Comparing the spatial accuracy of Digital Surface Models from four unoccupied aerial systems: Photogrammetry versus LiDAR. *Remote Sensing*, 12(17), 2806.
- Sánchez-Romero, L., Benito-Calvo, A. & Rios-Garaizar, J. (2022). Defining and Characterising Clusters in Palaeolithic Sites: a Review of Methods and Constraints. *J Archaeol Method Theory* 29, 305–333 <https://doi.org/10.1007/s10816-021-09524-8>
- Schmitt, S. A. (1969). *Measuring uncertainty: an elementary introduction to Bayesian statistics*. Addison-Wesley.
- Silván-Cárdenas, J.L., Caccavari-Garza, A., Quinto-Sánchez, M.E., Madrigal-Gómez, J.M., Coronado-Juárez, E., Quiroz-Suarez, D. (2021). Assessing optical remote sensing for grave detection, *Forensic Science International*, Volume 329, 111064, ISSN 0379-0738, <https://doi.org/10.1016/j.forsciint.2021.111064>.
- Speth, J.D. 2017. 13,000 years of communal bison hunting in western North America. In: *The Oxford Handbook of Zooarchaeology*, edited by U. Albarella, M. Rizzetto, H. Russ, K. Vickers, and S. Viner-Daniels, pp.525-540. Oxford University Press, Oxford, UK.
- Stott, E., Williams, R. D., & Hoey, T. B. (2020). Ground Control Point Distribution for Accurate Kilometre-Scale Topographic Mapping Using an RTK-GNSS Unmanned Aerial Vehicle and SfM Photogrammetry. *Drones*, 4(3), 55. <https://doi.org/10.3390/drones4030055>
- Štular B., Lozić E, Eichert S. (2021). Airborne LiDAR-Derived Digital Elevation Model for Archaeology. *Remote Sensing*, 13(9):1855. <https://doi.org/10.3390/rs13091855>
- Štroner, M., Urban, R., & Línková, L. (2021). A New Method for UAV Lidar Precision Testing Used for the Evaluation of an Affordable DJI ZENMUSE L1 Scanner. *Remote Sensing (Basel, Switzerland)*, 13(23), 4811–. <https://doi.org/10.3390/rs13234811>
- Thomas, H. (2018). Some like it hot: The impact of next generation FLIR Systems thermal cameras on archaeological thermography. *Archaeological Prospection*. 25, 81–87. <https://doi.org/10.1002/arp.1588>
- Transport Canada. (n.d.). *Find your category of drone operation*. Government of Canada. <https://tc.canada.ca/en/aviation/drone-safety/learn-rules-you-fly-your-drone/find-your-category-drone-operation>
- Transport Canada. (n.d.). *Transport Canada*. Government of Canada. <https://tc.canada.ca/>
- Verhoeven G. (2009). Providing an archeological bird's eye view - an overall picture of ground based means to execute low-altitude aerial photography (LAAP) in Archeology. *Archaeological Prospection*, 16: 233–249. DOI:10.1002/arp.354.
- Verhoeven. (2012). Near-Infrared Aerial Crop Mark Archaeology: From its Historical Use to Current Digital Implementations. *Journal of Archaeological Method and Theory*, 19(1), 132–160. <https://doi.org/10.1007/s10816-011-9104-5>

- Verhoeven, G., Doneus, M., Briese, C., & Vermeulen, F. (2012). Mapping by matching: a computer vision-based approach to fast and accurate georeferencing of archaeological aerial photographs. *Journal of Archaeological Science*, 39(7), 2060–2070. <https://doi.org/10.1016/j.jas.2012.02.022>
- Verhoeven, G., & Vermeulen, F. (2016). Engaging with the Canopy—Multi-Dimensional Vegetation Mark Visualisation Using Archived Aerial Images. *Remote Sensing*, 8(9), 752. MDPI AG. Retrieved from <http://dx.doi.org/10.3390/rs8090752>
- Waagen, J., Sánchez J. G., van. der Heiden M., Kuiters A., Lulof P. (2022). In the Heat of the Night: Comparative Assessment of Drone Thermography at the Archaeological Sites of Acquarossa, Italy, and Siegerswoude, The Netherlands. *Drones*. 6(7), 165. <https://doi.org/10.3390/drones6070165>
- Walker, S. (2020). Low-altitude aerial thermography for the archaeological investigation of arctic landscapes. *Journal of Archaeological Science*, 117, 105126. <https://doi.org/10.1016/j.jas.2020.105126>
- White, Devin A. (2016). Archaeology in the Age of Supercomputing. In: *Digital methods and remote sensing in archaeology: archaeology in the age of sensing*. Springer. March 19, 2024, United States. https://doi.org/10.1007/978-3-319-40658-9_15
- Whitehead, Hugenholtz, C. H., Myshak, S., Brown, O., LeClair, A., Tamminga, A., Barchyn, T. E., Moorman, B., & Eaton, B. (2014). Remote sensing of the environment with small unmanned aircraft systems (UASs), part 2: scientific and commercial applications. *Journal of Unmanned Vehicle Systems*, 2(3), 86–102. <https://doi.org/10.1139/juvs-2014-0007>
- Woywitka, R. J., & Michalchuk, B. (2021). Topographic setting of archaeological survey in the Boreal Forest of Alberta. *Archaeological Survey of Alberta Occasional Paper*, 41, 88–99. Archaeological Survey of Alberta.
- Zakšec, K., Oštir, K., Kokalj, Ž. 2011. Sky-View Factor as a Relief Visualization Technique. *Remote Sensing* 3: 398-415.
- Zhang, W., Qi, J., Wan, P., Wang, H., Xie, D., Wang, X., & Yan, G. (2016). An Easy-to-Use Airborne LiDAR Data Filtering Method Based on Cloth Simulation. *Remote Sensing*, 8(6), 501. MDPI AG. Retrieved from <http://dx.doi.org/10.3390/rs8060501>
- Zhou, T., Liu, J., Shin, S., and Habib, A. (2023). Multi-Primitive Triangulation of Airborne and Terrestrial Mobile Mapping Image and LiDAR Data. *Int. Arch. Photogramm. Remote Sens. Spatial Inf. Sci.*, XLVIII-1/W1-2023, 587–594, <https://doi.org/10.5194/isprs-archives-XLVIII-1-W1-2023-587-2023>, 2023.

APPENDIX

1) Results from Mavic Mini

GPS/GCP/3D Errors Details

GPS	Mean	Sigma	RMS Error
X Error (meters)	-0.019	0.930	0.930
Y Error (meters)	-1.678	3.105	3.530
Z Error (meters)	-512.866	1.025	512.867
Total			512.879

GCP	Mean	Sigma	RMS Error
X Error (meters)	0.000	0.001	0.001
Y Error (meters)	0.000	0.002	0.002
Z Error (meters)	0.000	0.000	0.000
Total			0.002

3D	Mean	Sigma	RMS Error
X Error (meters)	0.088	0.144	0.169
Y Error (meters)	0.096	0.167	0.193
Z Error (meters)	0.277	0.498	0.570
Total			0.332

	Absolute	Relative
Horizontal Accuracy CE90 (meters)	0.004	0.297
Vertical Accuracy LE90 (meters)	0.001	0.589

2) Predictive model for grave predictions using NDRE

CREATE A NDRE MULTISPECTRAL ORTHOGRAPHIC MODEL FROM A DATASET WITH USING INTENSITY

Step 1:

run a calibrated multispectral acquisition flight over desired area of interpretation

Step 2: process multispectral data in a photogrammetry software (make sure model type multispectral is selected to isolate each band and incorporate in the metadata

Step 3: output to raster (.tif) DEM Orthophoto with embedded multispectral metadata

Step 4: output raster to QGIS

Step 5: identify number associated with band RE and band NIR to verify the correct band numbers are used in the NDRE formula calculation in the next step

Step 6: run NDRE using raster calculator ($NDRE = NIR - RE / NIR + RE$)

Step 7: colorize raster using properties > symbology

Step 8: select "Singleband pseudocolor", interpolation "Linear", mode "Continuous", Classes "5"

Step 9: select "Classify" and record the range of NDRE values from -1 to +1 across the spectrum of 5 colours at intervals of 0.5 with -1 and +1 at opposite ends of the spectrum and with the centermost value set to 0 and as a neutral color. the aim is to see the range of plants with either sufficient or insufficient chlorophyll contents. A good suggestion is for -1 to represent shades commonly associated with unhealthy or distressed plants (i.e. brown or red), while healthy vigorous plants such as those with high chlorophyll content should be represented by colours of green.

Step 10: select "Apply" and "OK"

NEXT

Step 11: obtain pixel values (represented as reflection values from -1 to +1) from individual graves

*to test this formulaic hypothesis, only one (1) single pixel was isolated, selected, and its reflectance value recorded. Pixels were selected visually based on a scale of darkness (or near darkest) and from within the near centre of each grave. The darkness is associated with higher NDRE values.

Step 12: use area mapping tool to size area dimensions of marked and unmarked graves if possible (if known) and create a dataset.

*if unknown, a sampled dataset can double as a

Step 13: average this dataset

Step 14: calculate the ground sampling distance if this number is not yet known. The ground sampling distance is the distance between the centermost point between two pixels in an image. this is considered the resolution of the model.

Step 15: square this measurement (GSD^2) to obtain size area per pixel

Step 16: divide average size of grave calculated in step 13 by the area per pixel = average pixels per grave

Step 17: plot known and unknown on frequency histogram,

Step 18: divide the frequency of pixel values in the dataset by the average pixels per grave = a predication of the number of graves present in that dataset using NDRE reflectance values from known graves as a predictor.

3) NDVI and NDRE grave statistics (marked and unmarked)

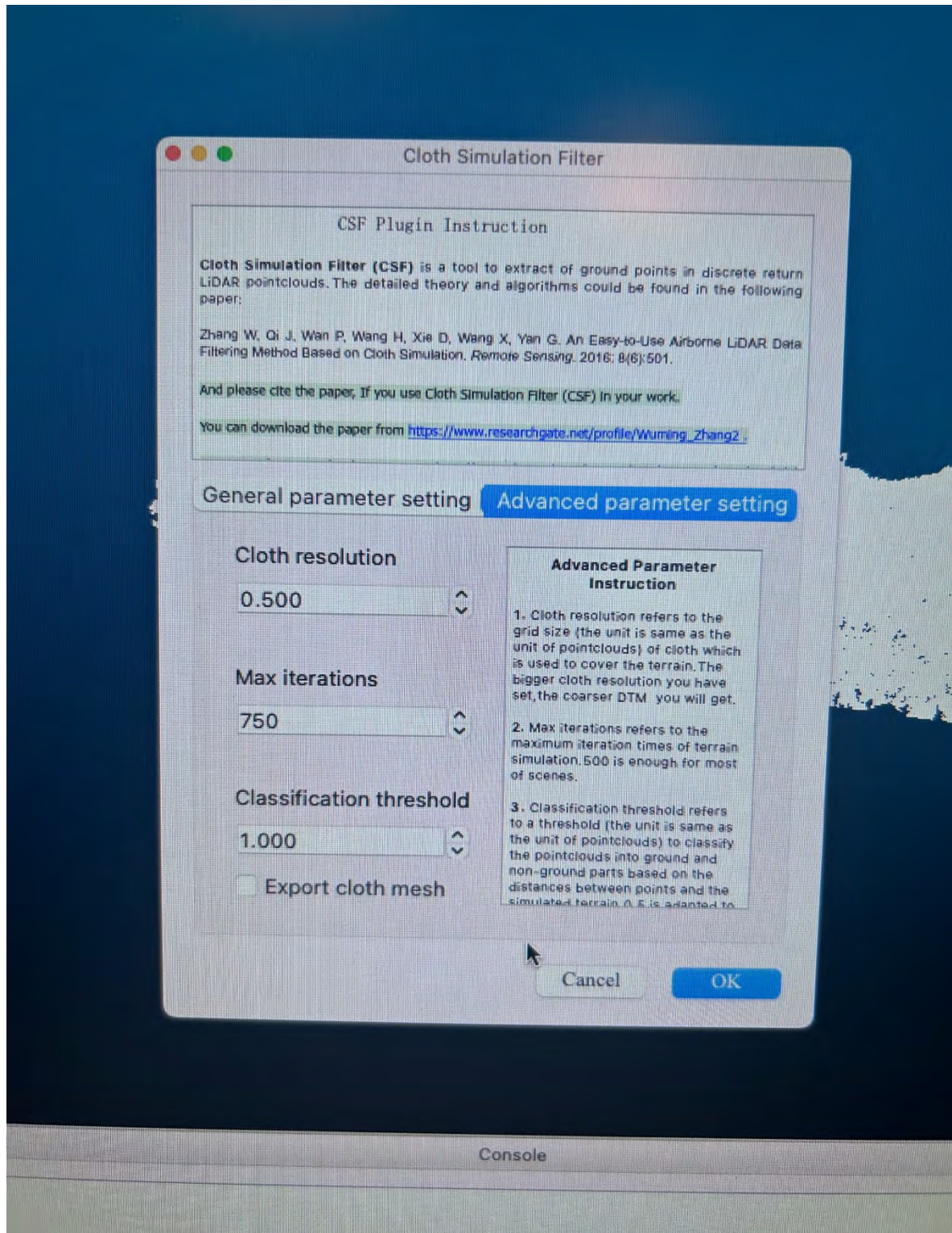
<u>Graves (Inside Cemetery)</u>				<u>Graves (Inside Cemetery)</u>			
<u>Unmarked Graves</u>		<u>Unmarked Graves</u>		<u>Unmarked Graves</u>		<u>Unmarked Graves</u>	
ID	NDVI	ID	NDVI	ID	NDRE	ID	NDRE
1	0.764142	1	0.536548	1	0.254265	1	0.158596
2	0.758552	2	0.555146	2	0.249566	2	0.13935
3	0.667494	3	0.504272	3	0.201269	3	0.140972
4	0.626308	4	0.701812	4	0.183468	4	0.229874
5	0.786762	5	0.505473	5	0.259599	5	0.156239
6	0.669471	6	0.461473	6	0.204824	6	0.1229355
7	0.723478	7	0.531059	7	0.189157	7	0.182672
8	0.686153	8	0.532981	8	0.238412	8	0.141927
9	0.733922	9	0.514838	9	0.202868	9	0.174467
10	0.688555	10	0.481652	10	0.24405	10	0.146606
11	0.577008	11	0.537588	11	0.15063	11	0.114004
12	0.643374	12	0.647302	12	0.195288	12	0.173036
13	0.525127	13	0.603984	13	0.088512	13	0.158378
14	0.651585	14	0.686049	14	0.185375	14	0.24474
15	0.629088	15	0.663959	15	0.141976	15	0.195398
16	0.568329	16	0.538919	16	0.151406	16	0.152778
17	0.78098	17	0.5714235	17	0.248077	17	0.161375
18	0.617434	18	0.611397	18	0.200841	18	0.182838
19	0.620966	19	0.572442	19	0.172864	19	0.125833
20	0.673151	20	0.577441	20	0.223984	20	0.167536
21	0.583671	21	0.596394	21	0.1632555	21	0.176265
22	0.503946	22	0.615453	22	0.146792	22	0.157002
23	0.726146	23	0.617008	23	0.240446	23	0.151288
24	0.668625	24	0.679836	24	0.204394	24	0.207923
25	0.801391	25	0.585062	25	0.348258	25	0.148447
26	0.580529	26	0.600093	26	0.186707	26	0.173452
27	0.679399	27	0.6819835	27	0.270141	27	0.168115
28	0.57404	28	0.589709	28	0.17875	28	0.174574
29	0.611988	29	0.613615	29	0.17869	29	0.19038
30	0.619818	30	0.560693	30	0.167671	30	0.163756
31	0.493616	31	0.509103	31	0.0974515	31	0.144827
32	0.531863	32	0.597222	32	0.152844	32	0.178316
33	0.602501	33	0.562589	33	0.174399	33	0.195621
34	0.643709	34	0.592022	34	0.202855	34	0.155508
35	0.526064	35	0.553852	35	0.1355395	35	0.158687
36	0.539687	36	0.583852	36	0.133389	36	0.18394

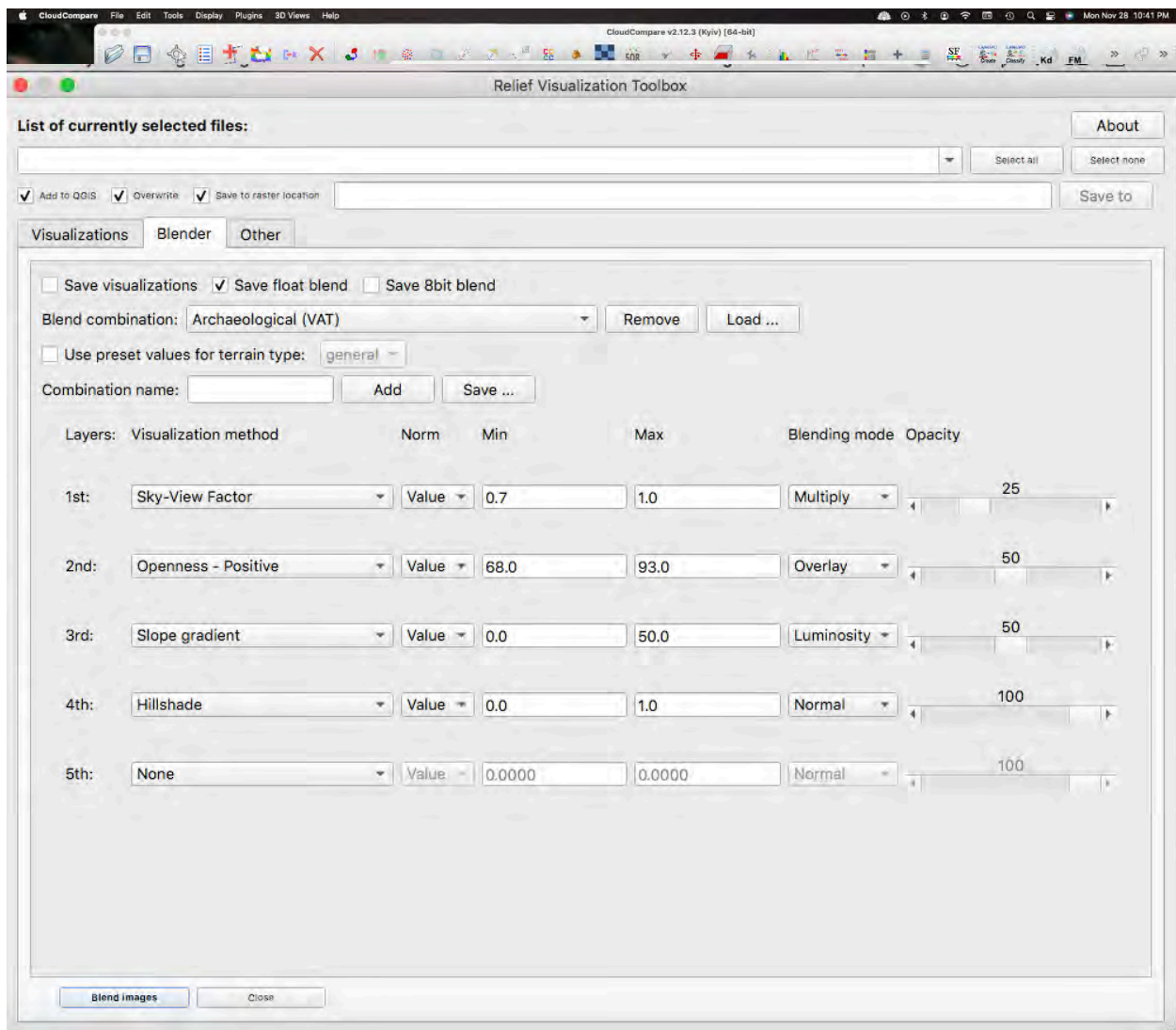
37	0.488132	37	0.419176	37	0.144396	37	0.124569
38	0.589822	38	0.514574	38	0.152446	38	0.138649
39	0.619977	39	0.553239	39	0.159062	39	0.150084
40	0.40182	40	0.54255	40	0.0800655	40	0.172379
MEAN	0.629465575		0.5725946		0.187599575		0.164583413
			0.056871				0.023016163
MEDIAN	0.623637		0.5719328		0.1844215		0.160031
			0.0517043				0.0243905

Graves (Inside Cemetery)		Graves (Inside Cemetery)		Unmarked Graves		Unmarked Graves	
ID	NDVI	ID	NDRE	ID	NDVI	ID	NDRE
1	0.764142	1	0.254265	1	0.536548	1	0.158596
2	0.758552	2	0.249566	2	0.555146	2	0.13935
3	0.667494	3	0.201269	3	0.504272	3	0.140972
4	0.626308	4	0.183468	4	0.701812	4	0.229874
5	0.786762	5	0.259599	5	0.505473	5	0.156239
6	0.669471	6	0.204824	6	0.461473	6	0.122936
7	0.723478	7	0.189157	7	0.531059	7	0.182672
8	0.686153	8	0.238412	8	0.532981	8	0.141927
9	0.733922	9	0.202868	9	0.514838	9	0.174467
10	0.688555	10	0.24405	10	0.481652	10	0.146606
11	0.577008	11	0.15063	11	0.537588	11	0.114004
12	0.643374	12	0.195288	12	0.647302	12	0.173036
13	0.525127	13	0.088512	13	0.603984	13	0.158378
14	0.651585	14	0.185375	14	0.686049	14	0.24474
15	0.629088	15	0.141976	15	0.663959	15	0.195398
16	0.568329	16	0.151406	16	0.538919	16	0.152778
17	0.78098	17	0.248077	17	0.571424	17	0.161375
18	0.617434	18	0.200841	18	0.611397	18	0.182838
19	0.620966	19	0.172864	19	0.572442	19	0.125833
20	0.673151	20	0.223984	20	0.577441	20	0.167536
21	0.583671	21	0.1632555	21	0.596394	21	0.176265
22	0.503946	22	0.146792	22	0.615453	22	0.157002
23	0.726146	23	0.240446	23	0.617008	23	0.151288
24	0.668625	24	0.204394	24	0.679836	24	0.207923
25	0.801391	25	0.348258	25	0.585062	25	0.148447
26	0.580529	26	0.186707	26	0.600093	26	0.173452
27	0.679399	27	0.270141	27	0.681984	27	0.168115
28	0.57404	28	0.17875	28	0.589709	28	0.174574
29	0.611988	29	0.17869	29	0.613615	29	0.19038

30	0.619818	30	0.167671	30	0.560693	30	0.163756
31	0.493616	31	0.0974515	31	0.509103	31	0.144827
32	0.531863	32	0.152844	32	0.597222	32	0.178316
33	0.602501	33	0.174399	33	0.562589	33	0.195621
34	0.643709	34	0.202855	34	0.592022	34	0.155508
35	0.526064	35	0.1355395	35	0.553852	35	0.158687
36	0.539687	36	0.133389	36	0.583852	36	0.18394
37	0.488132	37	0.144396	37	0.419176	37	0.124569
38	0.589822	38	0.152446	38	0.514574	38	0.138649
39	0.619977	39	0.159062	39	0.553239	39	0.150084
40	0.40182	40	0.0800655	40	0.54255	40	0.172379
MEAN	0.629465575		0.187599575		0.572595		0.164583
			0.441866				0.408011
MEDIAN	0.623637		0.1844215		0.571933		0.160031
			0.4392155				0.411902

4) Cloud Compare Settings (CSF)






5) VAT Algorithm Preset Values

6) DJI Mavic Mini Specs

Specifications	
Aircraft	
Maximum Take-Off Mass (MTOM)	249 g (including the battery, propellers, and a microSD card) 199 g (JP version)
Dimensions (LxWxH)	Folded: 140x81x57 mm Unfolded: 159x202x55 mm Unfolded (with propellers): 245x289x55 mm
Diagonal Distance	213 mm
Max Ascent Speed	4 m/s (S Mode) 2 m/s (P Mode) 1.5 m/s (C Mode)
Max Descent Speed	3 m/s (S Mode) 1.8 m/s (P Mode) 1 m/s (C Mode)
Max Speed (near sea level, no wind)	13 m/s (S Mode) 8 m/s (P Mode) 4 m/s (C Mode)
Max Service Ceiling Above Sea Level	3000 m
Max Flight Time	30 mins (measured while flying at 14 kph in windless conditions) 18 mins for JP version (measured while flying at 12 kph in windless conditions)
Max Wind Speed Resistance	8 m/s (Scale 4)
Max Tilt Angle	30° (S Mode) 20° (P Mode) 20° (C Mode)
Max Angular Velocity	150°/s (S Mode) 130°/s (P Mode) 30°/s (C Mode)
Operating Temperature Range	0° to 40° C (32° to 104° F)
GNSS	GPS+GLONASS
Operating Frequency	Model MT1SS5: 5.725-5.850 GHz Model MT1SD25: 2.400-2.4835 GHz, 5.725-5.850 GHz
Transmission Power (EIRP)	Model MT1SS5 5.8 GHz: <30 dBm (FCC); <28 dBm (SRRC) Model MT1SD25 2.4 GHz: <19 dBm (MIC/CE) 5.8 GHz: <14 dBm (CE)

Hovering Accuracy Range	Vertical: ± 0.1 m (with Vision Positioning), ± 0.5 m (with GPS Positioning) Horizontal: ± 0.3 m (with Vision Positioning), ± 1.5 m (with GPS Positioning)
Gimbal	
Mechanical Range	Tilt: -110° to $+35^{\circ}$ Roll: -35° to $+35^{\circ}$ Pan: -20° to $+20^{\circ}$
Controllable Range	Tilt: -90° to 0° (default setting), -90° to $+20^{\circ}$ (extended)
Stabilization	3-axis (tilt, roll, pan)
Max Control Speed (tilt)	$120^{\circ}/s$
Angular Vibration Range	$\pm 0.01^{\circ}$
Sensing System	
Downward	Operating Range: 0.5-10 m
Operating Environment	Non-reflective, discernable surfaces with diffuse reflectivity of $>20\%$ Adequate lighting of $\text{lux} > 15$
Camera	
Sensor	1/2.3" CMOS Effective Pixels: 12 MP
Lens	FOV: 83° 35 mm Format Equivalent: 24 mm Aperture: f/2.8 Focus Range: 1 m to ∞
ISO	Video: 100-3200 (Auto) Photo: 100-3200
Shutter Speed	Electronic Shutter: Video: 1/8000-1/fps (Auto) Photo: 4-1/8000 s (Manual), 1-1/8000 s (Auto)
Still Image Size	4:3: 4000 \times 3000 16:9: 4000 \times 2250
Still Photography Modes	Single shot Interval: 2/3/5/7/10/15/20/30/60 s
Video Resolution	2.7K: 2720 \times 1530 24/25/30 p FHD: 1920 \times 1080 24/25/30/48/50/60 p
Max Video Bitrate	40 Mbps
Supported File System	FAT32 (≤ 32 GB) exFAT (> 32 GB)
Photo Format	JPEG
Video Format	MP4 (H.264/MPEG-4 AVC)
Remote Controller	
Operating Frequency	Model MR1SS5: 5.725 - 5.850 GHz Model MR1SD25: 2.400 - 2.4835 GHz, 5.725 - 5.850 GHz

Max Transmission Distance (unobstructed, free of interference)	Model MR1SS5: 5.8 GHz: 4000 m (FCC); 2500 m (SRRC) Model MR1SD25: 2.4 GHz: 2000 m (MIC/CE) 5.8 GHz: 500 m (CE)
Operating Temperature Range	0° to 40° C (32° to 104° F)
Transmitter Power (EIRP)	Model MR1SS5: 5.8 GHz: <30 dBm (FCC); <28 dBm (SRRC) Model MR1SD25: 2.4 GHz: <19 dBm (MIC/CE) 5.8 GHz: <14 dBm (CE)
Battery Capacity	2600 mAh
Operating Current/Voltage	1200 mA 3.6 V (Android) 450 mA 3.6 V (iOS)
Supported Mobile Device Size	Max length: 160 mm Max thickness: 6.5 - 8.5 mm
Supported USB Port Types	Lightning, Micro USB (Type-B), USB-C
Video Transmission System	Enhanced Wi-Fi
Live View Quality	Remote Controller: 720p@30fps
Max. Bitrate	4 Mbps
Latency (depending on environmental conditions and mobile device)	170 - 240 ms
Charger	
Input	100 - 240V, 50/60 Hz, 0.5A
Output	12V 1.5A / 9V 2A / 5V 3A
Rated Power	18 W
Intelligent Flight Battery (General Version)	
Battery Capacity	2400 mAh
Voltage	7.2 V
Max Charging Voltage	8.4 V
Battery Type	Li-ion 2S
Energy	17.28 Wh
Weight	100 g
Charging Temperature Range	5° to 40° C (41° to 104° F)
Max Charging Power	24 W
Intelligent Flight Battery (JP Version)	
Capacity	1100 mAh
Voltage	7.6 V
Max Charging Voltage	8.7 V
Battery Type	LiPo 2S
Energy	8.36 Wh
Weight	50 g
Charging Temperature Range	5° to 40° C (41° to 104° F)

Max Charging Power	18 W
App	
App	DJI Fly
Required Operating System	iOS v10.0.2 or later; Android v6.0 or later
SD Cards	
Supported SD Cards	Requires UHS-I Speed Grade 3 rating microSD card
Recommended microSD Cards	<p>16GB: SanDisk Extreme, Lexar 633x</p> <p>32GB: Samsung PRO Endurance, Samsung EVO Plus, SanDisk Industrial, SanDisk Extreme V30 A1/A2, SanDisk Extreme PRO V30 A1/A2, Lexar 633x, Lexar 667x</p> <p>64GB: Samsung PRO Endurance, Samsung EVO Plus, SanDisk Extreme V30 A1, Lexar 633x, Lexar 667x, Lexar 1000x, Toshiba Exceria M303 V30 A1, Netac PRO V30 A1</p> <p>128GB: Samsung PRO Plus, Samsung EVO Plus, SanDisk Extreme V30 A1, SanDisk Extreme Plus V30 A1/A2, Lexar 633x, Lexar 667x, Lexar 1000x, Toshiba Exceria M303 V30 A1, Netac Pro V30 A1</p> <p>256GB: SanDisk Extreme V30 A1</p>
 <ul style="list-style-type: none"> • Aircraft takeoff weight includes battery, propellers, and a microSD card. • Registration not required in some countries and regions. Check local rules and regulations before use. • These specifications have been determined through tests conducted with the latest firmware. Firmware updates can enhance performance. It is highly recommended to update to the latest firmware. 	

7) MicaSense RedEdge-MX specs

	Multispectral
Pixel size	3.75 μm
Resolution	1280 x 960 (1.2 MP x 5 imagers)
Aspect ratio	4 : 3
Sensor size	4.8 mm x 3.6 mm
Focal length	5.4 mm
Field of view	47.2 degrees horizontal, 35.4 degrees vertical
Output bit depth	12-bit
GSD @ 120 m (~400 ft)	8 cm/pixel per band
GSD @ 60 m (~200 ft)	4 cm/pixel per band

8) DJI H20T Specs

Specifications

General	
Name	Zenmuse H20T
Dimensions	167×135×161 mm
Weight	828±5 g
Protection Rating	IP44
Laser Safety	Class 1M (IEC 60825-1:2014)
Supported Aircraft	Matrice 300 RTK
Gimbal	
Angular Vibration Range	±0.01°
Mount	Detachable
Zoom Camera	
Sensor	1/1.7" CMOS, Effective Pixels: 20M
Lens	Focal length: 6.83-119.94 mm (equivalent: 31.7-556.2 mm) Aperture: f/2.8-f/11 (normal), f/1.6-f/11 (night) Focus: 1 m to ∞ (wide), 8 m to ∞ (telephoto)
Wide Camera	
Sensor	1/2.3" CMOS, Effective Pixels: 12M
Lens	DFOV: 82.9° Focal length: 4.5 mm (equivalent: 24 mm) Aperture: f/2.8 Focus: 1 m to ∞
Infrared Thermal Camera	
Thermal Imager	Uncooled VOx Microbolometer
Lens	DFOV: 40.6° Focal length: 13.5 mm (equivalent: 58 mm) Aperture: f/1.0 Focus: 5 m to ∞
Laser Range Finder	
Wavelength	905 nm
Measuring Range	3-1200 m (Vertical reflecting surface with 12m diameter and 20% reflectivity)
Storage	
Supported SD Cards	Supports a microSD card with capacity of up to 128 GB. A UHS-I Speed Grade 3 rating microSD card is required.
Supported File System	FAT32 (≤32 GB), exFAT (>32 GB)
Environment	
Operating Temperature	-20° to 50° C
Storage Temperature	-20° to 60° C

9) DJI Zenmuse L1 Specs

General	
Product name	ZENMUSE L1
Dimensions	152×110×169 mm
Weight	930±10 g
Power	Typical: 30 W; Max: 60 W
IP Rating	IP54
Supported Aircraft	Matrice 300 RTK
Operating Temperature Range	-20° to 50° C (-4° to 122° F) when using RGB mapping camera: 0° to 50° C (32° to 122° F)
Storage Temperature Range	-20° to 60° C (-4° to 140° F)
System Performance	
Detection Range	450 m @ 80% reflectivity, 0 klx 190 m @ 10% reflectivity, 100 klx
Point Rate	Single return: max. 240,000 pts/s Multiple return: max. 480,000 pts/s
System Accuracy (RMS 1σ)*	Horizontal: 10 cm @ 50 m Vertical: 5 cm @ 50 m
Real-Time Point Cloud Coloring Coding	Reflectivity, Height, Distance, RGB
LiDAR	
Ranging Accuracy (RMS 1σ)*	3 cm @ 100 m
Maximum Returns Supported	3
Scan Modes	Non-repetitive scanning pattern, Repetitive scanning pattern
FOV	Non-repetitive scanning pattern: 70.4° (horizontal) × 77.2° (vertical) Repetitive scanning pattern: 70.4° (horizontal) × 4.5° (vertical)
Laser Safety	Class 1 (IEC 60825-1:2014) (Eye Safety)
Inertial Navigation System	
IMU Update Frequency	200 Hz
Accelerometer Range	±8 g
Angular Velocity Meter Range	±2000 dps
Yaw Accuracy (RMS 1σ)*	Real-time: 0.3°, Post-processing: 0.15°
Pitch/Roll Accuracy (RMS 1σ)*	Real-time: 0.05°, Post-processing: 0.025°
Auxiliary Positioning Vision Sensor	
Resolution	1280×960
FOV	95°
RGB Mapping Camera	
Sensor Size	1 in
Effective Pixels	20 MP
Photo Size	5472×3078 (16:9), 4864×3648 (4:3), 5472×3648 (3:2)
Focal Length	8.8/24 mm (equivalent)

Shutter Speed	Mechanical shutter speed: 1/2000-8 s Electronic shutter speed: 1/8000-8 s
ISO	Video: 100-3200 (auto), 100-6400 (manual) Photo: 100-3200 (auto), 100-12800 (manual)
Aperture Range	f/2.8 - f/11
Supported File System	FAT (≤ 32 GB); exFAT (> 32 GB)
Photo Format	JPEG
Video Format	MOV, MP4
Video Resolution	H.264, 4K: 3840x2160 30p
Gimbal	
Stabilized System	3-axis (tilt, roll, pan)
Angular Vibration Range	$\pm 0.01^\circ$
Mount	Detachable DJI SKYPORT
Controllable Range	Tilt: -120° to $+30^\circ$, Pan: $\pm 320^\circ$
Operation Modes	Follow/Free/Re-center
Data Storage	
Raw Data Storage	Photo/IMU/Point cloud/GNSS/Calibration files
Supported microSD Cards	microSD: Sequential writing speed 50 MB/s or above and UHS-I Speed Grade 3 rating or above; Max capacity: 256 GB
Recommended microSD Cards**	SanDisk Extreme 128GB UHS-I Speed Grade 3 SanDisk Extreme 64GB UHS-I Speed Grade 3 SanDisk Extreme 32GB UHS-I Speed Grade 3 SanDisk Extreme 16GB UHS-I Speed Grade 3 Lexar 1066x 128GB U3 Samsung EVO Plus 128GB
Post-Processing Software	
Supported Software	DJI Terra
Data Format	DJI Terra supports exporting standard format point cloud models: Point cloud format: PNTS/LAS/PLY/PCD/S3MB

* The accuracy was measured under the following conditions in a DJI laboratory environment: after a 5-minute warm up, using Mapping Mission with Calibration Flight enabled in DJI Pilot, and with the RTK in FIX status. The relative altitude was set to 50 m, flight speed to 10 m/s, gimbal pitch to -90° , and each straight segment of the flight route was less than 1000 m. DJI Terra was used for post-processing.

** The recommended microSD cards may be updated in future. Visit the DJI official website for the latest information.

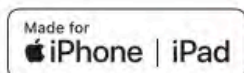
10) D-RTK2 Base Station Specs

GNSS Receiver	GNSS Frequency	Simultaneously receive: GPS: L1, L2, L5; BeiDou: B1, B2, B3 GLONASS: F1, F2; Galileo: E1, E5A, E5B
---------------	----------------	--

GNSS Receiver	Positioning Accuracy	Single Point Horizontal: 1.5 m (RMS) Vertical: 3.0 m (RMS) RTK Horizontal: 1 cm + 1 ppm (RMS) Vertical: 2 cm + 1 ppm (RMS) 1 ppm: For every 1 km increase in distance, the accuracy will be 1 mm less. For example, the horizontal accuracy is 1.1 cm when the receiving end is 1 km away from the base station.
	Positioning Update Rate	1 Hz, 2 Hz, 5 Hz, 10 Hz and 20 Hz
	Cold Start	< 45 s
	Hot Start	< 10 s
	Recapture Time	< 1 s
	Initialization Reliability	> 99.9%
	Differential Data Format	RTCM 2.x/3.x
	Data Link	OcuSync, LAN, 4G, Wi-Fi
Communication and Data Storage	Operating Frequency	2.4000-2.4835 GHz, 5.725-5.850 GHz
	EIRP	OcuSync 2.4 GHz SRRP/CE/MIC/KCC: < 20 dBm FCC/NCC: < 26 dBm 5.8 GHz SRRP/NCC/FCC: < 26 dBm; CE: < 14 dBm Wi-Fi 2.4 GHz SRRP/CE/MIC/KCC: < 20 dBm FCC/NCC: < 22 dBm 5.8 GHz SRRP/NCC/FCC: < 22 dBm
	OcuSync Communication Distance	Operating Mode 1/3 SRRP/NCC/FCC/MIC/KCC/CE: 2 km (Unobstructed and free of interference, when the D-RTK 2 Mobile Station is used as a base station and the distance from the D-RTK 2 antenna to the bottom of the tripod is 1.8 m, when the difference in height between the remote controller and D-RTK 2 is less than 2 m, and when the remote controller is 1.2 m from ground level)
		Operating Mode 4 Between the aircraft and mobile station: NCC/FCC: 7 km, SRRP/MIC/KCC/CE: 5 km Between the remote controller and mobile station: 200 m (Unobstructed and free of interference, at a flying altitude of about 120 m, when the distance from the D-RTK 2 antenna to the bottom of the tripod is 1.8 m, and when the remote controller is 1.2 m from ground level)
		Operating Mode 5 NCC/FCC: 12 km, SRRP/MIC/KCC/CE: 6 km (Unobstructed and free of interference, when the distance from the D-RTK 2 antenna to the bottom of the tripod is 1.8 m)
	Memory Capacity	16 GB

IMU	Features	Built-in high-precision 6-axis accelerometer D-RTK 2 movement monitoring Sloping measurements Electronic bubble level
Electrical Characteristics	Power Consumption	12 W
	Power Supply	16.5 to 58.8VDC
	Battery	Type: Lithium-ion battery Capacity: 4920 mAh Energy: 37.3 WH
	Run Time	WB37 battery: > 2 h
Physical Characteristics	Dimensions (D-RTK 2 body with extension rod)	168 mm × 168 mm × 1800 mm
	IP Rating	IP65
Operating Temperature	-4° to 131° F (-20° to 55° C)	

11) Juniper Systems GEODE-2 RTK Specs



GEODE GNS2 COMPATIBILITY

- iPhone 11 Pro Max, iPhone 11 Pro, iPhone 11, iPhone XS, iPhone XS Max, iPhone XR, iPhone X, iPhone 8, iPhone 8 Plus, iPhone 7, iPhone 7 Plus, iPhone SE, iPhone 6s Plus, iPhone 6s, iPhone 6 Plus, iPhone 6, iPod Touch (7th Generation), iPad Mini (5th Generation), iPad (7th Generation), iPad Pro 11-inch, iPad (6th Generation), iPad Pro 10.5 inch, iPad Pro 12.9 inch (1st, 2nd, and 3rd Generation.)
- Windows® PC (8/10)
- Windows® Embedded Handheld 6.5
- Android™ 4.x and above
- GeodeConnect™ software provides configuration, communications setup, and receiver settings

RECEIVER

- Receiver Type: GNSS single frequency with carrier phase tracking
- Signals Received: GPS, SBAS, GLONASS, BeiDou, GALILEO and QZSS¹
- Channels: 162
- SBAS Tracking: 3-channel parallel tracking
- Update Rate: 1 Hz standard, 2-10 Hz (optional)

ACCURACY

- SBAS (WAAS): <30 cm Horizontal RMS (<60 cm 2DRMS)²
- Cold Start: <60 sec typical (no almanac)
- Reacquisition: <1 sec

COMMUNICATIONS

- Bluetooth® 4.1 SPP, iAP2, EAP
- Bluetooth Range: Class 1 Long Range
- Ports: Micro USB Client 2.0; Serial RS232C DB-9 (optional)
- Serial Baud Rates: 4800-115200

RECEIVER PROTOCOLS

- Data I/O Protocol: NMEA 0183, Crescent Raw Binary (proprietary)
- Correction I/O Protocol: Hemisphere GNSS Proprietary, ROX, RTCM v2.3, RTCM v3.2, CMR, CMR+
- Other: 1PPS Timing Output, Speed Pulse, Event Marker Input (optional)

POWER

- Input Voltage: 5VDC @ 2A USB
- Power Consumption: 1.7-2 W nominal
- Overtime Technology™ Battery: 3.6V 6000 mAh Li-ion (10 hours)
- Charging Time: Less than 4 hours

ANTENNA

- Internal precision Multi-GNSS with integrated ground plane
- External Antenna Port: MCX type, 50 ohm 15VDC @ 20 mA maximum

JUNIPER RUGGED™

- Operating Temp: -20 C to +60 C
- Storage Temp: -30 C to +60 C
- Meets or Exceeds MIL-STD 810G (Drop, Vibration, Temperature, Ingress Protection)
- Enclosure Rating: IP68
- Dimensions: 4.4 x 4.4 x 1.7 inch (111 x 111 x 43 mm)
- Weight: 0.8 lb (360 g)
- Mount: ¼ x 20 camera stud and #6-32 AMPs

RECEIVER UPGRADES

- 2 Hz to 10 Hz update rate
- Multi-GNSS upgrade

INCLUDED ACCESSORIES

- 5VDC USB Universal Charger
- USB Data/Charging Cable (USB-A to Micro-B)
- 5/8 x 11 Pole Mount Adapter

CONFIGURATIONS

- Geode GNS2 GPS, 1 Hz
- Geode GNS2 Multi-GNSS, 1 Hz
- Geode GNS2 Multi-GNSS, with 9-pin serial port, 1 Hz
- Geode GNS2 Multi-GNSS, 10Hz
- Geode GNS2 Multi-GNSS, 10Hz with 9-pin Port



CONTACT JUNIPER SYSTEMS TODAY FOR A QUOTE

1. (Optional) used dependent on model configuration
2. GNSS accuracy subject to observation conditions, multipath environment, number of satellites in view, satellite geometry, and ionospheric activity.



Juniper Systems, Inc. Logan, UT, USA
Phone: 435.753.1881
Email: sales@junipersys.com

Juniper Systems Ltd. Bromsgrove, UK
Phone: +44 (0) 1527 870773
Email: info@junipersys.com

www.junipersys.com

FEATURE	SPECIFICATION
Receiver	<ul style="list-style-type: none"> Receiver Type: GNSS single frequency with carrier tracking Signals Received: GPS, SBAS, BeiDou (optional), Galileo (optional), GLONASS (optional) Channels: 162 SBAS Tracking: 3-channel parallel tracking Update Rate: 1 Hz standard, 2–10 Hz (optional)
Accuracy	<ul style="list-style-type: none"> SBAS (WAAS): <30 cm Horizontal RMS (<60 cm 2DRMS) Cold Start: <60 sec typical (no almanac) Reacquisition: <1 sec
Communications	<ul style="list-style-type: none"> Bluetooth® 4.0 (SPP, IAP2, EAP) Bluetooth Range: Class 1 Long Range up to 100 m (330 ft) depending on connection host device range. Ports: Micro USB Client 2.0; Serial RS232C DB-9 (optional) Serial Baud Rates: 4800–115200
Receiver Protocols	<ul style="list-style-type: none"> Data I/O Protocol: NMEA-0183, Raw Binary (proprietary), RTCM2, RTCM3 Other: 1PPS Timing Output, Speed Pulse, Event Marker Input (optional)
Power	<ul style="list-style-type: none"> USB Input Voltage: 5 VDC @ 2A Power Consumption: 1.7–2 W nominal Overtime Technology™ Battery: Rechargeable Li-ion battery pack, 3.6VDC 6000 mAh, 21.6 whr Run time up to 10 hours Charging Time 4 to 6 hours
Output Power	<ul style="list-style-type: none"> Output signals variable from 6 to -6 VDC

FEATURE	SPECIFICATION
Input Power	<ul style="list-style-type: none"> 0 to 5 VDC (max +/- 15 VDC)
Antenna	<ul style="list-style-type: none"> Internal precision multi-GNSS with integrated ground plane External Antenna Port: MCX type, 50 ohm 3.3VDC @ 20 mA maximum
Juniper Rugged™	<ul style="list-style-type: none"> 2-meter pole drop Operating Temp: -20° C to +60° C Storage Temp: -30° C to +60° C Battery Charging Temp: 0° C to 50° C Enclosure Rating: IP68 Dimensions: 4.4 x 4.4 x 1.7 inch (111 x 111 x 43 mm) Weight: 0.8 lb (360 g) Mount: 1/4" x 20 camera insert and #6-32 AMPS (diagonal)
Receiver Upgrades	<ul style="list-style-type: none"> 2Hz–10 Hz update rate Multi-GNSS Serial RS232C DB-9 port
Software	<ul style="list-style-type: none"> Geode Connect™ software provides configuration, communications setup, and receiver settings Available for: <ul style="list-style-type: none"> iPhone and iPad Android 4.2.x and above Windows PC (8/10) Windows Embedded Handheld 6.5
Included Accessories	<ul style="list-style-type: none"> 5VDC USB Universal Charger USB Data/Charging Cable (USB-A to Micro-B) Universal Plug Kit 5/8 x 11 Pole Adapter
Optional Accessories	<ul style="list-style-type: none"> Smart phone Adapter Tray External Patch Antenna Antenna Cable

FEATURE	SPECIFICATION
Models	<ul style="list-style-type: none"> ■ Geode GPS, 1 Hz ■ Geode GPS with 9-pin serial port, 1 Hz ■ Geode Multi-GNSS, 1 Hz ■ Geode Multi-GNSS with 9-pin serial port, 1 Hz ■ Geode Multi-GNSS Sub-meter Receiver, 10Hz ■ Geode Multi-GNSS Sub-meter Receiver, 10Hz with 9-pin Port
Compatibility	<ul style="list-style-type: none"> ■ All Geode models are compatible with Android 4.2.x and above, Windows 10, and Windows Embedded 6.5.3 devices. ■ Geode GNS2 is a registered Made for iPhone/iPad accessory. As of September 2019, Geode GNS2 models are compatible with the following: ■ iPhone 11 Pro Max, iPhone 11 Pro, iPhone 11, iPhone XS Max, iPhone XS, iPhone XR, iPhone X, iPhone 8, iPhone 8 Plus, iPhone 7, iPhone 7 Plus, iPhone SE, iPhone 6s Plus, iPhone 6s, iPhone 6 Plus, iPhone 6, iPod Touch (7th generation), iPad mini (5th generation), iPad (7th generation), iPad (6th Generation), iPad Pro 12.9 inch (3rd Generation), iPad Pro 12.9 inch (2nd Generation), iPad Pro 12.9 inch (1st Generation), iPad Pro 11-inch, iPad Pro 10.5 inch ■ Windows® PC (8/10) ■ Windows® Embedded Handheld 6.5 ■ Android™ 4.x and above

12) Signed data permission letter from PCSP



Peguis Consultation & Special Projects
P.O. Box 10, Peguis First Nation, MB R0C 3J0
T: (204) 645-2359 Ext.108
E: Proj.CC2@peguisfirstnation.ca



February 28, 2023

Chief & Council
P.O. Box
Peguis First Nation, MB
R0C 3J0

Dear Chief & Council

This letter is a request authorizing Nick Kuncewicz, employee of Peguis Consultation & Special Projects Inc. and student of Lakehead University, 955 Oliver Rd, Thunder Bay, ON P7B 5E1 to use the [REDACTED] and Lockport heritage files.

I request permission for Nick Kuncewicz to use the [REDACTED] and Lockport heritage information in the obtainment and earning of his Thesis to his examiners. Location and georeferencing of burials and cemetery site will remain discrete. However, any other use of this information will not be permitted.

If you approve consent to release and disclose heritage information please affix signature to document attached.

If you have any questions please do not hesitate to contact me at (204) 806-5712 or Specialproj.Director@peguisfirstnation.ca

Regards,

A handwritten signature in black ink, appearing to read 'Mike Sutherland'.

Mike Sutherland
Director
Peguis Consultation & Special Projects Inc.



Peguis Consultation & Special Projects
P.O. Box 10, Peguis First Nation, MB R0C 3J0
T: (204) 645-2359 Ext.108
E: Proj.CC2@peguisfirstnation.ca



HERITAGE FILE(S) RELEASE FORM PLEASE READ CAREFULLY

I hereby grant **Nick Kuncewicz**, employee of Peguis Consultation & Special Projects Inc. and student of Lakehead University, 955 Oliver Rd, Thunder Bay, ON P7B 5E1 to use the [REDACTED] and Lockport heritage files for his Thesis.

Nick Kuncewicz agrees to only use the [REDACTED] and Lockport heritage information in the obtainment and earning of his Thesis to his examiners. Location and georeferencing of burials and cemetery site will remain discrete. However, any other use of this information will not be permitted.

Name (printed): Chief Glenn Hudson

Signature: [Signature]

Date of Agreement: MARCH 2/23